

VICTORIA UNIVERSITY OF WELLINGTON  
*Te Whare Wānanga o te Ūpoko o te Ika a Māui*



School of Engineering and Computer Science  
*Te Kura Mātai Pūkaha, Pūrorohiko*

**Development and Evaluation of a Novel  
Mechatronic Percussion System**

Trent Little

March, 2019

Submitted in fulfilment of the requirements for  
the Degree of Master of Engineering at Victoria University  
of Wellington.



## Abstract

While numerous attempts at creating mechatronic percussion systems exist, many have been limited to only playing a single membranophone or idiophone. These systems inherently lack the ability to reproduce the expressive nature of strikes which human players are capable of and often require manual reconfiguration in order to vary the striking location, type of beater or striking angle. The few which are able to pan across multiple instruments often lack the ability to perform expressively.

We designed a mechatronic percussion system that provides expressivity through controllable variability of the acoustic properties inherent to percussion instruments. Our system can play across the range of an entire traditional drum kit, whether it is set up in a completely horizontal formation, vertically staggered or includes other percussion instruments. When continuously operating at maximum speed, the system is capable of playing for five hours before one subsystem is at risk of failing.

Our system possesses two "wrists", each capable of gripping a variety of beaters. A single wrist can reliably perform single drum strokes at a frequency of 21 Hz, surpassing that of the world's fastest drummer. Operating both wrists results in a striking frequency of 51.9 Hz. The level of force behind each stroke and resultant acoustic quality can be controlled to produce an expressive performance.

A unique feature of this system is the use of a compliant grip, applying variable pressure to the beater held and allows for a variety of beater diameters to be incorporated.



# Contents

<b>1 Introduction</b>	<b>1</b>
1.1 Motivation	1
1.2 Project Goals	2
1.3 Thesis Structure	3
<b>2 Literature Review</b>	<b>5</b>
2.1 Background	5
2.1.1 Drumkit Configuration	5
2.1.2 Drum membrane qualities	6
2.1.3 Grip Types	8
2.1.4 Stroke types	10
2.2 Human Characteristics	12
2.3 Contemporary Drummer Evaluation	13
2.4 Robotic Drumming Background	14
2.4.1 Individual Striking Systems	16
2.4.2 Multi-instrument Panning Percussion Systems	19
2.5 Conclusions	21

---

<b>3 Motion Design</b>	<b>23</b>
3.1 Chassis Selection . . . . .	23
3.2 Design Consideration's . . . . .	24
3.3 Shoulder Requirements . . . . .	25
3.4 Shoulder Design . . . . .	28
3.5 Elbow Requirements . . . . .	34
3.6 Elbow Design . . . . .	36
3.7 Wrist Requirements . . . . .	49
3.8 Wrist Design . . . . .	50
3.9 External sensor selection . . . . .	57
3.10 Summary . . . . .	60
<b>4 Grip Design</b>	<b>63</b>
4.1 Gripper Requirements . . . . .	63
4.2 Gripper Configurations . . . . .	64
4.3 Grip Design . . . . .	66
4.3.1 Gripper Material Selection . . . . .	75
4.3.2 Silicone grip design . . . . .	77
4.4 Grip Summary . . . . .	82
<b>5 Electronics Design</b>	<b>83</b>
5.1 System Communication and Power Topology . . . . .	83
5.2 Motherboard Design . . . . .	86

---

5.2.1 Power	87
5.2.2 Communication	90
5.2.3 Microcontroller	94
5.2.4 Additional Peripherals	96
5.2.5 Status Indicators	97
5.2.6 Physical Design	98
5.3 Daughterboard Design	100
5.3.1 Power Requirements	100
5.3.2 Power Management	103
5.3.3 Daughterboard to Dynamixel Communication	105
5.3.4 Microcontroller	106
5.3.5 Peripherals	106
5.3.6 Physical Size	107
5.4 Summary	108
<b>6 Software</b>	<b>109</b>
6.1 Daughterboard Communication to Dynamixel Actuators	109
6.2 Sub-System Calibration	114
6.2.1 Shoulder	114
6.2.2 Elbow	116
6.2.3 Wrist	118
6.2.4 Gripper	119
6.3 Calibration routine	121

---

6.4 Internal feedback	121
6.4.1 Temperature and load protections	122
6.4.2 Instrument Calibration	126
6.4.3 Movement	127
6.5 System Operation	128
6.5.1 Strike method written for custom use	128
6.6 Motherboard communication	131
6.7 Summary	132
<b>7 Results</b>	<b>135</b>
7.1 Shoulder	135
7.1.1 Range of Motion	135
7.1.2 Operation of the Shoulder	137
7.1.3 Shoulder Summary	142
7.2 Elbow	143
7.2.1 Range of Motion	143
7.2.2 Operation of the Elbow	144
7.2.3 Elbow Summary	147
7.3 Wrist	147
7.3.1 Range of Motion	147
7.3.2 Sound Pressure Level	149
7.3.3 Audio Analysis	153
7.3.4 Strike Rate	155

---

7.3.5	Operation of the Wrist	159
7.3.6	Wrist Summary	161
7.4	Gripper	162
7.4.1	Range of Motion	162
7.4.2	Effect of grip variation	163
7.4.3	Operation of the Gripper	165
7.5	System Overview	165
7.5.1	Noise Characterisation	165
7.5.2	Simultaneous Operation	167
7.6	Summary	168
<b>8</b>	<b>Conclusion</b>	<b>169</b>
8.1	Summary	169
8.2	Future Work	171
8.3	Conclusions	172



# List of Figures

2.1 A standard drum kit configuration. . . . .	6
2.2 Modes of an ideal circular membrane. . . . .	7
2.3 Illustration of the four main modes of play available on a snare drum . . . . .	7
2.4 Pronated and Supinated grip . . . . .	9
2.5 The three variations of matched grip: French, German and American. . . . .	10
2.6 The standard 4 stroke positions used by human drummers. . . . .	11
2.7 Additional range of motion provided by the elbow when performing a strike	13
2.8 The rotary solenoid actuated TrimpTron (a) and the linear solenoid actuated KalTron (b) . . . . .	17
2.9 The crank system of BreakBot's brushed actuator and a wide shot of Break- Bot's complete system . . . . .	17
2.10 Haile, an intuitive percussionist robot. . . . .	18
2.11 ZMachine's mechatronic percussionist: Ashura. . . . .	19
2.12 Nudge's solenoid actuated and variable height system. . . . .	20
2.13 Compressorhead's mechatronic percussionist: Sticks. . . . .	21
3.1 Render of the PT785 chassis . . . . .	23

3.2 Comparison of a traditional drum kit (left) and a horizontally ordered drum kit (right) . . . . .	24
3.3 Labelled diagram of the computer rendered, robotic drumming arm . . . . .	25
3.4 Illustration of the three modes of backlash . . . . .	30
3.5 Positioning of shoulder gears with acceptable backlash . . . . .	30
3.6 Side view of the shoulder sub-system with no vertical separation above gears . . . . .	31
3.7 Side view of the final shoulder sub-system design . . . . .	32
3.8 Design of the shoulder sub-system . . . . .	33
3.9 Design of the shoulder bracket . . . . .	34
3.10 Range of motion capable with the human elbow . . . . .	34
3.11 Free body diagram of the system . . . . .	36
3.12 MX-64T Performance curve . . . . .	39
3.13 elbow sub-system . . . . .	40
3.14 Design of the MX-64T mounting platform . . . . .	41
3.15 Design of the Top support . . . . .	41
3.16 Result of lower infill 3D printer percentages breaking . . . . .	42
3.17 Design of the 6 mm acrylic side support . . . . .	43
3.18 Design of the flanged bearing holder . . . . .	44
3.19 Design of the elbow sub-system mounting platform . . . . .	45
3.20 Top view of the elbow sub-assembly . . . . .	46
3.21 Design of the worm wheel mount . . . . .	47
3.22 Design of the worm wheel mount with worm wheel in place . . . . .	47

---

3.23 Cutaway of the elbow sub-system at a minimum position . . . . .	48
3.24 Final design of the elbow sub-system. . . . .	48
3.25 Design of the AX-12A Bracket . . . . .	52
3.26 Wrist servomotors at maximum extension . . . . .	52
3.27 Wrist servomotor cutaway of maximum extension contacting the limit switch	53
3.28 Wrist sub-assembly angled at the neutral position . . . . .	54
3.29 Exposed thermal vents and mounting positions of the wrist sub-assembly . .	55
3.30 zTop down view of the wrist mount design . . . . .	55
3.31 Kinematic range of the elbow and wrist sub-systems . . . . .	56
3.32 Final design of the wrist sub-system . . . . .	56
3.33 Placement of the reed switch on the PT785 chassis . . . . .	57
3.34 Design of the reed switch holster . . . . .	58
3.35 Top down view of the PCB wing design . . . . .	59
3.36 Implementation of the PCB wing design . . . . .	59
3.37 Final physical design of the system . . . . .	60
3.38 Final physical design of the system . . . . .	61
4.1 Pronation and supination of the wrist . . . . .	65
4.2 Front view cutaway section of the AX-12A gripping sub-system . . . . .	66
4.3 Design of the AX-12A adaptor plate . . . . .	67
4.4 Cutaway of the AX-12A adaptor plate . . . . .	68
4.5 Cutaway of the lead screw and lead nut setup . . . . .	69
4.6 Initial design of a 3D printed raising platform . . . . .	70

4.7 Design of a 3D printed lead platform . . . . .	70
4.8 Design of the machined lead platform . . . . .	71
4.9 Unsecured lead platform rotation . . . . .	71
4.10 Lead platform at various levels of engagement . . . . .	72
4.11 Initial designs of the AX-12A mounting bracket . . . . .	73
4.12 Location of the top gripper pad on the AX-12A Mounting bracket . . . . .	74
4.13 Design of the AX-12A mounting bracket . . . . .	74
4.14 Maximum position of the lead platform in the gripper sub-system . . . . .	75
4.15 Minimum position of the lead platform in the gripper sub-system . . . . .	75
4.16 Hardness testing using a Shore Durometer . . . . .	76
4.17 Shore hardness Scale . . . . .	77
4.18 Angled view of the bottom silicone grip pad . . . . .	78
4.19 Side view of the bottom silicone grip pad . . . . .	78
4.20 Angled view of the top silicone grip pad . . . . .	79
4.21 Underside of the bottom silicone grip pad . . . . .	79
4.22 Renders of the index and thumb molds used in this project . . . . .	79
4.23 Minimum (45 mm) and Maximum (135 mm) grip settings. . . . .	80
4.24 3D printed layer structure . . . . .	81
4.25 Final design of the Gripper sub-system . . . . .	82
5.1 Control Flow Diagram for a serial electronics systems. . . . .	84
5.2 Control Flow Diagram for a parallel electronics system. . . . .	85
5.3 5 V Regulator. . . . .	88

---

5.4 Reverse Polarity Protection Circuit. . . . .	89
5.5 Opto-Isolator Circuit. . . . .	91
5.6 RS-485 Master-Slave topology. . . . .	93
5.7 RS-485 Circuit schematic. . . . .	94
5.8 Pinout of the Teensy 3.5. . . . .	96
5.9 Circuit schematic of broken out GPIO pins on the Motherboard. . . . .	97
5.10 Design of the RS-485 communication LEDs (Left) and the implementation of communication LEDs (Right) . . . . .	98
5.11 Image of Final Motherboard . . . . .	100
5.14 Half-Duplex Asynchronous communication circuitry . . . . .	105
5.15 Half-Duplex Asynchronous communication circuitry . . . . .	106
5.16 Design of status LEDs (Left) and the implementation of status LEDs to indi- cate code 11 (Right) . . . . .	107
5.17 Image of Final Daughterboard Design . . . . .	108
6.1 Packetisation of Dynamixel instructions . . . . .	110
6.2 RX-24F Area of Operation . . . . .	114
6.3 MX-64T Area of Operation . . . . .	116
6.4 Control flow diagram for the strike function. . . . .	129
7.1 Maximum and minimum range of the shoulder sub-system. . . . .	136
7.2 Maximum recorded temperature of the RX-24F Package. . . . .	137
7.3 Temperature of shoulder servomotor operating at 100% speed. . . . .	138

7.4 Temperature response of the shoulder servomotor operating at the maximum recommended torque and lower speed. . . . .	139
7.5 Evaluation of the Torque setting and its impact on the shoulder sub-system. . . . .	140
7.6 Temperature response of the shoulder servomotor operating at the torque levels above the recommended value. . . . .	141
7.7 Evaluation of the Torque and Speed settings of the shoulder sub-system. . . . .	141
7.8 External temperature of the shoulder sub-system at 30% torque limiting after 35 minutes. . . . .	142
7.9 Maximum and minimum range of the elbow sub-system. . . . .	143
7.10 Resultant load acting on the elbow sub-system servomotor shaft during upward and downward motion. . . . .	145
7.11 Internal temperature of the elbow sub-system servomotor during continuous operation. . . . .	146
7.12 Thermal profile of the elbow sub-system after operating for 60 minutes . . . . .	146
7.13 Maximum and minimum range of the wrist sub-system. . . . .	148
7.14 Sound level variance of an identical strike across three instruments. . . . .	150
7.15 Sound level variance of altering the range for a single strike of a snare drum. . . . .	151
7.16 Sound level variance of altering the velocity for a single strike of a snare drum. . . . .	152
7.17 Sound level variance of altering the range for a free falling strike of a snare drum. . . . .	153
7.18 A standard piezoelectric contact microphone. . . . .	154
7.19 Amplitude of a single strike across various percussion instruments. . . . .	155
7.20 Evaluation of the practice pad's response to a single strike. . . . .	156
7.21 Maximum controllable strike rate of a single actuator. . . . .	157

---

7.22 Maximum strike rate of a single actuator. . . . .	158
7.23 Maximum strike rate of dual actuators. . . . .	159
7.24 Temperature characteristic to operation of the wrist sub-system as maximum strike rate and maximum speed. . . . .	160
7.25 Thermal profile of the wrist sub-system after operating for 30 minutes . . . .	161
7.26 Minimum and Maximum positions of the lead platform of the gripper sub- assembly. . . . .	162
7.27 Effect of grip actuator rotation on the FSR reading. . . . .	163
7.28 Effect of grip setting on the response of the beater. . . . .	164
7.29 Sound level of all recorded systems. . . . .	166
7.30 Sound level of the overall system test playing the snare and crash cymbal. . .	168



# Chapter 1

## Introduction

### 1.1 Motivation

In recent years, the field of musical robotics has grown significantly, with many mechatronic attempts at re-creating the expressivity and quality of a professional human musician's performance [1]. This surge in musical mechatronics can be attributed to increased accessibility of technology and a decrease in price over time, allowing people with a non-technical background to create and develop robotic systems [2]. A large number of the robots developed relate to percussion systems [2].

The underlying structure of music which has been written for percussion instruments was determined in part by the physical limitations and capabilities of human drummers [3]. In the last 50 years with the advent of synthesizers and artificial note replication, composers have been able to experiment with compositions which play at speeds higher than what a human is capable of [2]. Drum machines and music production software can imitate the performance of percussion instruments through analog synthesis or pre-recorded samples. However, the characteristics of the sounds played are limited to the synthetic reproduction of sound or the instrument notes recorded live. Both of these lack the real-time qualities of a drum performance such as specific tuning of instruments, visual feedback for audiences, type of beaters, and the influence of previous strikes.

Musical robots allow composers to experiment with new compositions or instruments and hear the resultant live qualities in real time, without the need of a human player. Professional musicians are limited by the length of time that they can perform before becoming fatigued; the ability to play a composition based on previous experience; and the strike rate they can achieve [4]. It takes years of practice for musicians to be able to play the drums effectively and play high strike rates. Mechatronic systems can reduce these limitations by not requiring practice or experience to carry out complex tasks for extended periods of time. However, a professional human drummers' performance is dynamic and expressive, a quality which mechatronic attempts have so far lacked.

Percussion instruments are among the simplest in the musical field [3]. However, achieving controllable variance in the quality of the strike can be complex. While a strike of a drum can be easily achieved, there are several characteristics inherent to the strike and resultant sound [1]. These are dependant on the type of beater used, the force behind each strike, how long the stick is in contact with the instrument and the position in which the instrument is struck.

Previous approaches, discussed in more detail in Chapter 2 have been divided into those that strike across an individual instrument and those that can pan between multiple instruments. Individual striking systems generally have a lower expressivity than their panning counterparts due to many requiring manual re-positioning to strike different locations or with variable force.

Individual striking systems can achieve expressive striking of instruments through the incorporation of additional actuators. However, the requirements of a system to expressively play one instrument are similar to that of a panning system. Both panning systems and individual striking systems often require custom instrument configurations, limiting the modularity of their overall design.

The natural compliance of the human hand is a desirable quality as this impacts the reflection of the beater and resultant acoustic signal when striking a percussion instrument and should be considered in the design of an effective mechatronic percussion system.

## 1.2 Project Goals

Existing mechatronic percussion robots currently lack the expressivity and ability observed in human drummers. We aim to design a system that is not a reproduction of a musician's arm, but rather focus on extracting the qualities that determine what make a human drummer able to play a wide variety of music. The components of a 'good drummer' can be abstracted into a set of characteristics that are achievable in a non-anthropomorphically inspired style, discussed further in Chapter 2. We do not intend to replicate the fingers of the human hand, it is the innate elasticity and pliability which allows dynamic grip of a range of beaters that is desirable. The degrees of freedom and functionality of the wrist is not required to strike an instrument but the ability to vary the force applied in a controllable manner.

The ability to position the system in front of a traditional drum kit or one intended for use by a professional drummer and calibrate our system to play with no further alterations to the setup would be advantageous.

We hypothesise that modelling these extracted characteristics in a mechatronic system will result in it being capable of producing the variability of strikes and expressivity without the inherent limitations of human musicians. These include the maximum time that a drum roll can be performed, or the ability to co-ordinate the position of drum instruments dynamically without practice. The goal of this project is to design and construct a mechatronic system that is capable of playing a large range of percussion music with at least some of the expressivity that professional drummer's exhibit.

### 1.3 Thesis Structure

Chapter 1 has outlined the motivation for the design of a mechatronic system which incorporates the characteristics that allow humans to strike percussive instruments and provided hypotheses for its projected performance. Chapter 2 presents background information regarding the features of a drum kit, an evaluation of professional drummers, presents the human limitations, and provides an analysis of the existing field of mechatronic percussion. This is followed by Chapter 3, where the requirements of an ideal mechatronic percussion system are discussed and the design process surrounding the hardware development of the system is illustrated. Chapter 4 discusses the design requirements of a modular gripping system and how this is integrated into the overall system. Chapter 5 centres on the design of the electronics and the control configuration of the overall system. Chapter 6 details the implementation of software to operate the electronics and actuators selected in Chapters 3 & 4 & 5. In Chapter 7 the performance of the percussion robot is evaluated against the requirements discussed in Chapter 3 to establish the functionality of the system. The thesis concludes in Chapter 8 with a summary of the performance evaluation and outlines potential work that may be completed in the future.



## Chapter 2

# Literature Review

This chapter provides an introduction to percussion systems, the characteristics of professional drummers required to effectively play a drumkit, and a review of previous mechatronic percussion systems and their limitations. From this evaluation, the design requirements of our proposed mechatronic percussion system will be determined.

### 2.1 Background

This section introduces the underlying terminology and behaviour of instruments in a drum kit and the generalised approaches which humans use to strike these effectively.

#### 2.1.1 Drumkit Configuration

Percussion instruments can be divided into two main categories: idiophones, which produce sounds primarily through the vibration of the entire instrument, and membranophones, which produce sounds through the vibration of a stretched membrane [5]. Idiophones are often un-pitched instruments and are used to provide rhythm or accents<sup>1</sup>. An example of an idiophone is a cymbal, a thin round plate of metal which produces sound through the vibration of the plate. Membranophones can be pitched or un-pitched depending on the desired sound. The snare drum and bass drum are both un-pitched membranophones, whereas tom drums are generally tuned to fundamental notes and frequencies depending on the number of toms used and the sound required [6].

---

<sup>1</sup>an accent is an emphasis, stress, or stronger attack placed on a particular note



Figure. 2.1: A standard drum kit configuration, complete with cymbals, toms, snare and bass drum [4].

A drum kit has no defined configuration or set number of instruments. The instruments required are defined by the composition played. The drummer can freely place these components in any layout that they find most comfortable to play. Common layouts utilised in drum kit setup often place the components with the highest number of strikes required in the centre of the kit to minimise the travel time required [7]. A standard drum kit consists of one bass drum, three tom drums, three cymbals and one snare drum, seen in Figure 2.1 [7].

### 2.1.2 Drum membrane qualities

As previously discussed, tom drums can be tuned to change the fundamental frequency of a strike. When the instrument is struck, the vibration of the drum membrane occurs at resonant frequencies based on the modes present within the circular membrane [8]. Theoretically, a single strike at the centre of the drum will result in radial modes being excited, seen in (0,1), (0,2) and (0,3) of Figure 2.2. Additional diametric modes are present where the total movement of the membrane is equal to zero.

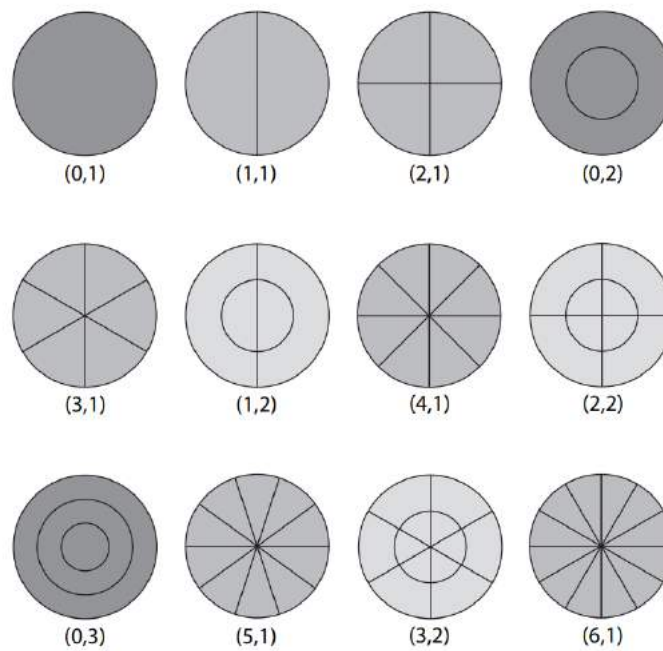


Figure. 2.2: Modes of an ideal circular membrane. Values  $(m,n)$  denote the nodal diameters  $m$  and nodal circles  $n$  [8].

The position struck on a membranophone determines which radial and diametric modes are excited, altering the resultant sound of the strike. Most membranophones have four audible radial modes of play: rim, two-thirds, off-centre and centre, shown in Figure 2.3 [8]. High tom drums have the smallest diameter of the traditional percussion instruments, 250 mm [9]. This results in a radial mode displacement of approximately 30 mm.

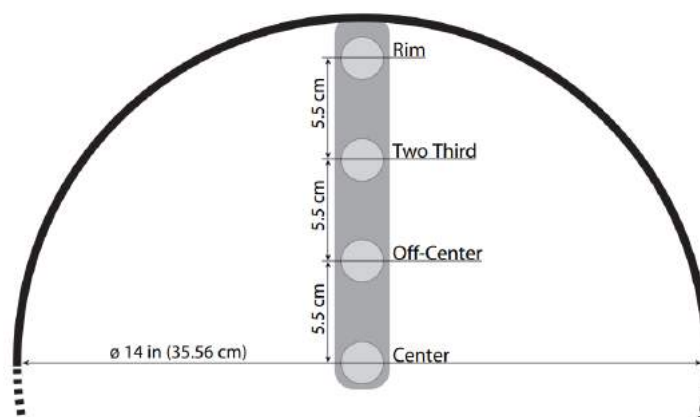


Figure. 2.3: Illustration of the four main modes of play available on a snare drum [8].

The strikes of professional drummers are reflected off the skin of the drum due to the tension of the membrane being greater than the absolute force of the human hand (applied by a beater) [8]. This decreases the response time necessary from the drummer, as the stick is naturally rebounded from the membrane by a factor of the force applied to the strike. The resultant sonic characteristics of a drum stroke provide a unique sound. Inhibiting the vibration of the drum causes the sonic response to be musically lacking and does not resemble the intended sound [10]. At any time, the drummer is able to dynamically grip the stick to increase the gripping force if the stick is about to come loose [11].

### 2.1.3 Grip Types

The style with which the beater is gripped alters the force, precision, and control over the beater as well as the resulting post-strike acoustic qualities [8]. The style of grip that a professional drummer uses is generally consistent throughout their career as they practice and develop muscle memory specific to that grip [8]. There are two predominant approaches to gripping a drum stick: traditional and matched [12]. A traditional grip style is asymmetric while the matched grip holds the beaters symmetrically. While the following sections deal with properties of human drummers, an understanding of grip styles and their implications on the resulting drum stroke proves useful in the design of a mechanical drum stick gripper.

#### Traditional Grip

The traditional grip originates from military marching drummers who carried a snare drum, with the drum riding against the hip at a tilted angle, allowing the drummer to play without impeding movement [12]. This resulted in the left hand playing at an awkward angle into the raised side of the drum, disincentivising the use of an identical grip when holding a drum stick. Traditional grip utilises both a supinated and pronated grip between the two hands, seen in Figure 2.4, to allow the drummer to comfortably hold a drum stick.

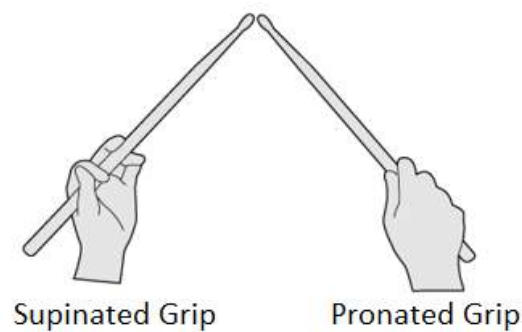


Figure. 2.4: Pronated and Supinated grip [13].

One hand uses a pronated grip, with the palm facing downward, similar to gripping a tool, while the left hand plays with the palm facing upward, as shown in Figure 2.5. Both grips result in a fulcrum between the index finger and the thumb, allowing the stick to rotate about the fulcrum after striking the drum membrane. The pronated provides strength to a strike while the supinated grip is precise.

This grip style is favourable amongst marching drummers but is less popular for seated drummers as it can result in the left and right hand play sounding differently during play as well as being more difficult to play across multiple drums due to the angle of the supinated hand.

### Matched Grip

Matched grip consists of both hands performing in a pronated fashion [8]. This is the widely accepted norm for players worldwide due to the ease of playing across a drum kit. Matched grip utilises the same muscles, resulting in a nearly identical sound being produced by both hands. There are three variations of the matched grip: French, German and American, seen in Figure 2.5. French grip consists of the thumbnails facing toward the ceiling and the palms of each hand facing one another, allowing for maximum control with the fingers. German grip has the palms faced downwards, relying on the wrists to provide power to the strike [8]. American has the palm facing at  $45^\circ$  to the drum membrane, utilising both the wrist and fingers for control and power. The choice of grip configuration for our system is further discussed in Chapter 4. Matched grip is implemented in the design of the robotic drumming systems evaluated in 2.4 due to the design for each beater being identical.

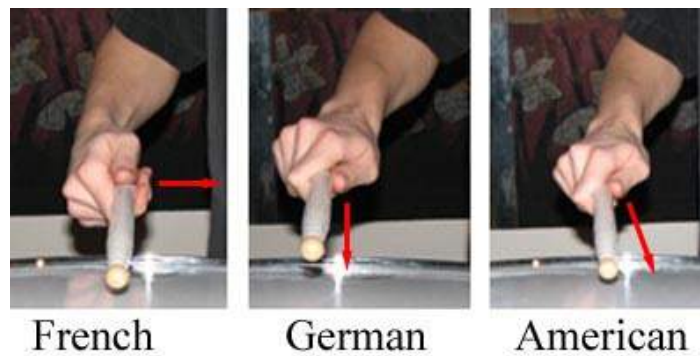


Figure. 2.5: The three variations of matched grip: French, German and American [14].

### 2.1.4 Stroke types

For a mechatronic percussion system to expressively play musical compositions it must be able to vary in the type of accents and strike power it is capable of. The majority of drum strikes use the wrist to provide power to the strike [15]. The elbow can be used to provide additional striking power but is mainly used to provide additional range to the wrists. Due to the external rim of the drum head being raised, the angle of the strike is almost always  $10^\circ$  toward the drum.

As the drum stick strikes the membrane, the membrane resists the force causing the stick to bounce back [8]. The resultant movement of the drum stick can be modelled as an under-damped system, with the stick oscillating back and forth as it strikes the membrane at lower velocities. A stronger grip on the stick reduces the rebound of the stick and damps the overall response [15]. The under-damped hold on the stick can allow for faster play speeds as the player can use the bounce to their advantage, reducing time spent physically raising the stick back to the starting position.

While striking the membrane of a drum is relatively simple, there are four styles of stroke that are primarily used by professional drummers [16]. Each of these strokes results in a different accent to the note being played. When designing a mechatronic percussion system, an understanding of these stroke types will inform the requirements of the striking system. Figure 2.6 provides a visual representation of the four predominant stroke types used by human drummers.

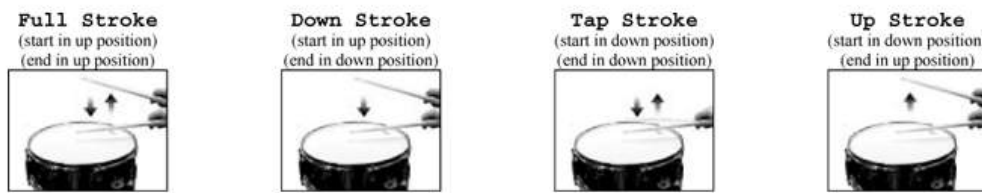


Figure. 2.6: The standard 4 stroke positions used by human drummers: Full, Down, Tap and Up [14].

### Full Stroke

The full stroke begins with the drumstick being held almost perpendicular to the drum, with the tip around 150 mm above the head of the drum. The head is struck and then the stick is returned to the starting position, creating a louder note or accent note due to the additional force gathered behind a longer strike.

### Down Stroke

The down stroke starts in the same position as the full stroke, but finishes with the stick just above the membrane of the drum. This allows the player to transition into softer strokes after an accent note.

### Tap

The tap is the most recognisable of the strokes, starting just above the drum head. After striking the head, the stick returns to the same position. This is generally used during continuous drum rolls due to the smaller range requiring less time to strike the drum.

### Up Stroke

The up stroke starts just above the head of the drum, followed by striking the surface and bringing the stick back up to a full stroke position. This is the opposite of the down stroke, allowing a soft stroke to be followed by an accented note.

## 2.2 Human Characteristics

There are several characteristics when playing percussion instruments that are a result of human limitation. These include the beat rate, length of play and compositions that can be played [4]. An evaluation of these limitations could highlight areas that can be matched or improved upon by a mechatronic percussion system.

Professional drummers' ability to play high speed striking patterns is predominantly attributed to practice [4]. Musical instruments often require complex patterns to be performed by multiple muscle groups. Repetition of these tasks increases a musician's fine motor skills and develops long-term muscle memory, allowing complex actions to be repeated without conscious effort being made by the player [4]. The maximum rate that humans can achieve voluntarily is approximately 7 Hz [4]. However, the maximum strike rate achieved by a professional drummer using single strikes was 1247 beats per minute (BPM) [4], or approximately 10 Hz per hand. The difference between these two striking rates is attributed to specifically developed, inherent muscle coordination in drummers attempting to reach a maximum strike rate and is not a controllably varied movement. The evaluation of the BPM occurs over one minute of testing and refers to the total number of strikes that a human drummer can perform in this time-frame. The strain that is placed on the human body to play at this speed prevents playing at a maximum strike rate for lengths of time much greater than one minute.

Another limitation on human drummers is the length of time for which the drums can be played. While muscle memory reduces the strain on the body to perform a drum roll, there are still limitations to the human body. The longest continuous drum roll achieved is 22 hours, playing on a snare drum [17]. However, the majority of compositions which involve percussion are between one and two hours. This is somewhat determined by a musician's ability to play for sustained periods of time without injury due to muscle fatigue. Previous attempts at this record have resulted in the drummer being hospitalised as a result of demands placed on the muscles [18].

For a mechatronic percussion system to be considered successful in its ability to recreate the majority of compositions, it should be capable of at least matching the outlined requirements and playing for sustained periods of time without risking damage to the system.

## 2.3 Contemporary Drummer Evaluation

A qualitative analysis of contemporary drummers was performed to establish the ranges of motion that are used in the elbow and wrist. Drummers from two different genres were analysed to inform the range of motion required of a mechatronic percussion system.

Professional drummers display a wide variety of drumming styles for different performances based upon the genre in which they perform. Buddy Rich, a jazz drummer known for his high speed drumming utilises his wrist heavily when drumming while Dave Grohl, a rock drummer, uses his whole arm as shown in Figure 2.7 [19][20].



Figure. 2.7: Additional range of motion provided by the elbow when performing a strike [21].

The style that a drummer plays with is dependent on the tempo that they are playing [22]. They adjust their movement between strikes proportionally to the tempo that is being played. This is done to increase the total length of time for which they can play, adapting the speed at which they move to what is required of the composition. Jazz drummers must be able to play a wide range of tempos due to the variance in the tempo of jazz compositions [22]. In contrast, in rock compositions, the drums form the backbeat to a song and have a generally consistent tempo, with only a small variance in the speed required of the drummer [23].

When performing, gestural flair is a significant factor in the way professional drummers play. Rich shows flair through speed, which is done through as little range of motion as possible, resulting in only the wrist being utilised [19]. The rest of his body is only utilised

when panning between the different instruments to allow him to reach. This movement is dynamic and varied dependant on the instrument which is played, resulting in the exact position of the beater varying with each strike [19].

Grohl expresses visual flair through the movement of his arm [20]. His elbow and shoulders are perhaps as much part of the performance as the sound of the strike itself. While they are not needed to make the same sound, live performances would be more visually dull if he did not utilise his entire arm and exaggerate the movement behind each strike. As discussed previously, the force behind the beater determines the sound level of a strike and larger ranges of motion can be used to provide more force. However, during live performances, the drums are usually amplified with loudspeakers using microphones and have their sound levels adjusted externally to a suitable sound level [24]. Therefore, the visual performance of the drummer is more important than the level of sound they are making. This results in the flair seen in Grohl's drumming performances [20].

The way in which a drummer achieves an individual strike on an instrument is of less importance than the sonic qualities of the strike itself. Therefore, if a mechatronic percussion system can achieve the same sound level and dynamic acoustic quality of striking an instrument, the range of motion used by human drummers is irrelevant. A complete discussion of musical performativity and embodiment is outside the scope of this thesis as our objective is to inform our mechatronic designer, not directly copy a human performer.

## 2.4 Robotic Drumming Background

Mechatronic percussion systems can be divided into two categories: individual striking systems and panning percussion systems. An individual striking system implements one actuated beater for each individual instrument. This results in a single position of the instrument being struck, limiting overall acoustic range. Additionally, the angle of attack that is used is limited to a single position, requiring manual re-positioning to alter the angle.

The expressivity afforded using the individual striking system is related to the number of actuators that are integrated into its operation. To provide a variable angle of attack, ability to pan the full instrument's modal range, vary the grip on the beater and strike the instrument requires a total of four actuators. Individual striking systems can achieve very

high strike rates, dependant on the actuator that is used, as it does not suffer from a travel delay to position the beater above the instrument. A number of such systems are presented and discussed below in Section [2.4.1](#).

A panning percussion system implements one or more beaters in a configuration that allows the robot to position the beater above multiple instruments. This reduces the required number of beaters and actuators as the same setup can play across multiple instruments. The total actuators required for a panning percussion system is the same for playing one instrument as it is for playing multiple, only the range of motion utilised changes.

Panning percussion systems allow for any instrument to be played as they do not require a dedicated setup tied to each instrument and remain the same regardless of the drum configuration or instruments provided. However, the performance of the system is limited to the speed with which it can pan between instruments before it can strike, potentially limiting the strike rate and ability to play polyphonically.

As discussed previously in Section [2.2](#), there are several attributes which impact the quality of sound for a drum performance. The key attributes of a mechatronic percussion system which allow for greater expressivity are as follows:

- Panning of the Drum Head: Playing across greater areas of the membrane results in a wider range of sounds
- Striking Power: Loudness of the strike should be variable to suit the performance.
- Strike Rate: The compositions that can be played are limited by the maximum controlled strike rate.
- Stick Grip: Variability of grip on the stick changes the acoustic response of the instrument, increasing expressivity and providing enhanced ability to play rolls.

These four attributes determine the acoustic quality of strikes against percussion instruments and can be used to evaluate the performance of existing mechatronic percussion systems.

### 2.4.1 Individual Striking Systems

The core of a mechatronic percussion system is the ability to strike a percussive instrument. The actuator used impacts the musical quality and rate at which the beater can strike. Previous systems have used a variety of actuators to achieve different ranges of motion and range such as solenoids, servomotors and stepper motors.

Solenoids can provide linear or rotary motion by energising a coil to provide movement of a shaft or angular rotation of an end effector [25]. As they use an energised coil, the motion of the solenoid is affected by the current and voltage supplied. This can provide high-speed strike rates. Solenoid based percussion systems form the majority of previous approaches across mechatronic implementations due to their simple operation and low acoustic noise.

Our discussion of previous systems is not an exhaustive survey of the entire field of mechatronic percussion systems but an evaluation of select designs which are exemplars in their approach to striking percussion instruments.

#### NotomotoN

A good example of an individual striking system is Ajay Kapur's KarmetiK NotomotoN [26]. The Karmetik NotomotoN is a robotic drum with 12 individual solenoid beaters spread across the top and bottom skins of a drum [26]. NotomotoN uses both linear and rotary solenoids to strike the drum, dubbed TrimpTron and KalTron, shown in Figure 2.8. Both actuator styles are mounted at the edge of the membrane and strike inwards to different modes of the drum head, providing a dynamic range of sounds. The maximum strike rate that can be achieved with the rotary actuated TrimpTron is 39.9 Hz, whilst the linearly actuated KalTron can perform at 68.9 Hz. While the individual KalTron actuator is capable of high strike rates, the overall system is limited by requiring manual re-positioning of the drum to strike different modes on the drum membrane.

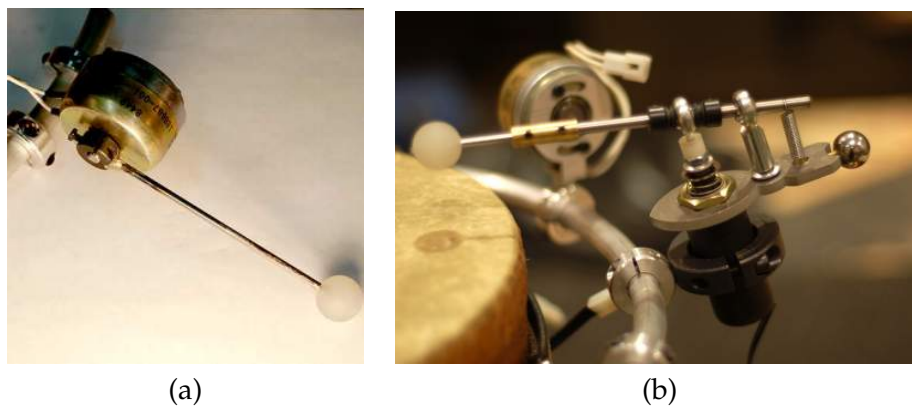


Figure. 2.8: The rotary solenoid actuated TrimpTron (a) and the linear solenoid actuated KalTron (b) [26].

### BreakBot

BreakBot is selected for evaluation as it introduces the concept of variation in striking position. The design of BreakBot is similar to that of NotomotoN except for the use of a brushed beater to play against a snare drum [27]. Four actuators are used to play the snare drum of BreakBot. Three solenoids are used to strike two drum sticks and one brushed beater against the membrane of the snare, with a DC motor controlling a crank mechanism to rotate the brush across the head of the snare drum, creating a brushed snare pattern. This crank mechanism is visible in Figure (a) of [29], with the curving of the crank creating the brushed snare's distinct sound. While a form of panning is introduced with the crank mechanism, this is limited to the shape of the crank and cannot be easily altered. Additionally, the control system of BreakBot is open-loop, lacking precision control over the placement of the crank mechanism.

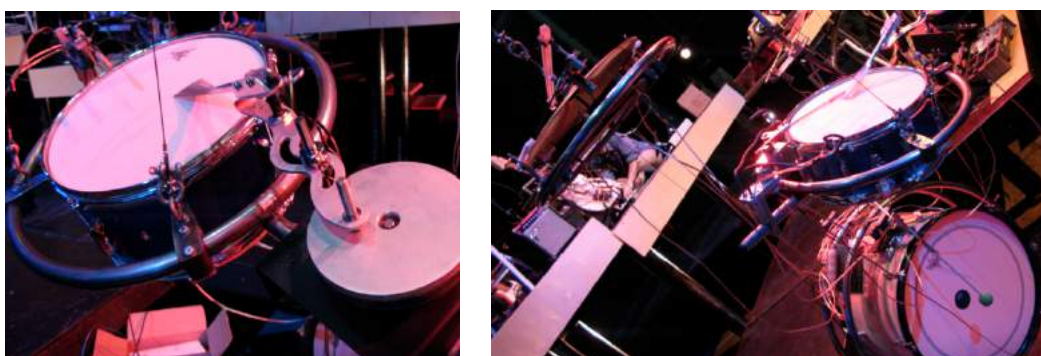


Figure. 2.9: The crank system of BreakBot's brushed actuator (left) and a wide shot of BreakBot's multi-mounted snare drum (right) [27]

## Haile

Haile, built by Gil Weinburg in 2005 [28], introduces dynamic positioning across a drum using a linear slide to alter the position of the striking beaters. This allows the left arm, driven by a linear motor, and right arm, solenoid driven, to pan across the width of a snare drum and play different modes with ease. The linear motor provides a greater range and force behind strikes whilst the solenoid is responsible for playing softer notes. The total design requires three actuators to play across a single drum. However, the separation of the beaters used on Haile results in strikes being produced in differing modes on the snare drum.



Figure. 2.10: The two varying drivers of the percussion system Haile [28].

## Z-Machines: Ashura

While Haile uses multiple actuators on a single drum, Ashura is designed to play across 22 individual instruments with 22 actuators, shown below in Figure 2.11. Each beater strikes an instrument using pneumatic linear actuators, allowing for fast strike rates. Ashura is part of a mechatronic ensemble of instruments created by the University of Tokyo in 2013 [29]. Due to the size of the system, the time taken to set up limits the dynamic capabilities of Ashura. Each actuator is physically mounted to the instrument that it strikes and requires manual re-positioning to change the angle of attack and mode of the instrument which is struck.

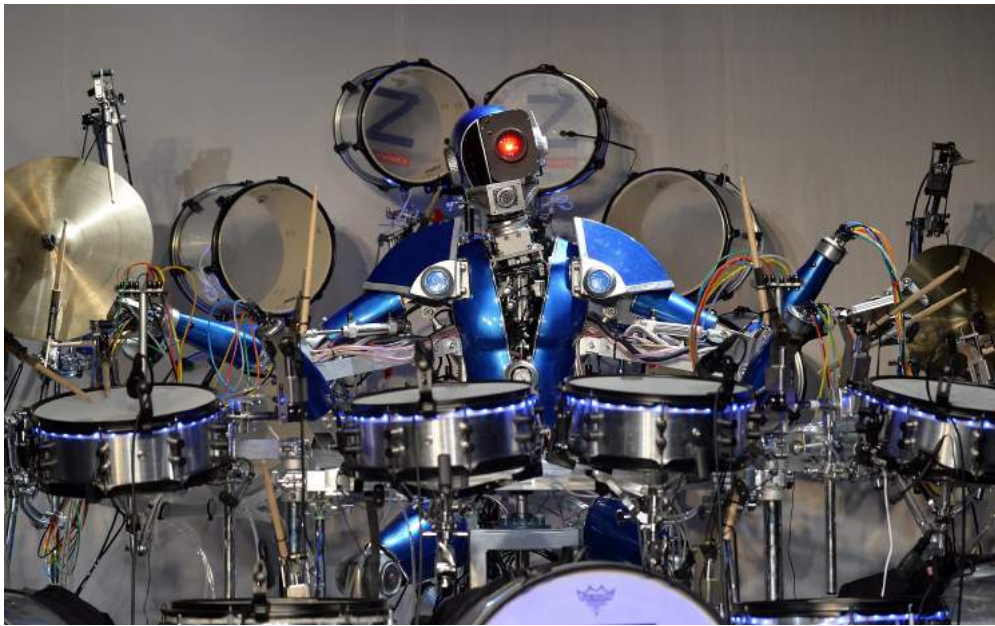


Figure. 2.11: The pneumatically actuated percussionist of the ZMachines [29].

## 2.4.2 Multi-instrument Panning Percussion Systems

A panning percussion system implements one or more beaters in a configuration that allows the robot to position the beater above multiple instruments. This reduces the total number of beaters required and depending on the number of instruments used, the overall number of actuators as the same system can play one or multiple instruments. The total number of actuators required for a panning percussion system is the same for playing one instrument as it is for playing multiple, only the range of motion utilised changes.

Panning percussion systems allow for any instrument to be played as they do not require a dedicated setup tied to each instrument and remain the same regardless of the drum configuration or instruments provided. As previously mentioned, the panning speed determines the ability to effectively play instruments.

### Nudge

The design of Nudge, created by Jim Murphy in 2014 [30], introduces the concept of panning between multiple instruments using a controllable actuator. Nudge uses a DC motor, a servomotor and one solenoid actuator to achieve dynamic range across a drum kit and

variable striking. One DC motor is used to provide  $360^\circ$  panning, whilst the other alters the angle of the beater from  $0^\circ$  to  $45^\circ$ . This setup requires the same number of actuators as are utilised in Haile, but provides an effective range far greater and allows the system to play across multiple instruments.

Nudge improves upon the design of NotomotoN and BreakBot through the incorporation of a servomotor to provide  $360^\circ$  of panning. A strike rate of 22.6 Hz is achieved through the use of a rotary solenoid to actuate the beater. The range of the solenoid from the drum can be varied with a servomotor to provide a greater sound level and varying acoustic qualities. However, the range which Nudge can play across is limited by the length of the beater used, restricting the design to custom drum kit configurations. Additionally, the beater used by Nudge was customised to suit the design and is directly mounted to the actuator using 3D printed ABS plastic, limiting the modularity of the design.

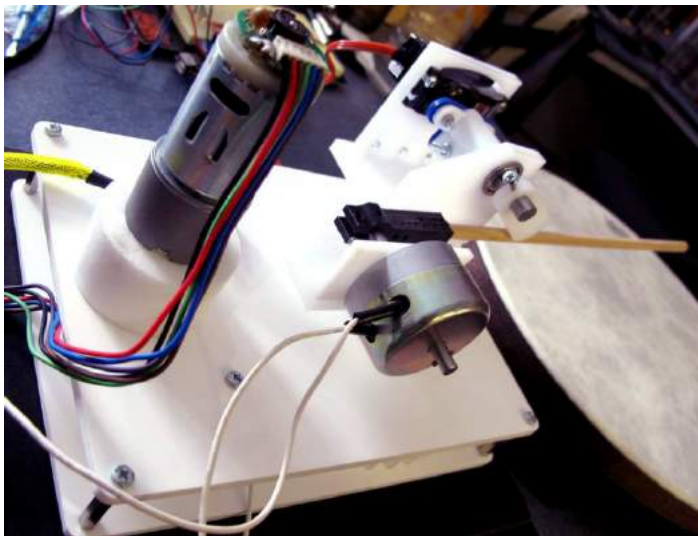


Figure. 2.12: Nudge's solenoid actuated and variable height mechatronic percussion system [30].

## Sticks

Compressorhead's mechatronic drum 'Sticks', created by Frank Barnes in 2013 [31], uses four arms to play a 10 piece drum kit and addresses the limitations of Nudge by using additional actuators to provide extra reach. This is achieved with pneumatic linear actuators, limiting the positional control of each actuator to two positions, similar to a solenoid. The

use of pneumatic actuators also limits the strike rate to 3 Hz per arm. However, the implementation of four arms and additional range allows Sticks to be placed in front of a drum kit configured for human play and, after calibration, successfully play across all the instruments included, as shown in Figure 2.13.

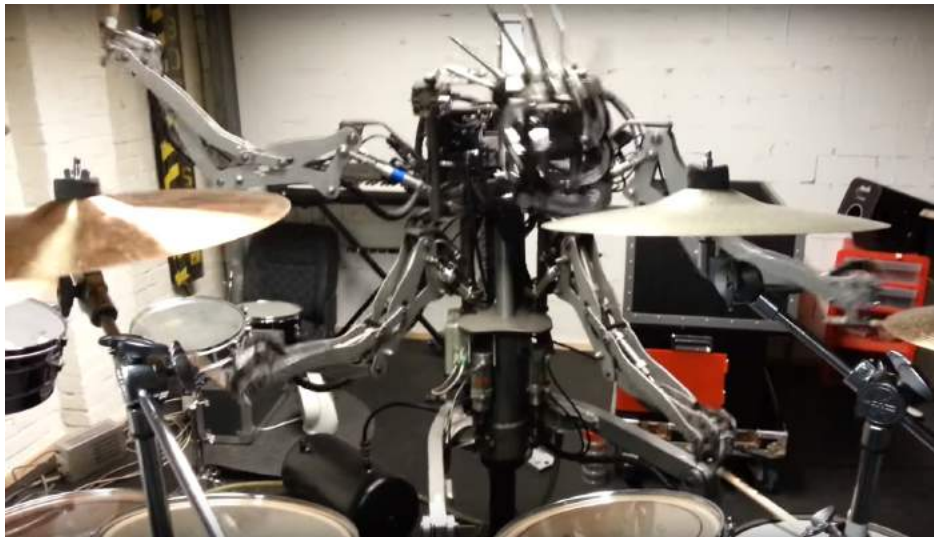


Figure. 2.13: The pneumatically actuated, panning percussionist of Compressorhead [31].

## 2.5 Conclusions

Individual striking systems use dedicated actuators to strike instruments at high speeds. However, this often comes at a cost to expressivity and modularity as well as an increased number of actuators that need to be controlled. While some of the evaluated systems use creative methods to achieve horizontal panning and alter the angle of the drumstick, they ultimately lack the modularity that is seen in panning systems. Modularity can reduce the time required to set up the system and allows for a wider range of drum configurations to be used.

Pneumatic actuators and solenoids provide fast striking systems but suffer from a lack of controllable range. For this project, solenoid actuators will be forgone in exchange for servomotors due to the ease of positioning that can be achieved with servomotors without losing significant speed.

A human drummer's ability to play the drums can be categorised into four separate biomechanical sub-systems: The elbow, capable of providing additional force to strike the drum and raising/lowering the beaters; the shoulder, responsible for panning between instruments; the wrists, used for striking the instruments; and the fingers, which vary their grip on the beater, allowing for differing levels of expressivity. These four groups constitute the functionality required to play across a drum kit and will be modelled using servomotors as the joint actuators. The design of each of these sub-groups will require similar ranges of motion as was observed in professional drummers to be capable of playing across drum kits of differing configurations.

## Chapter 3

# Motion Design

This chapter describes the design process required to achieve the realisation of a mechatronic system capable of playing across a traditional drum kit through the integration of an elbow, wrist and shoulder sub-system.

### 3.1 Chassis Selection

A chassis is required to support each of the robotic arms. The chassis must be capable of supporting the weight of the system, compact enough to allow complete rotation of the arm, and preferably be free-standing. The PT785 Panning system<sup>1</sup> is chosen as the central structure for the system due to its heavy steel frame and 25.4 mm shaft with bearing tracks built into the carriage. The shaft, seen in Figure 3.1, consists of an aluminium tube with a hollow centre, which allows for cabling to be routed through the centre of the system, reducing the risk of damage from the cables winding.



Figure. 3.1: Render of the PT785 chassis.

<sup>1</sup><https://www.servocity.com/pt785-s>

The mechatronic percussion system needs to be stable and easy to set up, and so it was decided to secure the PT785 chassis to the same tripod assemblies to which the toms and cymbals are mounted in a standard drum kit. The tripod stand greatly increases the stability of the system, whilst being familiar to potential users and having easy to adjust height and tripod leg widths.

The telescopic setup of the stand allows for a maximum extension vertically of 600 mm from the point of extension, giving the system a total possible height of 1200 mm.

The general setup of a traditional drum kit has the cymbals placed above the toms and kick. This is due to the dynamic reach that human drummers are capable of, as discussed in Chapter 2. Therefore, the system should be capable of playing both a vertically and horizontally staggered setup seen below in Figure 3.2.



Figure. 3.2: Comparison of a traditional drum kit (left) [32] and a horizontally ordered drum kit (right)

### 3.2 Design Consideration's

As stated in Chapter 1. The goal of this project is to design and construct a mechatronic system that is capable of playing a large range of percussion music without losing the expressivity in the way that single actuator systems do. Figure 3.3 illustrates the drumming arm and where in this chapter each sub-system is discussed.



Figure. 3.3: Labelled diagram of the computer rendered, robotic drumming arm

There are inherent limitations in a human drummer's ability to play the drums. These were discussed in Chapter 2, and include the length of time that a human can reliably play, reaction time and the ability to play different tempos. A mechatronic percussion system would benefit composers by being able to overcome these limitations while still achieving the speed, Beats-Per-Minute (BPM) and expressivity required of a live performance.

This will be accomplished using the Dynamixel servomotors as actuators [33], discussed further below; 3D printed parts, laser cut acrylic and machined metals to build the structure; and external sensors to provide feedback.

In Chapter 2 the human drumming technique and several robotic approximations which attempted to replicate these were discussed. The design of the robotic arm will incorporate the characteristics extracted from this analysis by using them to inform the minimum requirements of the motion based sub-systems in Sections 3.3, 3.5, 3.7. The design of the fourth sub-system, the gripper, which secures the beaters will be discussed in Chapter 4.

### 3.3 Shoulder Requirements

Human drummers utilise the shoulder for panning about the drum kit, and to raise or lower the elbow to provide additional reach which is useful for playing across the staggered instrument positions of a traditional drum kit [34]. However, the shoulder's main function is to position the elbow in an arc around the drummer.

A traditional five-piece drum kit consists of three cymbals, three toms, a snare and a kick drum [35]. The kick drum is outside of the scope of this project as they produce a tone of indefinite pitch regardless of strike location and generally requires a beater of different material and size than what is used on other percussion instruments. Additionally, the kick drum is actuated with the feet, not the human hand. By adding together the maximum diameter of all drums, listed in Table 3.1, we can establish the arc length that needs to be panned across by the shoulder. A range of 2640 mm is required to play across all the instruments. This calculation uses the strikable area of the cymbals as opposed to the maximum diameter because cymbals have different modes of play to the drums and cannot be struck at the midpoint in normal playing styles. A horizontally aligned configuration would be the widest spread that the shoulder sub-system would need to play across.

Table 3.1: Dimensions of a standard drum kit [35]

Drum	Strikable Area (mm)	Max Diameter (mm)
Snare	350	395
Low Tom	300	345
Hi Tom	250	295
Floor Tom	400	445
Hi-Hat	305.6	355.6
Crash	386.4	406.4
Ride	468	508

The tempo of a composition is the speed at which the piece is intended to be played. Chapter 2 established that for our system, tempo and BPM are the number of drum strikes per minutes. This determines the minimum speed at which the shoulder should be able to pan from the minimum location to the maximum location of the required instruments. On the scale of basic tempo markings, Presto is described as very, very fast at a BPM of 168-200 with Prestissimo described as 200 BPM and over. Compositions with a BPM over 200 are rare due to both limitations of the musicians and the frequency of notes sounding equivalent to 30 Hz. Therefore, the upper limit of Presto is selected to define the speed requirement of the shoulder. This BPM is not limited to strikes on a single drum and therefore the shoulder must be capable of panning between instruments with each individual beat.

A strike rate of 200 BPM is equivalent to one strike of an instrument every 0.33 s. This would require a panning time of less than 0.33 s between the maximum and minimum locations of the shoulder. To mitigate the panning time required, we use three arms to accomplish play across the drum kit. Therefore, as a maximum tempo requirement, an individual arm should be capable of panning the entire range of a drum kit within one second. A panning time between instruments of 0.5 s would be advantageous for operation of a single arm, allowing common tempos of 120 BPM to be played.

The accuracy with which the shoulder can position a drum strike is an essential component given the sonic variance that the positioning of the sticks can make. Figure 2.2 shows four striking positions possible on the membrane of a snare drum. A radius of 55 mm defines four locations on the snare drum based on the modal response of the drum membrane. However, the snare drum is not the smallest diameter drum in a traditional kit. The Hi-tom has the smallest drum modes diameter, with a 45 mm diameter between each mode. As the difference between modes is a gradual change over this 45 mm, a strike at the centre of the mode has a different response than at the edge of the mode.

A variance of 30 mm between strike locations for each mode was noted in Chapter 2. The equivalent sonic response within this range still resembles that of a centre strike. Therefore, a panning resolution of 10 mm will allow the arm to produce a response that is characteristic of the desired mode.

The shoulder must also be capable of operating for a sustained period of time. The average length of a contemporary song is three minutes, however, operatic performances have been known to last for four hours [36]. An experienced human drummer is typically capable of performing at a sustained, fast pace for an hour before tiring [37]. The shoulder should be capable of at least matching and preferably doubling this (i.e. operate continually for 2 hours).

The selected actuator and drive system for the shoulder should be capable of providing the torque required to move the expected load of the arm.

As previously mentioned in Section 3.1, the PT785 pan-tilt carriage offers a 25.4 mm rotating shaft. This can be used as a system mounting point and would allow the use of a geared configuration to drive the load of the arm, reducing the strain on the shoulder servomotor.

### 3.4 Shoulder Design

The Dynamixel servomotors are selected as the actuators for the system due to their wide range of characteristics that allow for high speed or high torque configurations and daisy-chained communication system [33].

The characteristics of each series of Dynamixel servomotor are a trade-off between size, speed and stall current [33]. The AX series are a discrete set of servomotors that weigh approximately 50 g, but are only capable of 1.5 Nm of torque, while the MX series servomotors have four times the stall torque but are 2.5 times the weight of the AX series, detailed below in Table 3.2 [38] [39] [40].

Table 3.2: Dynamixel Servomotor Characteristics [38] [39] [40]

Dynamixel Servomotor Characteristics			
Name:	AX-12A	RX-24F	MX-64T
Weight (g)	53.5	67	135
Resolution (°)	0.29	0.29	0.088
Communication Type	Asynchronous Serial	RS-485	Asynchronous Serial
Stall Torque (Nm)	1.5	2.6	6.0
Stall Current (A)	.900	2.4	4.1
Operating Voltage (V)	9-12	9-12	10-14.8
Addressable Range (°)	0 - 300	0 - 300	0 - 360
Running Temperature (° C)	-5 ~+ 70	-5 ~+ 80	-5 ~+ 80
No-load Speed (RPM)	59	126	63

The RX series, 24F servomotor is capable of a no-load speed of 126 RPM, with a resolution of 0.29°. Using equation 3.1 below, the arc length can be calculated if the radius of the arm,  $r$ , and the centre angle,  $\Theta$  is known. Given that the projected length of the arm is 530 mm, and the addressable range is 300°, the arc length is calculated to be 2775 mm. Therefore, the RX-24F is capable of spanning the total range required of the shoulder.

$$Arc = 2\pi r \frac{\Theta}{360} \quad (3.1)$$

Assuming the RX-24F has a similar loss of performance with an increased load as the MX-64T, discussed in Section 3.6, the projected speed when operating at the maximum allowable torque threshold of 25% is 94 RPM. The projected time taken to travel the required

$300^\circ$  between the maximum and minimum operating points at this speed is approximately 0.53 s. This is above the required threshold stated in Section 3.3 of 0.5 s. However, this is a conservative calculation based on the worst case scenario torque level.

The 25.4 mm shaft of the PT785 carriage is used as the rotational centre of the arm. This requires a method of driving the shaft with the RX-24F at the required speed. This can be accomplished by mounting a gear to the shaft of the PT785 and another gear to the servo horn of the RX-24F. Using gears reduces the torque acting on the RX-24F when stationary, as the load of the arm is decoupled and does not act directly on the shaft of the servomotor. The RX-24F is capable of driving the 25.4 mm shaft using a 1:1 gear ratio as there is no requirement for additional speed or torque through gearing. The gear with the lowest number of teeth which fits the 25.4 mm shaft has 76 teeth and is made from aluminium.

The shoulder is to play across the 2640 mm drum kit with a 10 mm resolution, this equates to 264 individual positions, or  $1.56^\circ$  of accuracy. The RX-24F is capable of  $0.29^\circ$  resolution, satisfying this requirement.

The resultant arc length for a change in angle of  $0.29^\circ$  can be calculated using equation 3.1. Given the 530 mm length of the arm from the fulcrum of the elbow to the tip of the beater, a change in centre angle of  $0.29^\circ$  causes a resultant 2.68 mm change in arc length.

The working depth of a gear helps determine the centre distance between the two gears [41]. If the working depth is too small, the teeth will bind and result in overheating and additional wear due to increased pressure between the gear faces, visible in the left side of Figure 3.4. If the depth between teeth is too large (right image of 3.4), backlash between the gears will result in lower efficiency performance and lead to increased backlash angle, the difference between a clockwise and anti-clockwise movement driving the gear. Larger backlash angles result in lower accuracy of positioning [41]. It is worth noting that a small amount of backlash can be advantageous to allow for lubricant to be applied between the gears [41]. The backlash angle can be adjusted using the rail slots of the PT785.

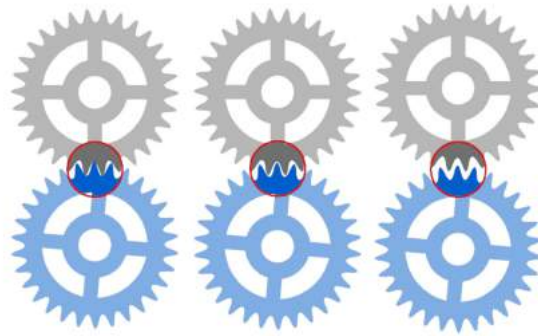


Figure. 3.4: Illustration of too little backlash (left), a good amount of backlash (middle), and too much backlash (right) [42].

Initially, 3D models of the gears were used to determine the centre distance of the shoulder drive gear and the shaft gear. While this modelling results in the recommended working depth between the teeth of the gears, the real world implementation of this resulted in the working depth being too small. The asymmetrical load of the system caused misalignment of the gear faces with the driven gear angling slightly downward. Any change in angle results in a decrease of working depth. With a smaller working depth, the strain on the shoulder servomotor driving the gears is increased past the recommended torque limit for sustained operation.

Revisions to the centre distance were made to further separate the gears, with a resulting increase in the backlash angle when driving the lower load side of the driven gear. The level of backlash allowed is visible in Figure 3.5, with enough working depth between the gears to allow for lubrication.



Figure. 3.5: Positioning of shoulder gears with acceptable backlash

In the first iteration of the design, the asymmetric loading of the driven gear caused the gear face to be angled downward by approximately 0.3 mm. This increased the total strain of the system by shifting the central angle of the load on the shaft downwards, resulting in the elbow platform contacting the shoulder gears. However, this only occurs due to the shoulder gears being perfectly level with one another. The vertical separation cannot be decreased between these gears as the drive gear is mounted to a 25.4 mm clamp beneath it which secures it to the shaft, as shown in Figure 3.6. Therefore, another solution is required to negate the impact of an angled gear face.

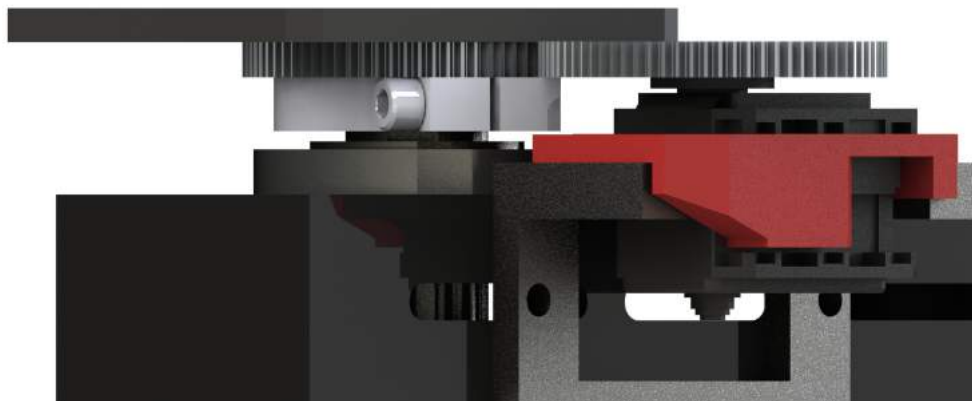


Figure. 3.6: Side view of the shoulder sub-system with no vertical separation above gears.

The 76T gear chosen for the driving/driven gear is 31.6 mm in radius and by using the arc length equation 3.1, the central angle can be found, using the 0.3 mm displacement as the arc length. This displacement results in a central angle deviation  $0.54^\circ$ . As the arc length increases with the radius, this deviation will have the greatest impact at the furthest point from the centre of the driven gear. The furthest separation is the edge of the RX-24F drive gear, at a radius of 94.79 mm. Equation 3.1 can be used to calculate the total vertical deviation, where the radius is 94.79 mm and the central angle is  $0.54^\circ$ . The asymmetrical loading of the shaft results in a 0.89 mm vertical displacement. Due to the level mating of the shoulder gear system, this deviation results in undesirable strain placed upon the shaft of the shoulder servomotor when the platform mounted to the shaft gear passes across the face of the RX-24F gear. This strain severely limits the playtime of the shoulder sub-system due to the increased current and resultant heating of the servomotor.

The shoulder sub-system is revised to incorporate a separating disc which sits between the mounting platform and the driven gear. Acrylic is selected for the separator disc material as it requires only 2D features to be implemented and could thus be laser cut with a 2 degree of freedom laser cutter. A thickness of 6 mm is selected for the acrylic disc, as this will provide a separation of 2.8 mm between the face of the drive gear and the mounting platform, once the depth of the drive gear is accounted for, seen in Figure 3.7. The use of the separator disc allows the vertical positioning of the drive gear to be above that of the driven gear, reducing the risk of contact with the clamp beneath.

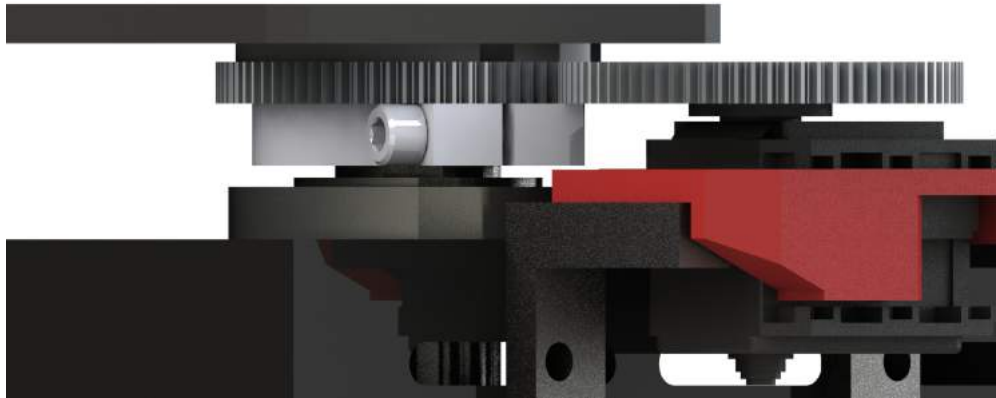


Figure. 3.7: Side view of the final shoulder sub-system design.

The features of this disc include the mounting holes required to secure the driven gear to a 25.4 mm clamp used to secure the system to the shaft, a hollow centre for cables to run through and a cutout for the elbow limit switch (discussed further in Section 3.6). The placement of the limit switch is noted in Figure 3.8 and routes the sensors' cables through the middle of the shaft.

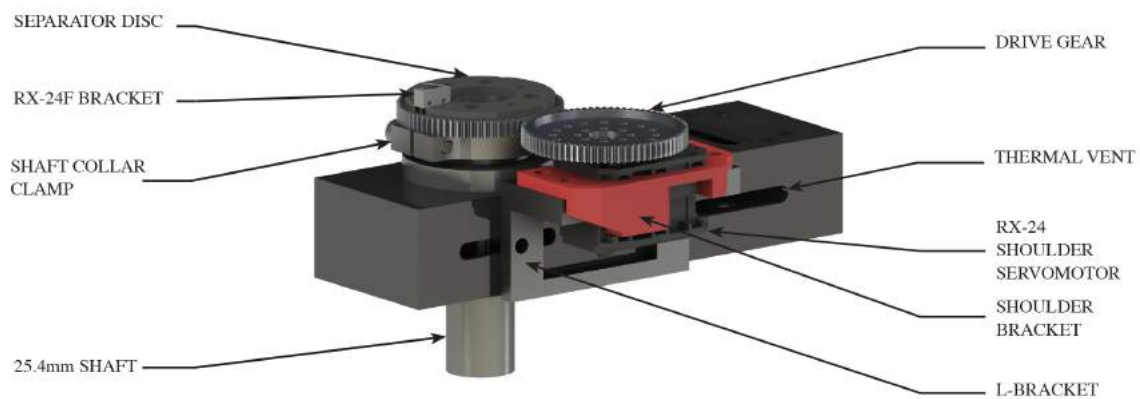


Figure. 3.8: Design of the shoulder sub-system.

To secure the RX-24F shoulder servomotor, a bracket is required that can mount from the PT785 to the RX-24F. The mounting bracket designed mounts to an L-bracket which interfaces with the inbuilt slots of the P785, seen in Figure 3.8. The thermal vents of the RX-24F are intentionally left un-concealed to increase passive airflow to the motor, reducing potential thermal buildup.

Due to the torque that the shoulder servomotor will be transmitting to the drive gear, the RX-24F must be securely fixed to the PT785 carriage. This is because any torsion or movement of the servomotor under high torque would result in a mismatch of gear faces and increase the torque further. The design of the shoulder bracket secures the RX-24F in place by using the mounting holes inherent to the servomotor to fasten to nuts embedded in the bracket. Eight of the potential sixteen mounting holes are used and their locations are denoted in Figure 3.9.

The shoulder bracket mounts to the previously mentioned L-bracket of the PT785 chassis using four M3 threaded mounting holes. The thickness of the 3D printed material where the shoulder bracket secures against the L-bracket is 5 mm, which is the recommended thickness of 3D printed ABS [43].

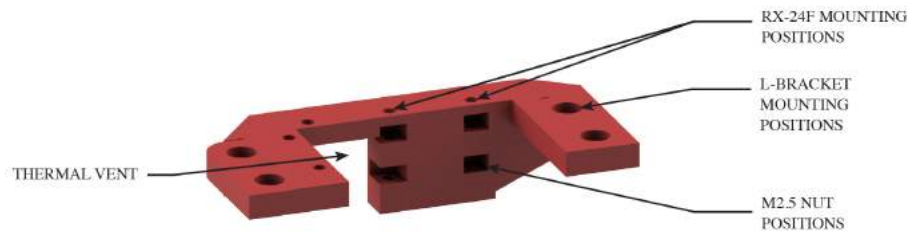


Figure. 3.9: Design of the shoulder bracket

The direction of the 3D printed layers is perpendicular to the torsion that is expected upon the servomotor. This increases the strength of the component as any twisting motion will not cause any splits in the layers of the 3D print.

### 3.5 Elbow Requirements

The maximum angle which a human forearm is capable of achieving is approximately  $140^\circ$  due to the limitations of the triceps and biceps, seen in Figure 3.10 [44]. However, the range which is used by professional drummers is closer to  $45^\circ$  [19]. This is due to the shoulder joint moving the position of the elbow to suit striking the instruments. Additionally, human arms are not detached from the rest of the body and the body requires a large area with which to comfortably operate. This reduces the angle required by the elbow as the arms are naturally separated over a larger area.

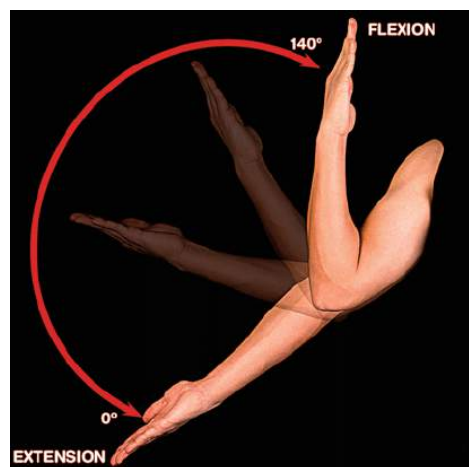


Figure. 3.10: Range of motion capable with the human elbow [44].

For a horizontally placed drum kit, the angle required of the elbow is much lower as the wrist is capable of lifting the beaters away from contacting the instruments. Instead of  $45^\circ$ , the minimum angle necessary to raise the beater above the exterior lip of a drum would be  $5^\circ$ , using equation [3.1](#) with an arm length of 530 mm and a lip of 10 mm. However, to increase the performance of the overall system and allow it to play across arbitrarily configured drum kits, the minimum angle is decided as  $45^\circ$ .

When the elbow is used to provide additional force behind strikes, the time taken to pan between the maximum and minimum position is approximately 0.5 s. As the elbow is not providing striking force, the response time of the system is not as critical to overall performance. The shoulder sub-system provides panning between instruments in a horizontal drum kit setup. However, future implementation may see use of the arm in a vertically staggered capacity. A compromise must be made between the travel time of the elbow and the design of the elbow sub-system. A travel time of approximately one second is decided as the requirement of the elbow sub-system between the maximum and minimum position.

The shoulder and the elbow determine the positioning of the beaters and the range which the wrist actuators can strike. The shoulder sub-system is capable of a resolution of 2.68 mm. The elbow sub-system should provide a resolution that is at least equivalent to the shoulder in order to position the wrist actuators in the widest number of configurations. This will allow the elbow to adjust the beaters between positions on the drum that the shoulder system is incapable of moving to. Therefore, the resolution of the elbow is set at the minimum of 2.68 mm to accurately control the positioning of the beaters.

The elbow can be used to provide additional striking power to accompany the wrist. However, as discussed in [Chapter 2](#) in the evaluation of human drummers, when the elbow is utilised for striking purposes the wrist is generally locked. This results in the elbow acting as a pseudo-wrist, reducing strain on the wrist. As the majority of live drummers in popular music contexts have microphones amplifying the sound of the strike, the elbow is not used for additional power.

The actuator used to raise and lower the elbow should be capable of supporting the combined weight of the grip sub-systems and wrist sub-system at the required distance from the pivot point. Additionally, the actuator must be capable of playing for a period of two hours.

### 3.6 Elbow Design

The Dynamixel servomotors offer a range of varying hardware characteristics and have been previously selected for use as the actuators of the sub-systems. Table 3.2 shows the hardware characteristics of the Dynamixel servomotors. The MX-64T has the highest stall torque at 6.0 Nm and so it is selected as the actuator for the elbow. The recommended operating load for the Dynamixel servomotors if intended for a long duration of use is approximately 25% of the total load the servo is capable of [40]. This lowers the level of torque acting on the shaft of the MX-64T to 1.5 Nm. Loads greater than 25% will cause overheating and eventual motor burnout when operating for long periods of time.

A free body diagram is used to visualise the forces applied and their distance from the fulcrum, and the centre of gravity of the arm is shown in Figure 3.11. The centre of gravity is the point from which the weight of the system is considered to act [45]. This can be used to find the total torque which is placed upon the fulcrum. This is the minimum value of torque which must be supplied by the MX-64T to support the static load of the arm.

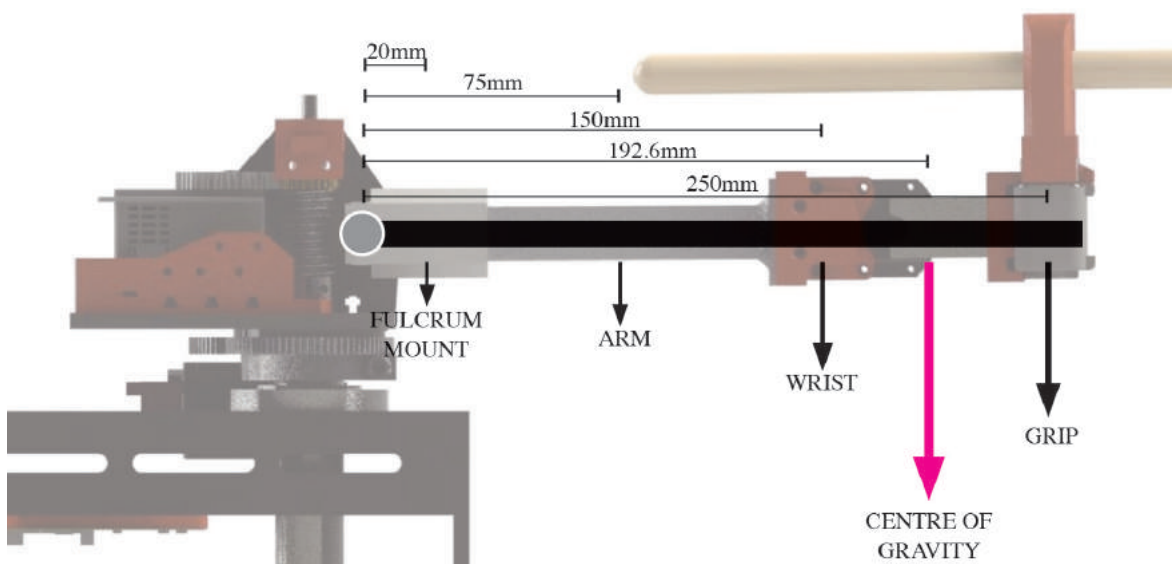


Figure. 3.11: Free body diagram of the system.

The centre of gravity of the system is calculated by summing the individual torques acting upon the elbow and dividing them by the total mass of the system, shown in Equation 3.2.

$$CG = \frac{\tau_{Grip} * \tau_{Wrist} * \tau_{Arm} * \tau_{Gear}}{M_{Grip} + M_{Wrist} + M_{Arm} + M_{Gear}} \quad (3.2)$$

To calculate the torque, the weight of the individual components and their distance from the fulcrum is required. These values are listed in Table 3.3.

Table 3.3: Weights of individual components acting on the elbow

<b>Grip Sub-assembly:</b>		<b>Wrist Sub-assembly:</b>	
Component	Weight (g)	Component	Weight (g)
AX-12A adaptor plate	4	RX-24F	71
Raising platform	11	Wrist Bracket	59.38
C-bracket	15	Total:	200.38
Drum Stick	55		
Silicone Pads	4	<b>Arm Components:</b>	
AX-12A bracket	26.98	Aluminium arm	50
Total:	350	Worm gear bracket	32.69

Using the weights of the individual components, shown in Table 3.3 and the distances listed in Figure 3.11 the individual moments of torque can be calculated using Equation 3.3

$$\tau_{total} = \tau_{grip} + \tau_{wrist} + \tau_{arm} \quad (3.3)$$

$$\tau_{grip} = F_{grip} * D_{grip}, \quad \tau_{wrist} = F_{wrist} * D_{wrist}, \quad \tau_{arm} = F_{arm} * D_{arm}$$

$$\tau_{grip} = F_{grip} * D_{grip} = (0.350 * g) * 0.250 = 0.86 \text{ Nm}$$

$$\tau_{wrist} = F_{wrist} * D_{wrist} = (0.200 * g) * 0.150 = 0.29 \text{ Nm}$$

$$\tau_{arm} = F_{arm} * D_{arm} = (0.050 * g) * 0.075 = 0.04 \text{ Nm}$$

$$\tau_{total} = 0.975 + 0.32 + 0.04 = 1.20 \text{ Nm}$$

where  $\tau$  refers to the torque,  $F$  is the force,  $g$  is the gravitational constant of earth and  $D$  is the distance from the fulcrum. The total torque applied to the fulcrum of the elbow calculated from equation 3.3 is approximately 1.2 Nm using conservative estimates of the sub-system weights.

The MX-64T is capable of a maximum output torque of 6.0 Nm; the intended load is approximately 20% of the maximum load which can be sustained by the servomotor. This is a static load approximation of torque and the force required to shift this load within one second would be far greater than this. Therefore, directly driving the elbow of the system with the MX-64T would result in overloading the shaft and potentially damaging the servomotor. An alternative solution is required that can support both static and moving loads of the shaft in approximately one second.

A common solution to de-loading the motor output shaft is to use a worm drive arrangement [46]. Worm drives reduce the rotational speed and increase the output torque by a factor of the gear ratio. A worm drive consists of two elements: a worm screw and a worm wheel. The exact configuration of these two gears is configurable based upon the exact system requirements. With a single start worm screw, each  $360^\circ$  rotation of the worm screw results in the worm gear advancing by a single tooth [46]. A dual start worm screw doubles the number of teeth per rotation. The angle panned by the arm using a single or dual start can be calculated using equation 3.4 [45], where  $N_{\text{teeth}}$  is the number of teeth to the worm wheel and  $N_{\text{start}}$  is the number of starts to the worm screw. With a single start worm screw and a 20 tooth worm wheel the central angle pans a total of  $18^\circ$ . This angle results in 2.5 rotations being necessary to satisfy the  $45^\circ$  range of motion required.

$$\text{Centre Angle} = \frac{360^\circ}{N_{\text{teeth}} * N_{\text{start}}} \quad (3.4)$$

The speed of the MX-64T is limited by the torque placed upon the shaft of the servomotor. The no-load speed of 63 RPM is achieved when the shaft torque is below 0.15 Nm. As previously stated, the recommended torque for sustained operation is 1.5 Nm. Figure 3.12 shows that operating at this torque results in an output speed of approximately 46 RPM. This equates to 1.3 s per complete rotation of the MX-64T and would take 3.26 s to complete the range required of the elbow. A single start worm screw and 1:1 gear ratio does not meet the requirements. Conventional suppliers of worm screws do not typically offer worm

screws and gears with starts higher than four without being custom machined. Having both a worm screw and worm wheel custom manufactured increases the lead time to source the component significantly. A dual start worm screw is selected as it doubles the central angle which can be achieved and is the highest conventional start worm drive readily available.

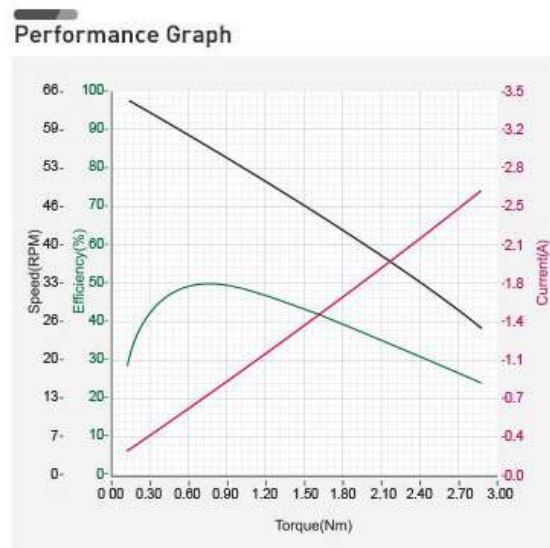


Figure. 3.12: MX-64T Performance curve [40].

Using a dual start worm screw results in a  $36^\circ$  change per complete rotation. As the resolution of the MX-64T is  $0.088^\circ$ , the controllable change in arc length is  $6.79 \times 10^{-6}$  degrees. This is several orders of magnitude below the minimum requirement, therefore, halving the accuracy by using a dual-start is insignificant. Assuming the same operating torque and a speed of 46 RPM, a complete rotation of the required range would take half that of the single start, 1.63 s. This is still higher than the outlined requirement of one second. As the number of starts cannot easily be increased further, the gear ratio of the MX-64T must be increased. A gear ratio of 2:1 would halve the travel time from 1.63 s to 0.82 s, with the maximum required travel time.

A 2:1 gear ratio from the MX-64T to the worm screw shaft, shown in Figure 3.13, has the added benefit of disconnecting the torque acting upon the worm screw shaft from the shaft of the MX-64T, further reducing the strain on the servomotor. A 48 tooth aluminium gear is chosen for the MX-64T as the features of the gear match those of the MX-64T adaptor plate

making it easier to secure. Accordingly, a 24T gear is selected for the worm screw shaft. A bore diameter of 6 mm is selected as this is a commonly used diameter and has a wide range of components which are readily available to source.

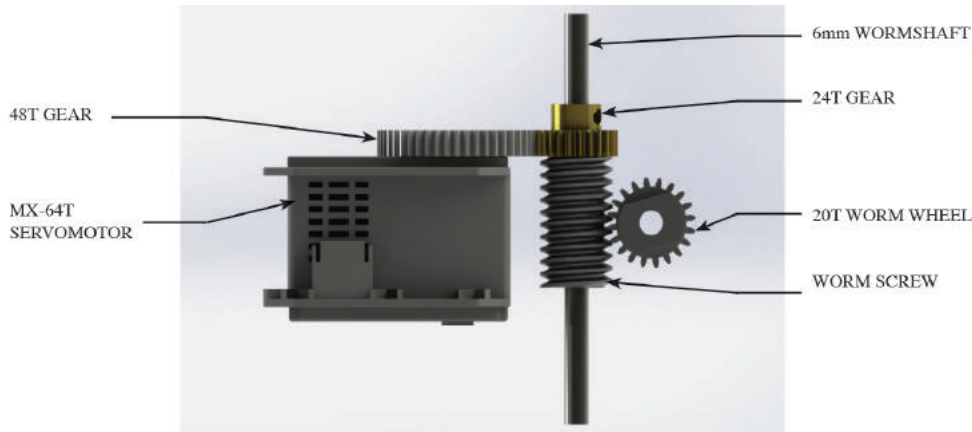


Figure 3.13: Gear setup of the elbow sub-system.

A 100% efficient system would result in  $75.6^\circ$  of movement per second or 660 mm arc length. However, this assumes zero losses in the friction of the shafts and gears and a significant torque reduction on the shaft of the servomotor. A realistic approximation of the range capable in under a second would be a 48 RPM operating speed, accomplishing  $57.6^\circ$  of rotation per second or 502 mm arc length. This exceeds the requirements listed in section [3.5](#).

The MX-64T must be held in place while actuating the worm drive as the torque is only applied to the worm drive if the servomotor is secured. To prevent movement of the MX-64T, a 3D printed component is designed that both press fits the features of the base of the MX-64T but also screws through the eight mounting holes. This component feeds the vertical worm screw shaft through it to prevent torsion from moving the shaft. A shaft clamp is incorporated into the base of the 6 mm shaft to prevent vertical movement. A section is cut away from the MX-64 platform to press this circular clamp into and can be seen in Figure [3.14](#). Additionally, the thermal vents of the MX-64T package are similar to those of the RX-24F, located on the non-shaft side of the package. As with the shoulder design in Section [3.4](#), the elbow sub-system leaves these vents exposed for passive heat dissipation.

The design of the 2:1 worm drive disconnects the torque from the shaft of the MX-64T,

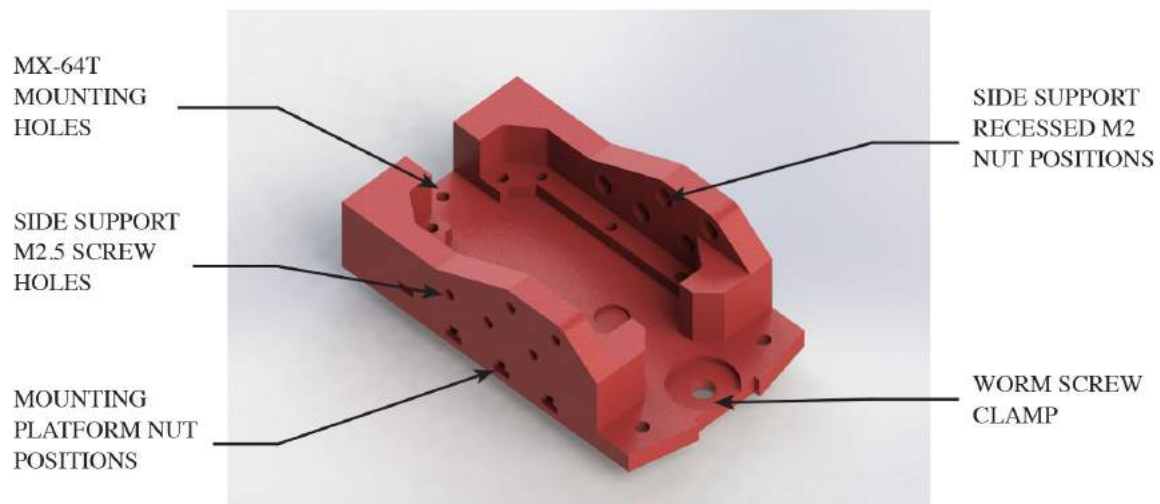


Figure. 3.14: Design of the MX-64T mounting platform.

instead the worm screw shaft and worm wheel shaft support the torque. These shafts must be held securely to prevent dislodging or misalignment of gears. Vertical movement of the worm screw can be prevented by securing either side of it within the design of the system. Movement upward is limited by a top support component that is designed to integrate with the side supports using two M3 screw holes and a press fit block on each side. The recessed fit of M3 screws is shown in Figure [3.15](#).

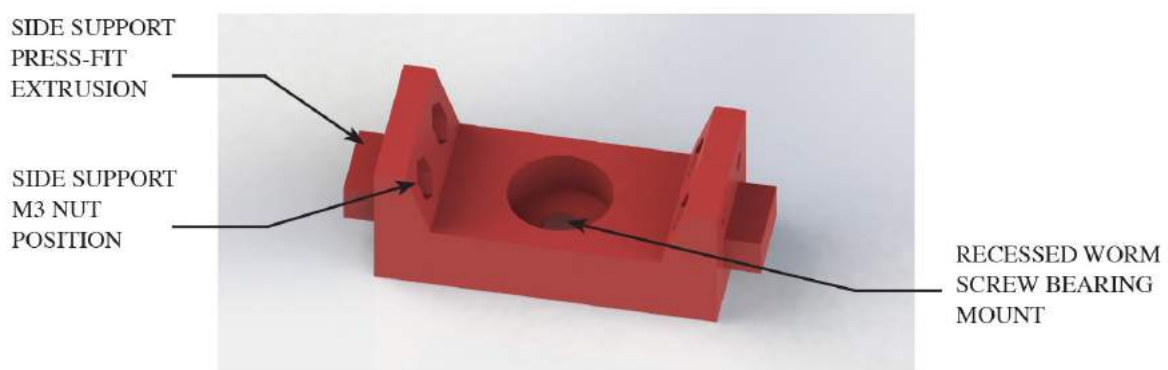


Figure. 3.15: Design of the Top support.

To allow for free rotation of the 6 mm vertical shaft, a bearing is recessed into the top support. Initially, a flanged bearing was used as any motion upward would press the flanged bearing further into the top support. However, the flanged bearings which were readily

available at a 6 mm bore diameter had inner diameters which were less than that of the 24T worm gear. This results in the 24T gear rubbing against the outer diameter of the flanged bearing, increasing the total torque required to rotate the shaft as the gear is pressed against a stationary component. The additional strain on the MX-64T resulted in an equivalent load on the shaft of 70% to actuate the worm gear.

A greater outer diameter is used in the second revision to decrease the total strain on the worm gear. The orientation of the top support when 3D printed is such that it allows the individual layers to flex with any vertical motion as opposed to breaking due to forces greater than the tension between layers. However, initial prints which used infill percentages of 40% resulted in larger amounts of backlash in the worm gear setup due to excessive flex in the 3D printed material. After completing range of motion tests with the elbow, the increase in flex caused by this backlash cracked the 3D printed top support on the same layer as the recessed bearing. The face of the bearing was thrusting against this layer with enough force to eventually overcome the force binding the 3D printed layers together and sheared the component, shown in Figure [3.16](#).

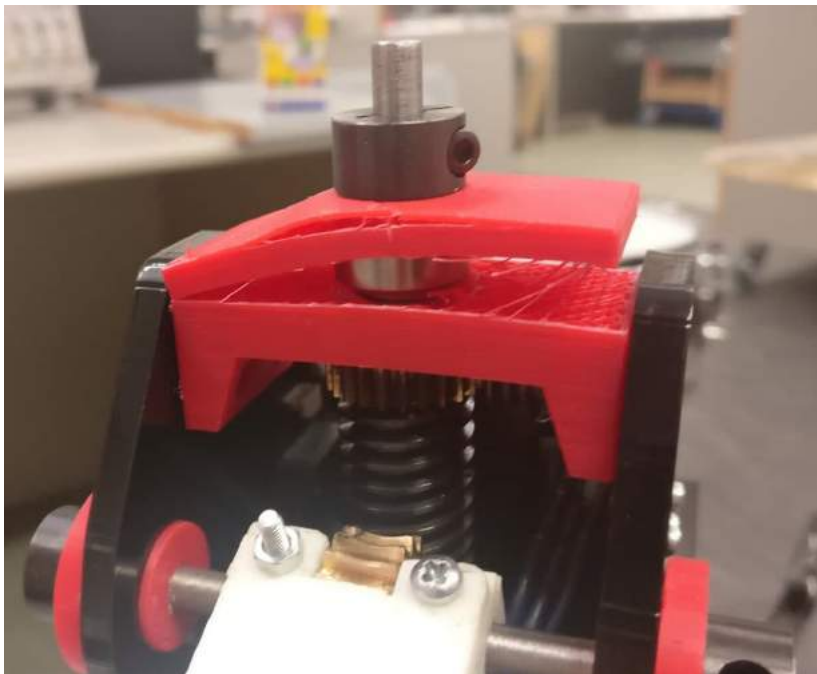


Figure. 3.16: Result of lower infill 3D printer percentages breaking.

To prevent movement of the worm gear, side supports are mounted either side of the gear. These supports mount to the top support as previously mentioned. They also mount to the MX-64 platform through a series of five holes across two different heights, with a thickness of 6 mm into recessed M3 nuts labelled in Figure 3.15. A third separate area of support is found by mounting the side supports to the base platform which the shoulder gear connects, depicted in Figure 3.17.

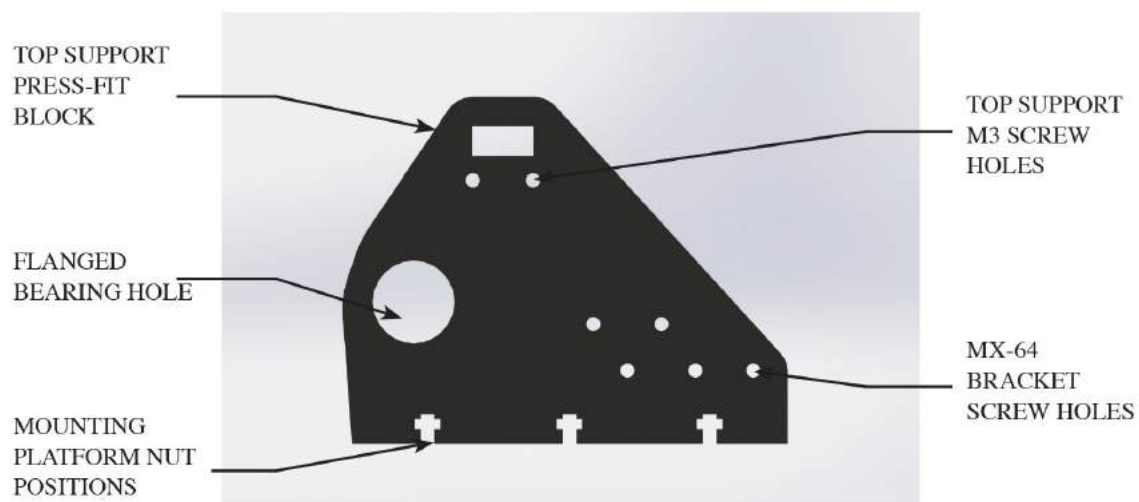


Figure. 3.17: Design of the 6 mm acrylic side support.

To prevent torsion on the horizontal worm gear shaft, flanged bearings can be mounted to the side supports. By facing the flanges outwards, any horizontal motion which could dislodge one bearing will cause the opposing flange to press against the side support, preventing motion. However, the flange diameters of the bearings with a 6 mm bore diameter were only 2 mm greater than the outer diameter of the flange. Placing the lip of the flange directly against the acrylic side support places all the tension into the 2 mm flange, potentially cracking the acrylic due to the small area of contact. A holster can be used to recess the flanged bearing into with a wider outer flange which increases the surface area contacting the side support. This increase in surface area is seen in Figure 3.18 with the initial contact area of the flange and the final contact area labelled.

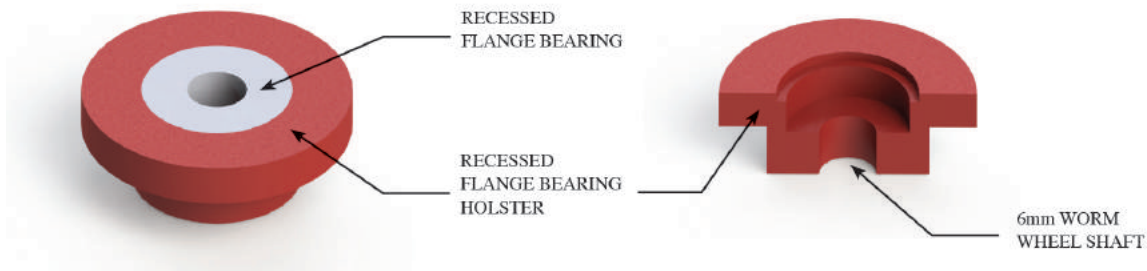


Figure 3.18: Design of flanged bearing holder.

The mounting platform that connects the shoulder gear to the side supports and MX-64 platform is larger than what the 3D printers available for this project can produce. Instead, 6 mm laser cut acrylic is used. As will be discussed further in Section 4.3, 3D printing with larger bases results in additional flex and warping due to a non-uniform temperature across the ABS. The maximum bed dimensions of the printers available are 100 mm  $\times$  100 mm. If the mounting platform were 3D printed with the available printers, the vertical deviation at the edges of the print would be approximately 3 mm. Acrylic maintains the same level of flex, which is very low, across larger sizes due to the composition of the plastic. The thickness of readily available acrylic sheets varies in step size between 0.5 mm and 6 mm, shown in Table 3.4 [47]. As the step size increases, so too does the weight per square metre of acrylic. 6 mm thickness is selected due to its high tensile and compressive strength, whilst still having a relatively low weight per square metre [48].

Table 3.4: Acrylic thickness and weight

Acrylic Thickness (mm)	Weight per square metre (kg)
1.5	1.78
2	2.29
2.5	2.84
3	3.38
4.5	5.22
6	6.95
9	10.42
12	14.05
18	21.10
24	28.11

Additionally, the mounting platform must accommodate the routing of the motors and sensor cables through the rotating shaft. Complex features and patterns can be easily cut into the acrylic with a laser cutter. To allow this, a section is cutout through the centre that is the width and length of the Dynamixel terminal cables. The locations and designations of the mounting holes for the various parts with which the mounting platform interacts are highlighted in Figure 3.19

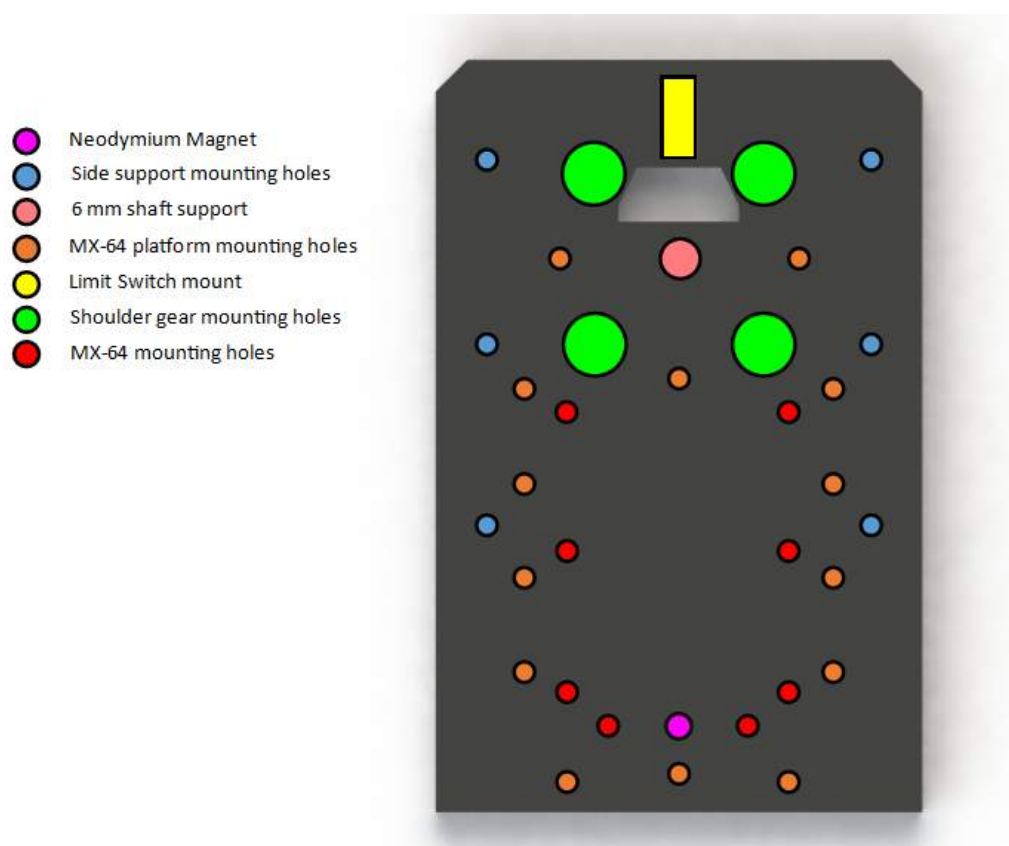


Figure. 3.19: Design of the elbow sub-system mounting platform.

The placement of the mounting platform relevant to the components which it secures is visible in Figure 3.20. The top view of the elbow sub-assembly shows the implementation of the flanged bearing holster and how the two being placed in an outward orientation prevents the worm wheel shaft from moving in either direction.

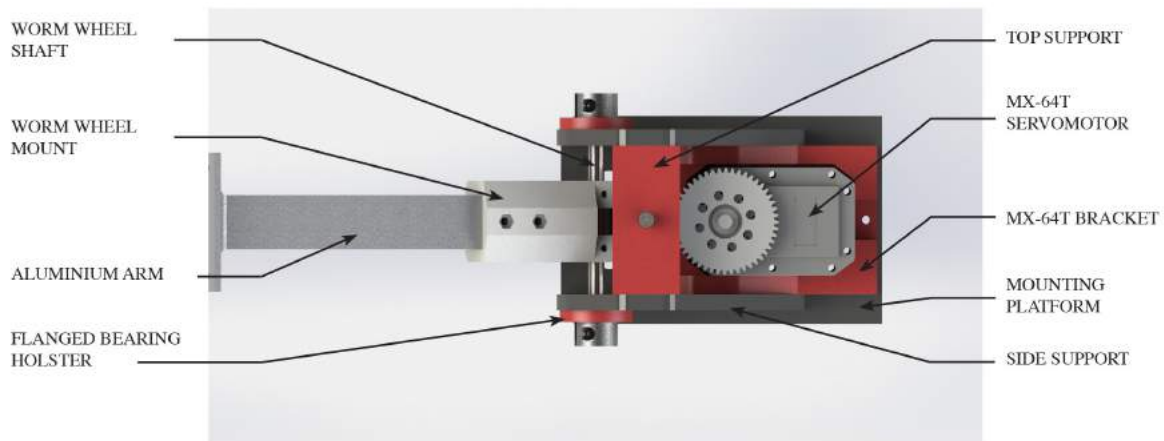


Figure. 3.20: Top view of the elbow sub-assembly platform.

The worm gear requires a way to connect to the aluminium extrusion that will also support the torque of the wrist and gripper sub-systems. This must securely mount the worm gear in place, as well as prevent movement of the aluminium extrusion.

A press fit is designed to suit the width and height of the aluminium extrusion, with a depth of 40 mm. This allows for two drill locations and an M3 screw to be secured by a recessed nut. The location of both recessed nuts and M3 thread locations are visible in Figure [3.21](#).

While a limit switch is discussed later as the means of detecting the minimum position to which the arm can be lowered, the upper limit is defined as the point at which the arm can no longer be raised. This is caused by the edges of the mount that is used to secure the worm wheel interacting with the worm screw past an angle of  $75^\circ$ . This angle is above the outlined requirement of Section [3.5](#) and was calculated the 3D model of the system and testing is required to determine the exact angle.

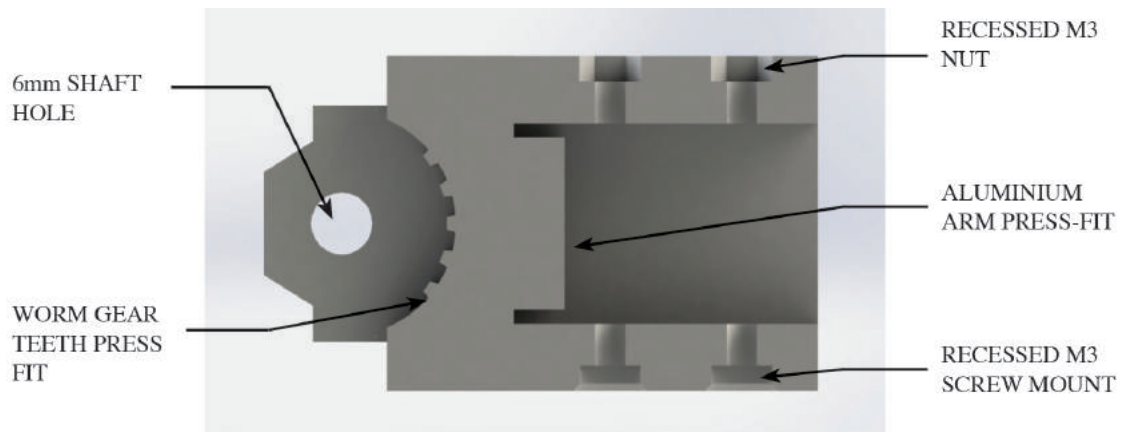


Figure. 3.21: Design of the worm wheel mount.

The feature depth and pattern of the teeth are modelled and embossed into the 3D printed part to bind against the teeth, increasing the contact area and is shown in Figure 3.21. To secure the worm gear, the boss face is flattened down on either side to press fit into a matching feature of the 3D printed part, and an M3 40 mm screw is tapped through the worm gear and 6 mm shaft. The flattened edge of the boss face can be seen in Figure 3.22. On the opposite side of the boss, an additional 40 mm screw is mounted through the 6 mm shaft, preventing the worm gear, 3D printed interface and shaft from rotating independently.



Figure. 3.22: Design of the worm wheel mount with worm wheel in place.

The MX-64T has internal sensor feedback that can be polled in software. This includes the encoder position of the motor, temperature and load. However, if the worm gear and worm wheel become dislodged and the angle of the arm changes whilst the system is powered down, this can impact the reliability of positioning the servomotor. By incorporating a limit switch into the base of the mounting platform, the elbow can calibrate itself to the minimum position [49]. As the range which the servomotor is limited to cannot change, the maximum position can be calculated from this value. This scenario is visualised by the render of Figure 3.23, with the worm gear interface applying pressure to the limit switch.

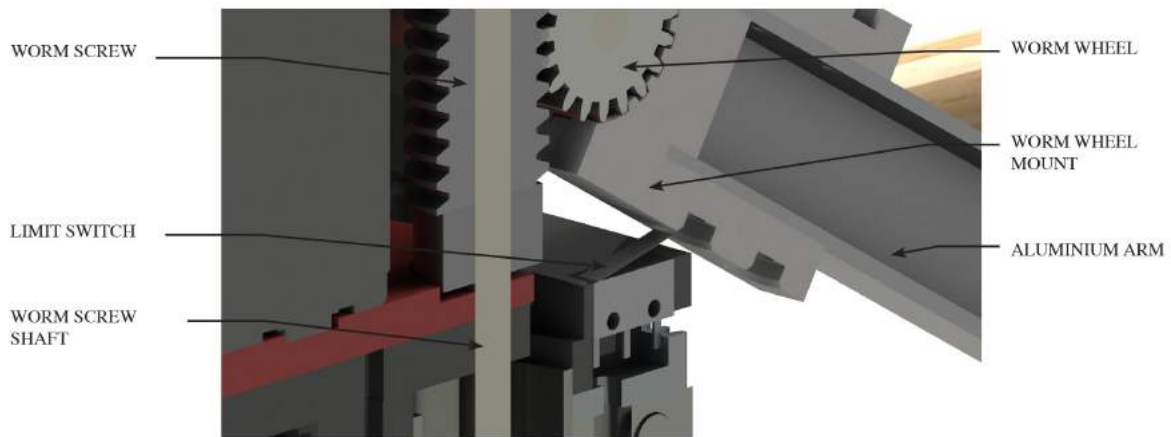


Figure 3.23: Cutaway of the elbow sub-system at a minimum position

In summary, the design of the elbow fulfills the requirements outlined at the start of Section 3.5 by being able to support the wrist and gripper sub-systems at the end of the aluminium extrusion and theoretically possessing the speed and resolution required. The MX-64T servomotor is geared up to provide more torque by using a worm drive. To increase the strength of the MX-64T's supporting structure, each component is interconnected to relieve the stress placed across each joint. This allows the MX-64T to be securely held in place while moving the worm drive with high torque, preventing dislodgement and potential damage. The final design of the elbow sub-system is displayed in Figure 3.24



Figure 3.24: Final design of the elbow sub-system

### 3.7 Wrist Requirements

While the world record sustained drum roll is 22 hours, this is an unreasonable feature to design the wrist sub-system to be able to achieve. Instead, the wrist actuator should be capable of supporting the torque of the gripping system and beater. The resultant steady-state temperature for different modes of wrist operation, evaluated further in Section 7.3.5, must be lower than the temperature threshold of the servomotor.

As discussed in Chapter 2, striking the elastic membrane of a drum results in initial deformation of the membrane and then rejection of the tip of the stick due to deflection. The resultant under-damped motion of the stick results in additional strikes against the membrane, decreasing force with each strike. The resultant bounce of the stick can increase the total BPM which is achievable by the wrist sub-system if the actuators can be fine-tuned.

The goal of the wrist is not necessarily to outperform a human drummer, but rather to be capable of at least playing the same compositions that humans do in a manner that is audibly similar. The wrist sub-system must be able to meet the play speeds discussed in Chapter 2, where the highest limit of single strike drum roll humans have achieved was defined as 1247 BPM.

The wrist should be capable of a range of  $45^\circ$  to allow for different combinations of elbow angle and wrist angle. This would accommodate play across a staggered drum kit as the elbow is designed to have a  $45^\circ$  range of motion. The combined range of motion of the elbow and wrist would allow multiple approaches to striking a single location. Additionally, the range which the wrists are capable of influences the loudness of strikes that can be generated.

The loudness of percussion instruments is determined by the impact force of the beater. The typical loudness of a drum kit is typically between 70 and 105 decibels (dB) depending on the type of performance [50]. Loudness is a subjective perception of sound pressure level by human ears [50]. Therefore, when referring to the loudness of strikes using dB within this thesis, it is the sound pressure level that is being described.

For live performances at concerts, the peak sound of a drum kit from 1 metre away can reach peaks of 120 dB [51]. While drum strikes are capable of creating sound levels this high, repeated or extended exposure at levels of 80 dB and higher can cause hearing loss.

The recommended maximum exposure time to noises above 80 dB is 8 hours per day and exposure to noises of 105 to 110 dB can result in permanent hearing loss within two to five minutes [51]. It would be advantageous for the wrist sub-system to strike the drum louder than 80 dB, but any louder than 100 dB can risk permanent hearing loss over considerably short periods of time.

Precision control of the human hands lets human drummers make minute adjustments to the placement of the beaters range before striking an instrument. Drums are designed to echo the strike through a resonant space, amplifying the sound naturally. This allows small strokes to have an audible response and therefore decrease the range required to travel by a drummer, further increasing possible play speed by reducing the time spent in motion. The wrist actuators must be capable of controlling the movement of the beater to a resolution of at least 2 mm to accurately position them across the modes of the drum. This is to maximise the control of the beaters and allow for a greater strike rate by travelling less distance.

The separation of the beaters must be small enough that the tips remain within the same mode of play on the membrane of the smallest instrument. This was previously discussed at the start of Section 3.3 and was calculated to be approximately 55 mm.

### 3.8 Wrist Design

The actuator that is selected for the wrist will determine the base speed and torque characteristics of the wrist sub-system and influence the overall design of the wrist. As the weight of the actuators selected directly impacts the loading of the elbow, the actuator must have a good torque-to-weight ratio. The torque required of each wrist actuator can be calculated using equation 3.5,

$$\tau_{wrist} = \tau_{grip} = F_{grip} * D_{grip} = (0.175 * g) * .100 = 0.17Nm \quad (3.5)$$

where  $\tau_{wrist}$  is the total torque acting on the wrist, and  $\tau_{grip}$  is the torque of a single grip sub-assembly, discussed further below in Chapter 4. The total torque applied to the fulcrum of the wrist calculated from equation 3.5 is approximately 0.17 Nm of torque, assuming that each gripper and stick has a combined weight of 175 g. The RX-24F has a stall torque of 2.6 Nm and a package weight is 67 g. This is a mid-ground servomotor of the available

Dynamixel actuators in torque and weight. The torque applied by each grip sub-system is 7% of the total torque that can be applied to the servomotor. This calculation is for a static load approximation of torque and the force required to shift it will be greater. However, as the static force is 18% less than the recommended torque for sustained operation, it is predicted that the RX-24F is suitable to be directly driven.

Two actuators are chosen for the wrist sub-system since this will double the strike rate which can be achieved. This allows the wrist to strike in an alternating fashion or, as discussed in Chapter 4, play across multiple instruments.

To determine whether the RX-24F is fast enough to meet the required BPM, the arc length and resolution must be calculated for the given stick distance from the servo horn. As the beater is being directly driven, the calculation is shown in equation 3.1. The resolution of the RX-24F is  $0.29^\circ$ , and given a distance of 295 mm from the fulcrum, the minimum arc length is 1.49 mm. This is more than the required resolution outlined at the start of Section 3.7.

The RX-24F is capable of a no-load speed of 126 RPM. This speed is unrealistic due to the loading of the shaft due to the weight of the servomotor. Assuming a depreciation in performance of 25% at the sustained torque threshold of 0.65 Nm, comparable to that of the MX-64T, the speed is approximately 94 RPM. This is equivalent to a complete rotation in 0.64 s, or one degree every 17.8 ms. Assuming a minimum distance of 5 mm is required to lift the stick sufficiently away from the membrane of the drum, this is equivalent to a strike rate of 50 Hz, or 3000 BPM. This satisfies the outlined requirements of Section 3.7.

A method of connecting the wrist servomotor to the AX-12A servomotor, selected below in Section 4.3, is required that allows for a direct-driven setup. To couple the RX-24F wrist servomotor and the AX-12A of the gripper, a servo horn C-bracket is used. This bracket mounts to the servomotor's horn on one side and a free spinning bearing to the underside shaft of the RX-24F. This shifts the force away from acting solely on the top of the servomotor's shaft, instead relying on the entire shaft. The bracket itself consists of various mounting positions that can be integrated with different bolt and screw sizes.

While the C-bracket mounts to the RX-24F, an interface is still required that connects it to the AX-12A. This interface is designed to mount to both the inbuilt screw holes of the AX-12A package and the previously mentioned C-bracket mounts. The AX-12A facing side of this bracket can be seen in Figure 4.13, and its implementation in Figure 3.25.



Figure. 3.25: Design of the AX-12A Bracket

The RX-24Fs have a controllable range of  $300^\circ$  and a resolution of  $0.29^\circ$ . However, with the gripper sub-system and beater being mounted, this will reduce the range dependant on the depth of the wrist actuator mount. The thickness of the wrist bracket will determine the maximum range achievable, as the beaters will collide with the wrist assembly potentially causing damage. A thickness of 10 mm allows the wrist servomotors to press-fit into place and results in a maximum achievable angle either side of the neutral point of  $105^\circ$ . To prevent the servomotors from extending past this angle, range blockers have been incorporated alongside the mounting of the RX-24F. These cause the aluminium C-bracket to make contact with the wrist bracket, as opposed to dislodging the beater. The minimum and maximum positions which the C-bracket will extend to are seen in Figure [3.27](#)

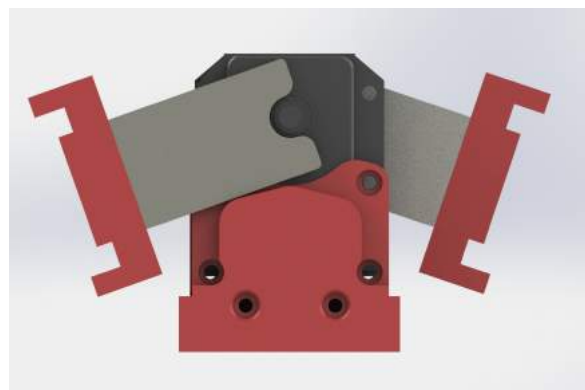


Figure. 3.26: Wrist servomotors at maximum extension

This limits potential damage to the gripper and instead increases the load on the servomotor shaft. This is an acceptable trade-off between causing damage to the gripper subsystem (which cannot easily be quantified) and increasing load on the RX-24F, whose present load can be polled for in software. The range of motion projected for the wrist servomotors is approximately  $210^\circ$ , above the outlined requirement at the start of Section 3.7.

Although the RX-24F's have internal feedback which can be polled for in software, external feedback should be incorporated to increase reliability. There are many sensors which could be used that provide sensing of the complete range of motion. However, the expected use case where external feedback is required would be a loss of the current position value of the RX-24F. The range which the servomotor can travel does not change. Therefore, a limit switch can be used to detect the upper limit of the servomotor's movement. The limit switches' incorporation is shown in Figure 3.27. Given that the range of the servomotor cannot change, the lower limit can then be calculated. As previously mentioned, range blockers are incorporated into either side of the servomotors to prevent potentially damaging movement. The limit switches are made to fit in such a way that when activated they are flush to one of the range blockers at maximum rotation.

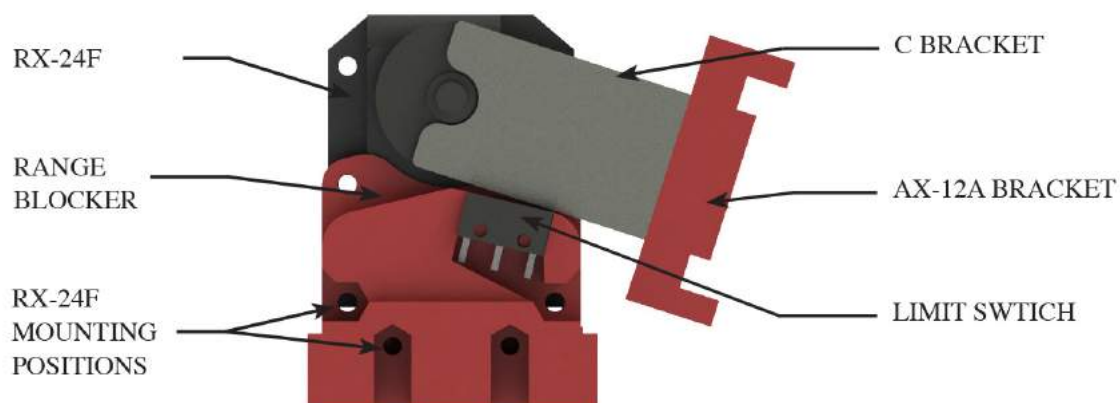


Figure. 3.27: Wrist servomotor cutaway of maximum extension contacting the limit switch

Human percussionists separate the beaters by a custom range depending on the piece that is being played, the location of instruments, player preference and the beater itself. The majority of documentation discussed in Chapter 2 highlights that the choice of stick distance

is up to personal preference. The base separation between the tips of the beaters was selected as 90 mm when parallel and is seen in Figure 3.28. While this is greater than the requirement listed at the start of Section 3.7, this is to allow separation between the wrist servomotors and gripper sub-systems. To achieve a closer placement of drum tips, the silicone moulds that determine the playing angle of the drum sticks could be altered to face inwards, discussed below in Section 4.3.

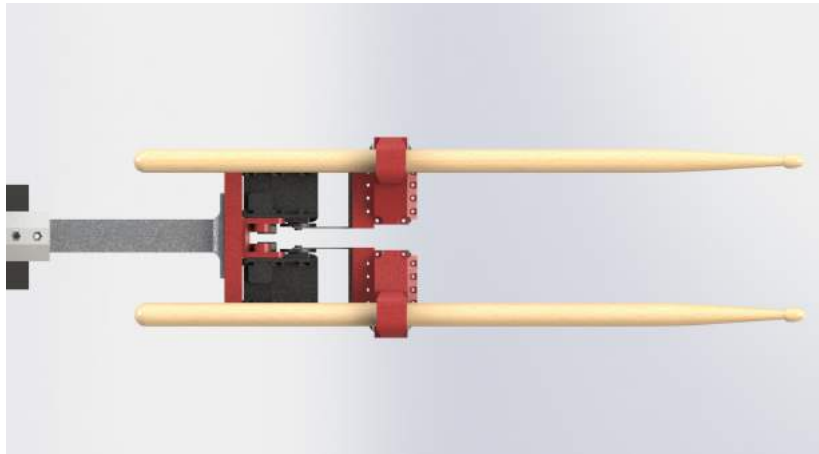


Figure 3.28: Wrist sub-assembly angled at the neutral position

The wrist sub-assembly mounts to the aluminium arm using mounting holes that are determined by the hole pattern of the aluminium arm. These holes are placed underneath the RX-24F servomotors and utilise the thick base of the wrist bracket to secure to the aluminium arm. The exact positions of the mounting holes are denoted in Figure 3.30.

The first round of design did not include thermal relief for the wrist servomotors. This severely inhibits the heat dissipation of the servomotors when operating at high speeds and does not allow the external detection of temperature. The thermal vent of the RX-24F is located in the back of the package in a 12 mm  $\times$  12 mm vent pattern [39]. To provide thermal relief, a 13 mm  $\times$  13 mm vent is included in the wrist sub-assembly, visible in Figure 3.29. By opening the back of the wrist design in this manner, the heat generated by the servomotor can be externally monitored using thermal imaging as well as providing airflow for heat dissipation. Temperature control is a major factor given that the wrists are where almost all of the power that strikes the drum comes from. As the wrist sub-system is directly driving the gripper sub-systems, temperature management and measurement is crucial.

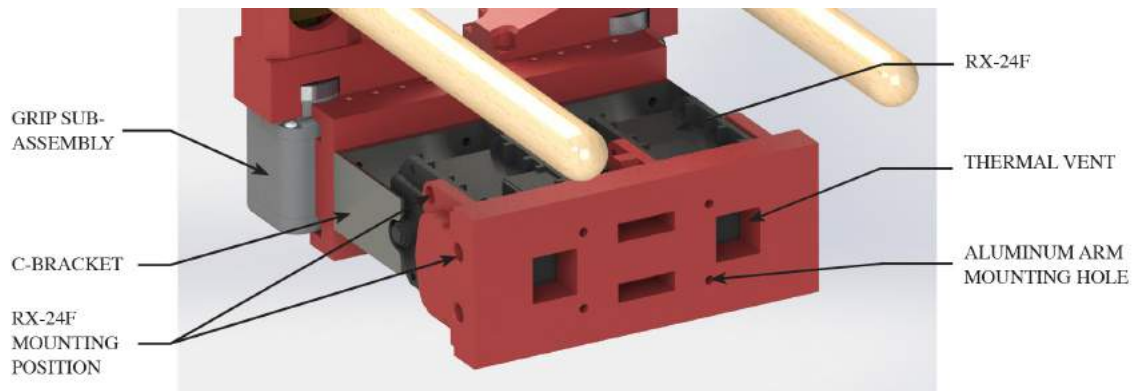


Figure. 3.29: Exposed thermal vents and mounting positions of the wrist sub-assembly

Torque is proportional to distance; as such, the furthest point from the fulcrum of the servomotor will experience the greatest force if the servomotor attempts to drive high loads. The initial design of the wrist assembly relied on using the mounting positions included on the RX-24F package to hold the servo in place. Over time the high torque which the servomotors are capable of resulted in the 3D printed mounting brackets wearing down and breaking. To reduce the impact of the torque on the servomotor, a press fit is used in the base of the assembly, where the farthest point to the RX-24F's fulcrum is located. The contours of the wrist mount design follow that of the RX-24F and are visible in the base of the design shown in Figure 3.30. The base of the assembly has an increased thickness of 3D print to provide more structural support.

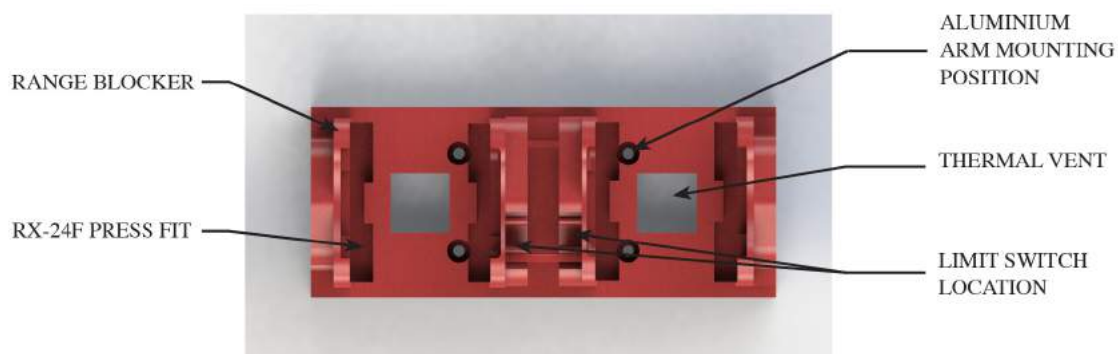


Figure. 3.30: Top down view of the wrist mount design

The wrist sub-assembly is connected to the worm gear via the aluminium extrusion discussed at the start of Section 3.5. To mount the aluminium extrusion securely, screw holes are included in the base of the wrist design which matches the pattern on the aluminium extrusion. Figure 3.31 shows the effective range of both the elbow and wrist sub-systems.

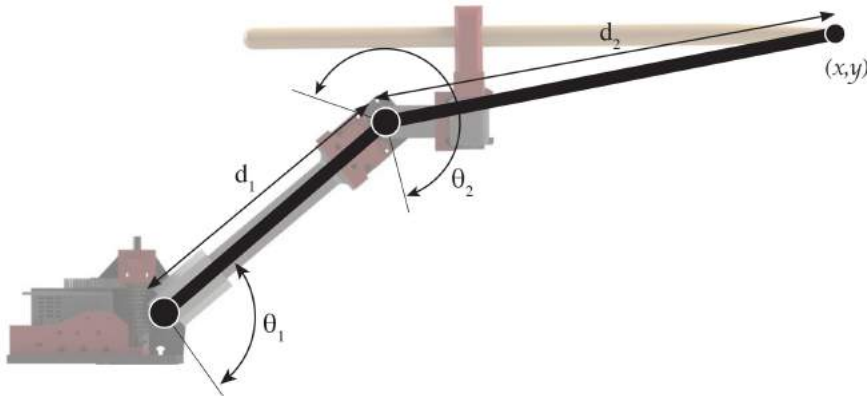


Figure 3.31: Kinematic range of the elbow and wrist sub-systems

The design of the wrist sub-assembly is capable of moving two gripper sub-assemblies at a range greater than the requirements outlined at the start of Section 3.7 and incorporates external sensors for positional feedback. The wrist sub-assembly includes vents for heat dissipation and range blockers to prevent potential damage to the system as shown in Figure 3.32.

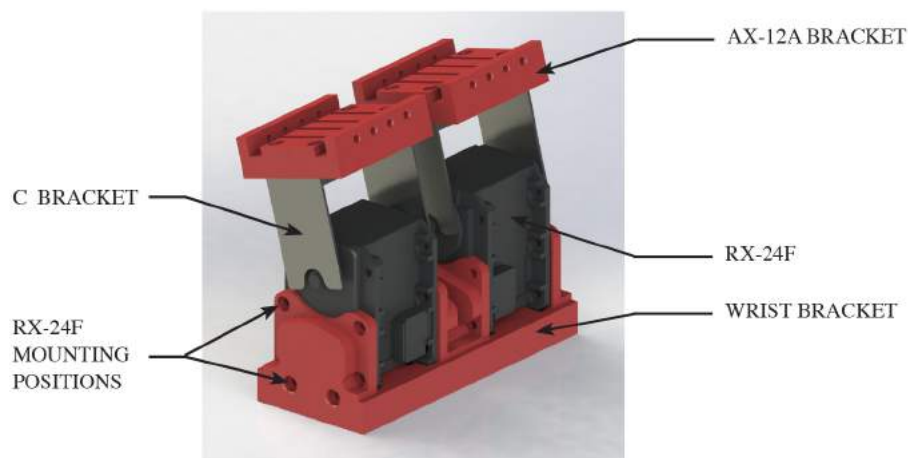


Figure 3.32: Final design of the wrist sub-system

### 3.9 External sensor selection

The RX-24F is capable of storing up to 4092 bytes of data on its non-volatile EEPROM that is retrievable after powering down the servomotor. However, the RX-24F is limited to an operating range of  $0^{\circ}$ - $300^{\circ}$ . Only in continuous operation mode can the RX-24F rotate about the complete  $360^{\circ}$  using clockwise or anti-clockwise commands. Continuous operation mode does not record the current position and therefore cannot track the current number of complete rotations, so an external sensor is required. A reed switch is implemented to keep track of rotation [52]. As the reed switch needs to be relatively close to the magnet in order to register a signal, it needs a separate part designed to adequately place it in line with the mounting platform. The holster designed for securing the reed switch is shown below, attached to the PT785 chassis, in Figure 3.33.

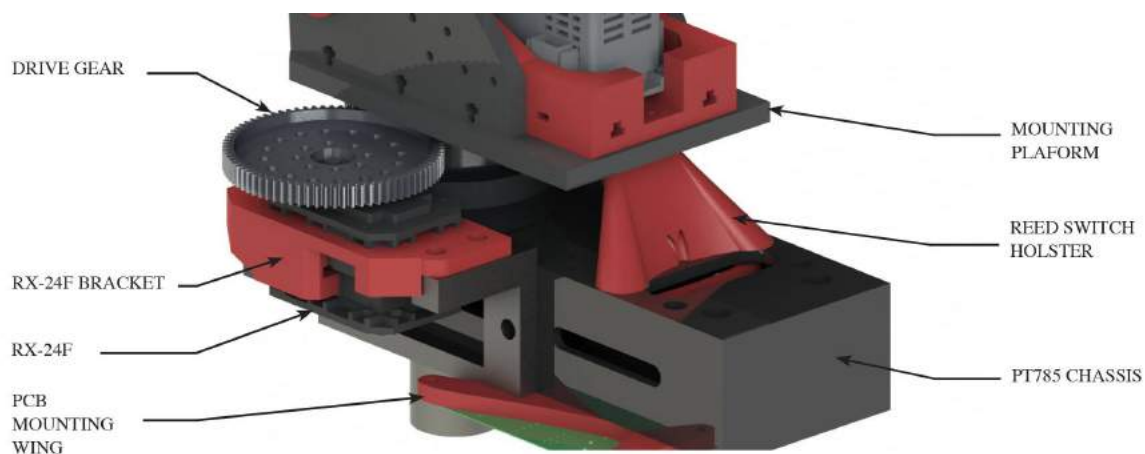


Figure 3.33: Placement of the reed switch on the PT785 chassis.

Placement of the reed switch closer to the gears would decrease the reliability with which a complete rotation could be detected. By placing the switch at a larger radius, the angular movement required to trigger the switch is decreased. A hole is made in the acrylic base platform that a neodymium magnet can press fit into to trigger the reed switch. This hole is placed opposite the mounting holes in the PT785 carriage that are used to hold the reed switch, shown in Figure 3.33. The reed switch is recessed into the package of the holster, seen below in Figure 3.34, with cable holes running through the centre of the part allowing them to be connected directly to the Daughterboard through the PT785 chassis.



Figure. 3.34: Design of the reed switch holster

The design of the platform for the reed switch to be mounted on utilises the mounting holes of the PX-75 carriage. By having a press-fit column slide through the carriage and clip in using an internal bracket, the 3D printed part cannot be lifted and stays flush with the carriage. The clip designed can be seen clipped into the base of the reed switch holster in Figure 3.34. The total contact area of the holster with the carriage is larger than the top end of the holster to reduce movement. The reed switch is seated flush into the holster and has two extruded tunnels for running the wires through.

To secure the daughterboard to the PT785 carriage, a component must be designed that can adequately separate the soldered headers from contacting the metal carriage. To accomplish this, a twin winged design is utilised which has a press fit and clip design similar to that of the reed switch to secure it to the carriage, shown below in Figure 3.35. The thickness of the wings is 6 mm to decrease the likelihood of the 3D print breaking.

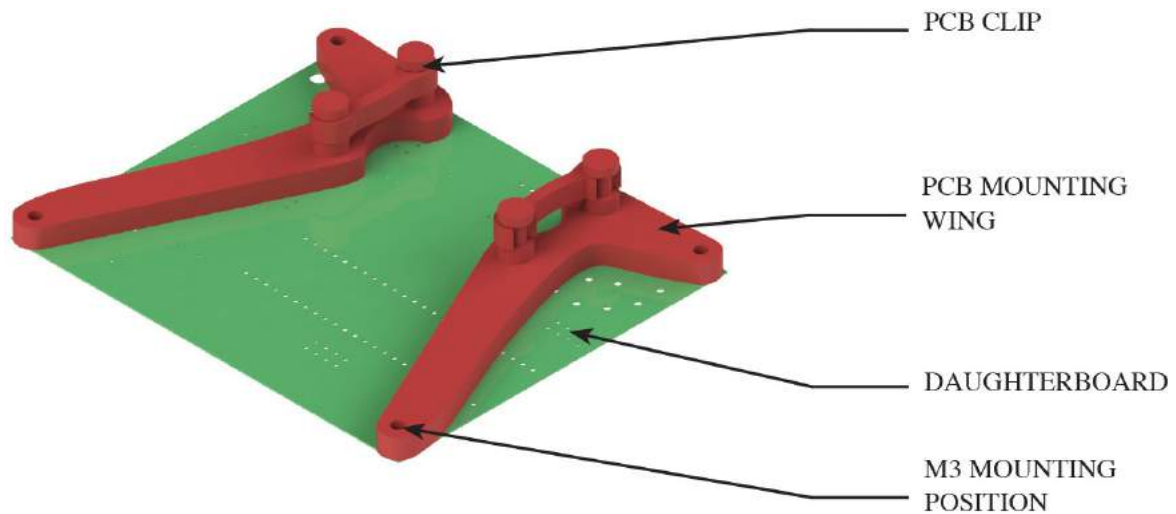


Figure. 3.35: Top down view of the PCB wing design

The wings are separated from the daughterboard using PCB standoffs to allow further room to prevent electrical interference. M3 mounting holes are incorporated in the daughterboard to connect to these standoffs. This design allows the power, control and sensor cabling to be run neatly and connected to the daughterboard whilst being out of the way, as shown in [3.36](#).

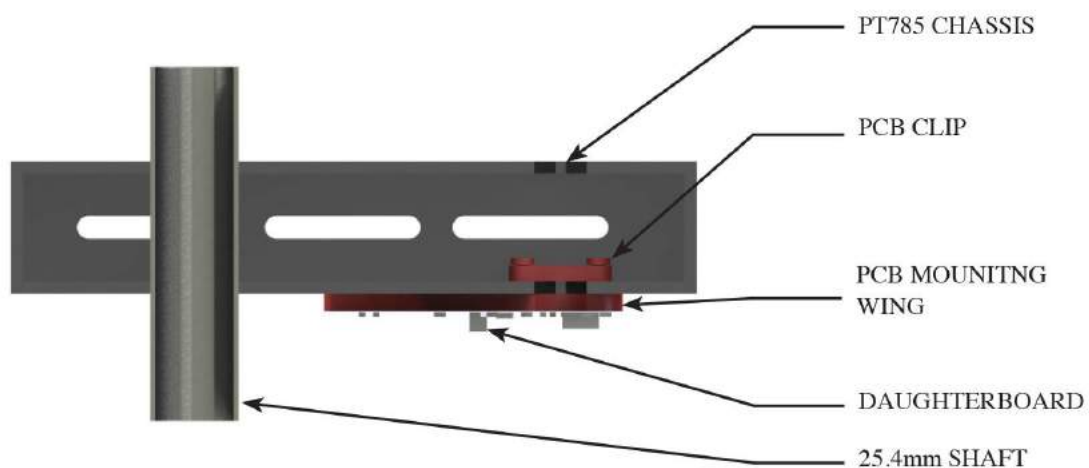


Figure. 3.36: Implementation of the PCB wing design

### 3.10 Summary

Three sub-systems have been designed which integrate together to provide the motion required to play across an entire traditional drum kit. Each sub-system incorporates external sensors to increase the reliability and operation of the servomotors. The final system, shown below in Figure 3.37, is designed to strike the drums at faster speeds than humans, with a similar range of motion achievable in pitch and yaw. The grip sub-system, discussed below in Chapter 4.3, is the final stage in the design of our mechatronic system and incorporates the functionality required to secure the beaters. The realisation of this design, and its subsequent replication into two more arms, can be seen below in Figure 3.38 splayed across a snare drum.

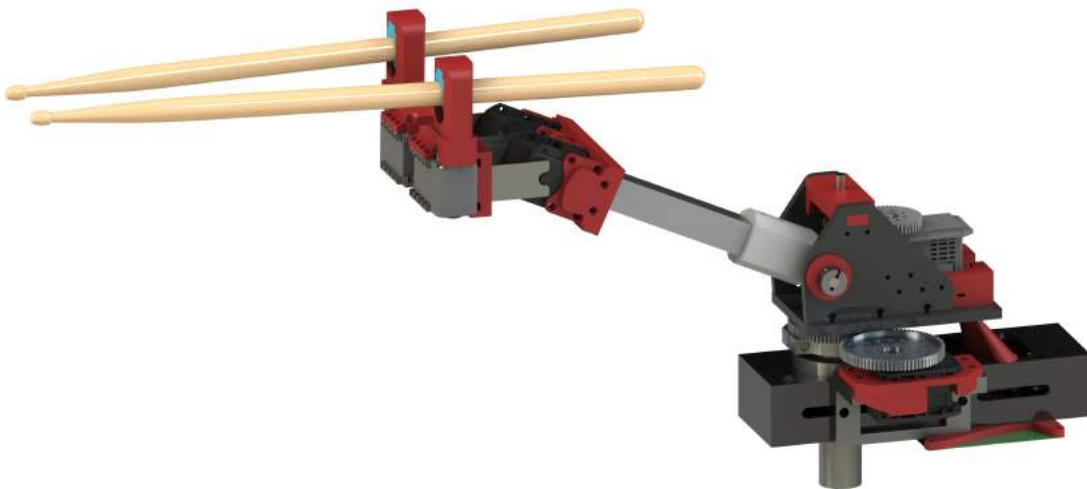


Figure. 3.37: Final CAD Render of the system design.



Figure. 3.38: Final realisation of three mechatronic percussion arms.



## Chapter 4

# Grip Design

This chapter discusses the requirements of a mechatronic percussion system that can expressively grip a beater and illustrates the design process surrounding the design of a compliant grip sub-system.

### 4.1 Gripper Requirements

Humans are able to utilise fine motor skills and sensory feedback from the cutaneous layer under the skin to dynamically grip beaters with very high levels of variation [53]. This is due to the human hand having one of the densest concentrations of nerve endings in the entire body with which to provide feedback. These nerve endings sense pressure, movement and vibration [53]. Force feedback is essential to percussionists to control the response of the beater after striking the membrane of the drum. A form of force feedback is required for the new robot drumming system to accurately interpret how tightly the stick is being gripped.

When human drummers grip a beater, the bio-mechanical properties of human skin naturally increases the surface area with an increase of force [54]. This is due to the palms and fingers of human hands being covered in small ridges that increase the overall flexibility of the human hand. This allows it to deform around objects and prevents potential damage from gripping non-uniform objects. The areas of the hand with ridged features are known as palmar surfaces [54]. The viscoelasticity of skin allows it to deform when force is applied, spreading the force from the muscles in the forearm across a greater area. This increases the stability of grip on the beater and the precision with which it is gripped.

Human drummers use their sense of touch to tell whether their current grip on a beater is great enough to keep it secured. The robotic gripper sub-system must securely grip the beater and minimise the chances of it becoming dislodged during extended play. Therefore, the material constituting the grips must have a certain level of compressibility to conform around the profile of the beater held.

The grip with which the drummer grips the beater has an impact on the musical expressivity of the note played. Looser grips cause an under-damped transient response to striking and the additional over/undershoot increases the number of minor strikes (bounces) due to the modes of the drum membrane [8]. Tighter grips result in a critically damped response with no overshoot or additional strikes. The system should be capable of varying its grip upon the beater to accommodate different styles of play.

Humans are capable of responding physically to a stimulus within 250 milliseconds [55]. While drummers can alter their grip in approximately this time frame, this is not required for the system as the grip is unlikely to change whilst playing the same routine or pattern. Therefore, the time required to shift between the minimum and maximum pressure is set at approximately one second as it is unlikely the grip will require the maximum change faster than this.

The diameter of traditional beaters used in drum kits ranges from 12.4 mm to 19 mm [56]. The gripper should be able to accommodate this range of diameter sticks, brushes and mallets to increase the total dynamic capabilities of the system. Should stick diameters out of this range be used, simple adapters may be constructed on a case-by-case basis.

## 4.2 Gripper Configurations

Human drummers conventionally grip the stick between the index finger and the thumb, creating a fulcrum. As discussed in Chapter 2, there are three different approaches to gripping the beater, which vary the position of the fulcrum from vertical to horizontal. These grips are vertical, horizontal and the hybrid grip, shown previously in Figure 2.5.

Vertical grip, or French Grip, provides a greater amount of control by positioning the beater vertically between the index and thumb. This grip provides stability and control over the beater and is used by professional drummers for precision. A horizontal grip, or German grip, uses the entire hand to hold the beater, pronating the wrist to strike the drum, shown in Figure 4.1. This provides greater force behind strikes but sacrifices accuracy and precision. Additionally, horizontal grips damp the motion of the beater after striking with the palm of the hand.

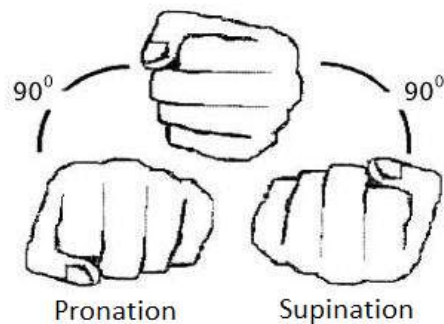


Figure. 4.1: Pronation and supination of the wrist [57].

The hybrid grip, also known as American grip, is a blend between the French and German grip, angling the sticks at  $45^\circ$  from either vertical or horizontal. This grip combines the precision of the vertical and the power of the horizontal, allowing the drummer to define a custom striking angle.

For an actuated gripper to be functional in a horizontal setup, there would need to be additional damping in the vertical axis to prevent the stick from dislodging itself at lower levels of grip. Professional drummers naturally provide additional support by resting the stick against the palm. Implementing a damped horizontal design increases the complexity and the number of components required, increasing the total torque acting on the elbow.

Additionally, an actuated horizontal grip that is non-invasive to the beaters used requires a mechanism for keeping it in place once the grip is loosened to the point that the weight of the beater is greater than the grip potential. In a vertical design, holding the stick away from the centre of gravity in a looser grip will result in it angling forward, resting the stick between the two grip locations. However, in a horizontal and hybrid design, the effects of gravity pulls the stick away from both of the grips.

The lack of additional components and lower complexity design makes the vertical approach easier to implement and reduces the total weight of the system. The vertical clamping style can effectively hold various diameter beaters in place.

### 4.3 Grip Design

A vertical grip reduces the chances of a beater becoming dislodged. However, extended play can cause the beater to become misaligned if the grip strength is not high enough to hold it in place. One approach to securing the beater would be to thread a rod through the centre of the beater which would prevent the beaters from becoming dislodged. However, this requires destructive alterations to be made to every beater which is used. This limits how flexible and configurable the overall system is, as beaters with these alterations must always be used.

We define a non-destructive manner of gripping as being able to secure a beater in place and vary the grip without requiring additional modifications to the beater. By implementing a non-destructive grip design, any beater may be used, from mallets to different thicknesses of drum sticks. However, a non-destructive design requires a way of detecting the beater drifting or if it has been released. This requires feedback to detect the current level of force exerted on the beater.

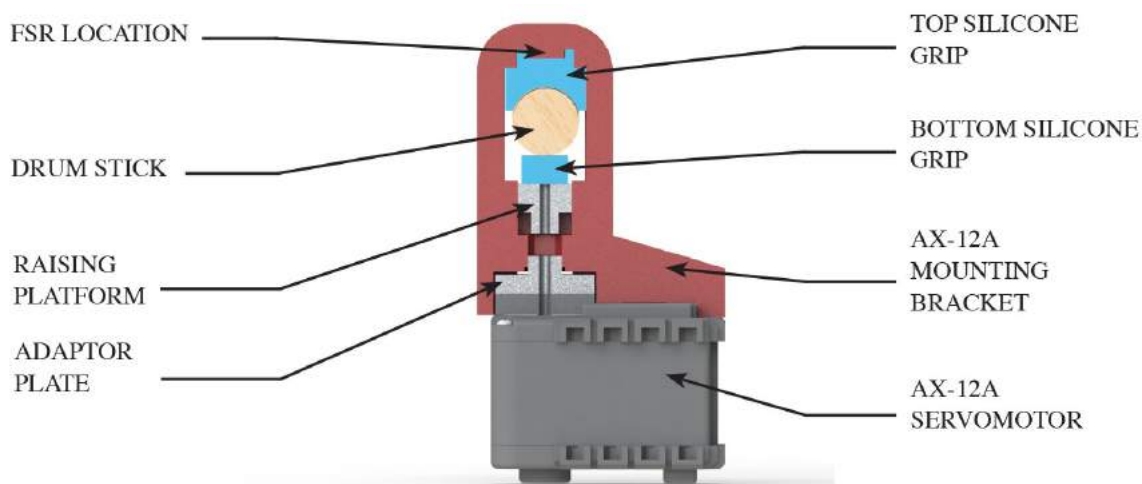


Figure. 4.2: Front view cutaway section of the AX-12A gripping sub-system.

Force feedback can be accomplished using a force-sensitive resistor (FSR). The FSR must be small enough in area that it can accurately detect the thinnest beater that may be used. The FSR selected for the gripper is the 0.25", short tailed resistor from Interlink [58]. The sensing area of this FSR is 6.35 mm  $\times$  6.35 mm, which makes it suitable for detection of the minimum diameter of a drum stick, 12 mm.

There is currently a lack of research available into the variations of grip strength that are exerted by human drummers when playing different compositions. As such, the FSR will be used to establish rudimentary grip strengths upon the stick from maximum to minimum. Further research should be conducted into the field to determine quantitative amounts of force that should be applied to either side of the beaters. The location of the force sensitive resistor is shown in Figure 4.2

The actuator used to alter the grip must be capable of accomplishing the range of motion desired in under a second. The AX-12A servomotor from the Dynamixel series is selected for actuating the gripper. This is due to its smaller size and weight but high RPM. Linear motion is required to shift the platform which will be used to grip a beater. To convert rotational motion into linear motion, a lead screw can be used. A lead screw is an externally threaded rod which rotates from a fixed position to shift an internally threaded nut linearly [46]. The lead nut must be secured to an external axis to prevent rotational motion. If the lead nut cannot rotate, this will cause the internal thread of the lead nut to travel up or down the external thread of the lead screw as it rotates. By affixing the lead screw to the centre of the AX-12A and securing a threaded platform to the AX-12A body, the rotational motion of the servomotor can be translated to linear motion of the platform. The location of the threaded lead screw can be seen clearly in Figure 4.3.

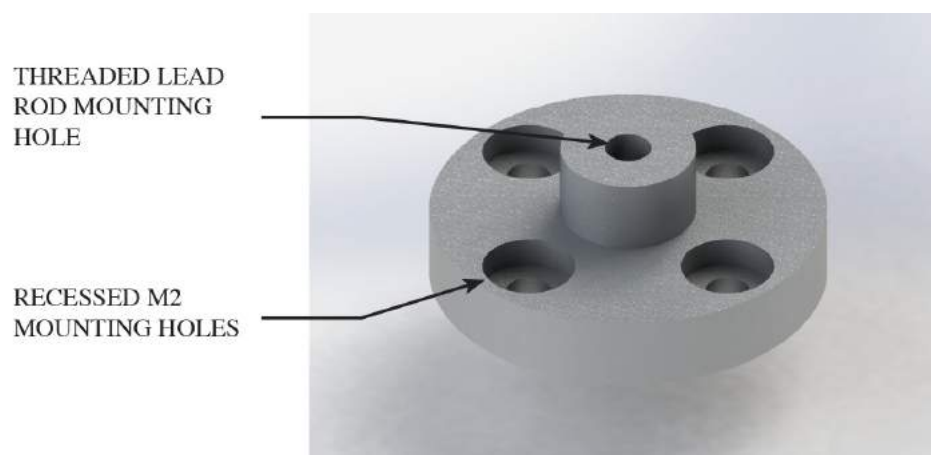


Figure. 4.3: Design of the AX-12A adaptor plate.

The servo horn of the AX-12A is recessed into the package of the AX-12A, meaning that a threaded lead screw cannot be attached directly. Therefore, an adaptor plate must be designed that interfaces with the AX-12A servo hub, allowing a lead screw to be secured to its centre. This adaptor plate should be of equal radius to the AX-12A servo hub to simplify the design. The AX-12A servo hub has four rotationally patterned mounting holes with which the adaptor plate is designed to interface. The mounting holes are recessed into the plate such that the heads of the screws are flush with the face of the adaptor plate, as shown in Figure 4.4.

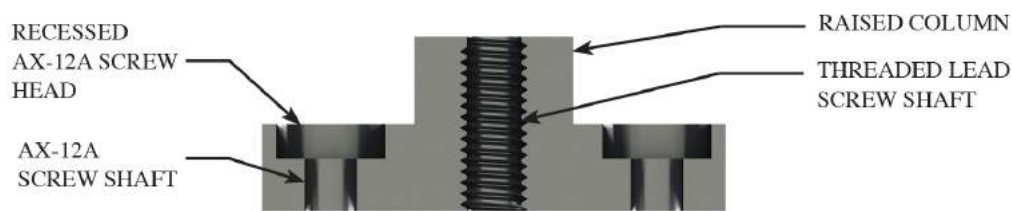


Figure. 4.4: Cutaway of the AX-12A adaptor plate.

The strength of the grip on the lead screw is determined by the total area that the screw contacts on a threaded column. To increase the hold of the adaptor plate on the lead screw, the internal thread length can be increased. A raised column is incorporated into the design to increase the total thread engagement. The diameter of this column provides 2 mm of material either side of the thread to prevent warping of the column. This increases the total surface area with which the screw is in contact. A thread locking fluid is applied to the thread on the adaptor plate to prevent loosening from shock and vibration. The adaptor plate is machined from aluminium due to its lightweight characteristics. 4.5 is a cutaway of the initial lead screw setup using a 3D printed lead platform showing the amount of thread engagement in both the adaptor plate and 3D printed approach.

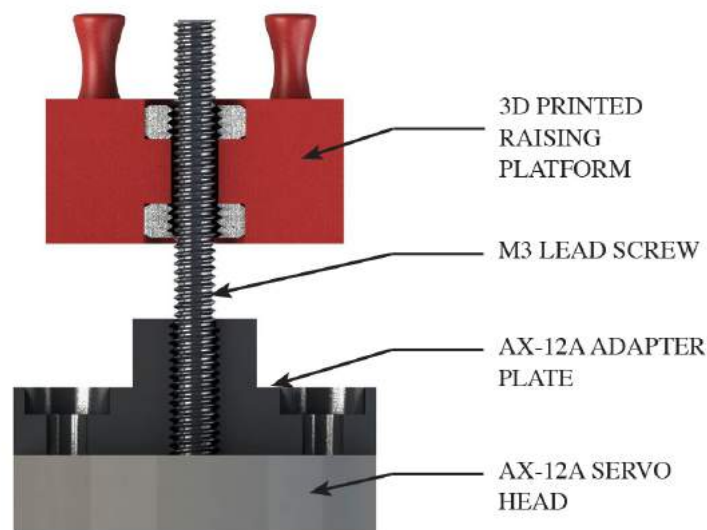


Figure. 4.5: Cutaway of the lead screw and lead nut setup platform.

The platform that raises and lowers with the rotation of the lead screw constitutes the bottom half of the vertical gripping design. If the platform is capable of rotational motion, it will move consistently with the lead screw instead of raising or lowering. Therefore the design must incorporate features that prevent rotational motion and limit movement to the Y-Axis only.

To prevent rotational motion, a press-fit slot is used to secure the platform into a square slot on the AX-12A mount. In order for the platform to move with the rotating thread, a matching thread must be incorporated. This can be achieved by 3D printing the platform, mounting M3 nuts to it and threading them onto the lead rod, as seen in Figure 4.6. However, early implementations of this design resulted in the nuts dislodging themselves or twisting the 3D printed ABS and breaking. As the tensile strength of ABS plastic was not high enough to prevent rotation of the nuts. Therefore, a platform must be designed which incorporates the thread of the lead rod into the platform as a single component.

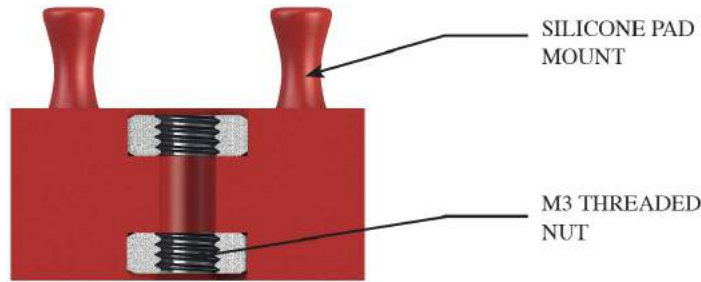


Figure 4.6: Initial design of a 3D printed raising platform.

The initial 3D printed approach also attempted to provide a mounting position for the gripper pads which are discussed further in Section 4.3.2. These raised columns were intended to provide a press-fit into the base of a silicone pad, using a narrow base and wide top to prevent the pads from being dislodged. However, early testing revealed that the 3D printed layers were not strong enough to withstand the compression and non-uniform load of a beater. This resulted in the mounting positions being snapped off at the weaker, narrower bases of the columns seen in Figure 4.7.

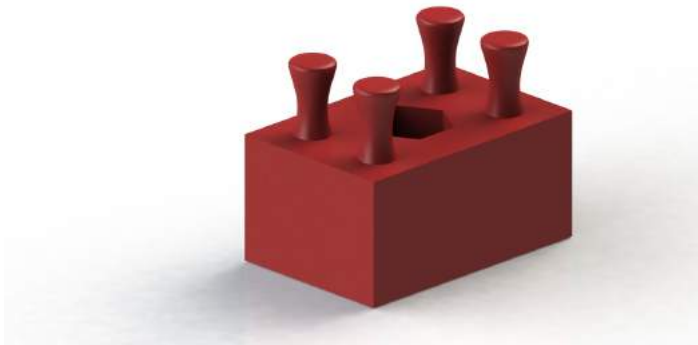


Figure 4.7: Design of a 3D printed lead platform.

The 3D printed design relied on the four square sides to prevent rotational motion in the lead screw assembly. However, this leaves the design prone to damage of the ABS plastic on both the platform and the AX-12A bracket over time due to the low contact area when in a raised position. To increase the surface area across which the force is dispersed, an H-pattern is used, shown in Figure 4.8. The additional surface area provided by the two square cutouts allows the platform to raise further without damaging the ABS print.

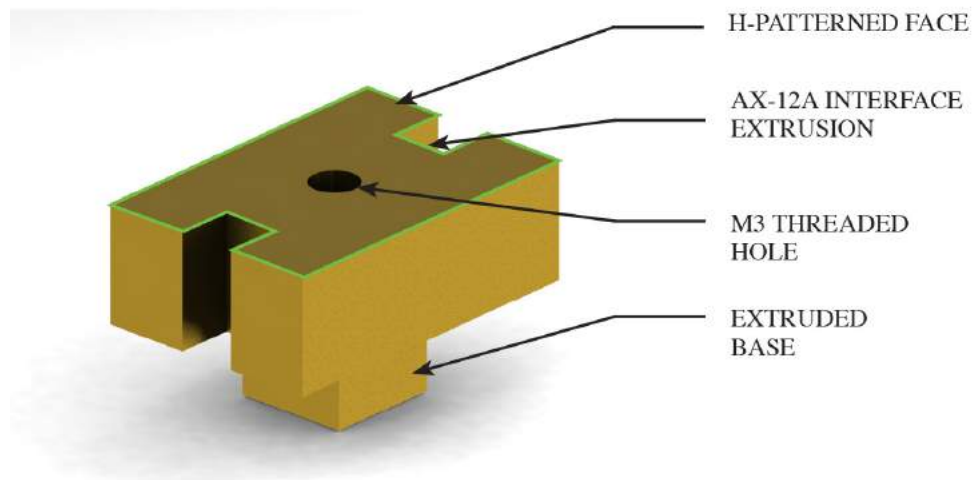


Figure. 4.8: Design of the machined lead platform.

An inverse of the H-pattern is featured on the AX-12A mounting bracket, with a cutout section shaped in an H for the lead platform to lower and recess into. The total number of contact points present on the lead platform is 12, decreasing the total force spread across each face. As with the design of the AX-12A adaptor plate, the lead platform features an extruded section to increase the total area which contacts the lead screw. If the lead platform is not secured properly then the platform will rotate with the lead screw and become unstable, visible in Figure [4.9](#).

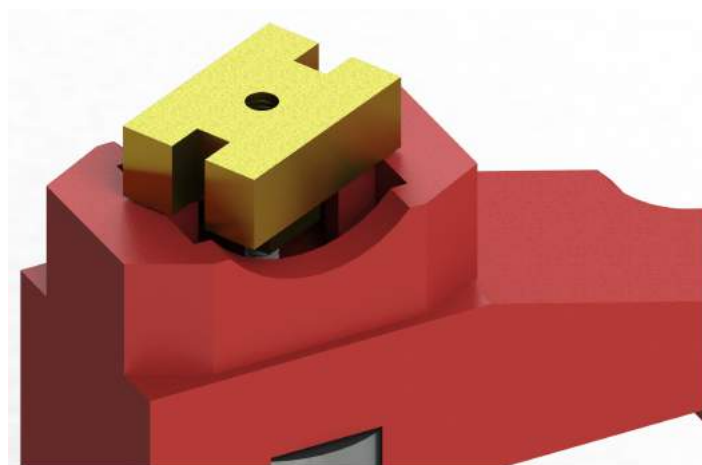


Figure. 4.9: Unsecured lead platform rotation.

The AX-12A mounting bracket discussed further below has matching inverted H-pattern features for the lead platform to recess into. The internal width of the AX-12A mounting bracket also matches that of the platform, providing a total of 12 contact areas on the platform to prevent rotation. The impact of the H-pattern is visible in Figure 4.10 and displays the contact area. To increase the surface area with which the thread is in contact, a square section is extruded on the underside of the platform, seen in the bottom of Figure 4.8.

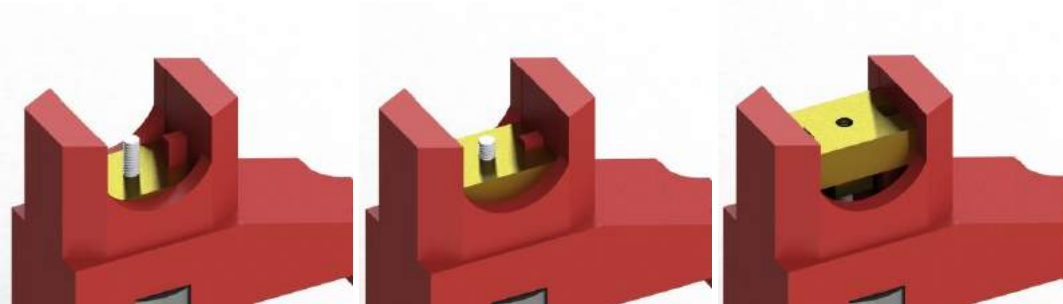


Figure. 4.10: Lead platform at various levels of engagement

The face of the platform that drives towards the beater is designed to be the same dimensions as the average index finger's proximal phalange that makes contact with the beater. This is approximately  $12 \text{ mm} \times 10 \text{ mm}$ . The thickness of the platform was designed to have 10 mm of length for thread engagement. The platform is made from brass due to the ease at which brass can be machined and its tensile strength [46].

The design of the AX-12A mounting bracket centres on mounting to the AX-12A package and supporting the upper half of the vertical gripper at a far enough distance to house a maximum diameter beater. The first version of the design was used to experiment with the implementation of the lead screw. As such, the top half of the grip was omitted and cutaways implemented in the side pillars so the full path travelled by the lead platform could be evaluated, seen in Figure 4.11 (left).

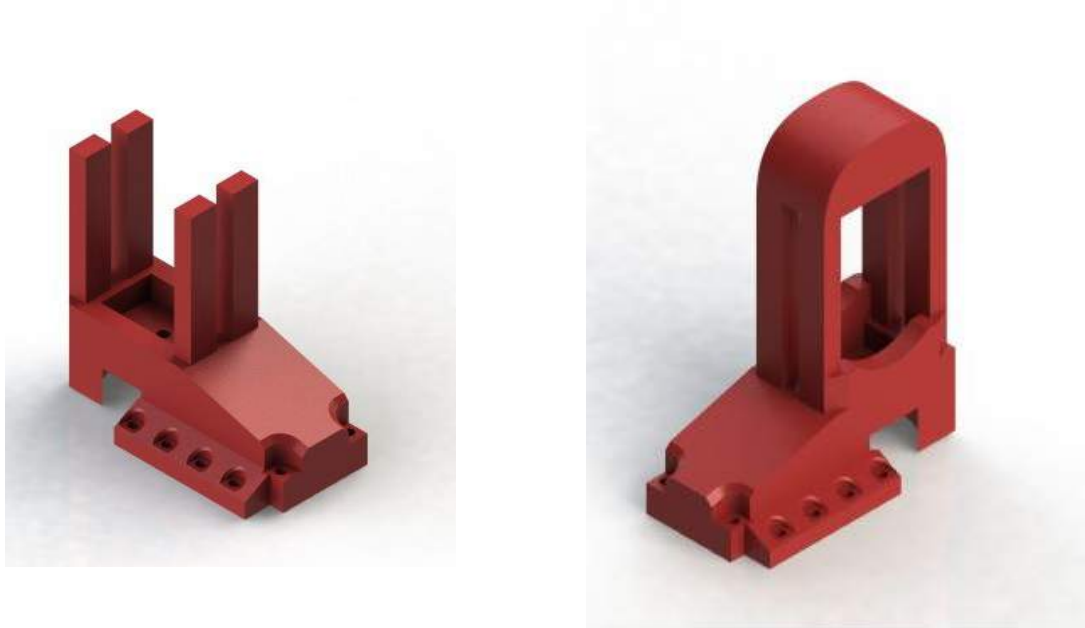


Figure 4.11: Initial designs of the AX-12A mounting bracket

Once the motion of the lead platform and screw had been observed and the initial problems with the 3D printed platform were resolved, the design progressed. This involved the inclusion of the top half of the vertical gripper but kept the side cutouts to make visible the complete beater engagement, shown in Figure 4.11 (right). However, this design could not sufficiently secure the silicone pads to the top half of the gripper (discussed in Section 4.3.2) and required alterations to incorporate them. The design of the gripping materials determines the total height of the AX-12A bracket and, as multiple revisions were seen, this height changed for each change in thickness of grip, as discussed in Section 4.3.

During printing, components with a large base area were prone to errors as because the time required to print each layer is larger, the plastic at the fringes of the design is able to cool before the next layer is melted to it [59]. This causes some warping and deformation in the final print. Multiple revisions were required due to this change of tolerance for larger models that could only be measured and revised in multiple prints. Often the deviation in the 3D print from the design would be between 0.2 mm and 1 mm, depending on the length of time required to print. A major issue with 3D printing is that exact dimensions require fine tuning and must occur for each component integrated.

In a vertical grip, the human hand can allow for up to 30° of rebounded motion in the drum stick due to the elasticity of the drum membrane and the force applied. To limit rotation past angles of 30°, a natural damper is incorporated into the design of the AX-12A

mount with semi-circle extrusions of equal diameter as the largest beater expected to be used, shown below in Figure 4.12. This limitation prevents stronger strikes from potentially dislodging the stick due to excessive rebounding.

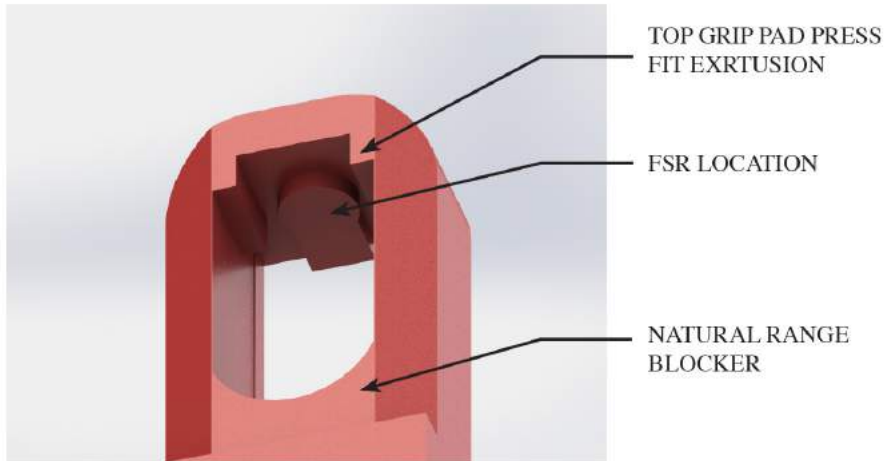


Figure. 4.12: Location of the top gripper pad on the AX-12A Mounting bracket.

The final design incorporates a recessed section for the platform to lower into and separate the platform at its lowest point from interacting with the aluminium adaptor plate. This redirects any potential damage from unwinding the platform too far onto the 3D printed material instead of metal, as the 3D printed material will deform before the metal will. The recessed section of the mounting bracket that allows for the lead platform to slot into is shown in Figure 4.13.

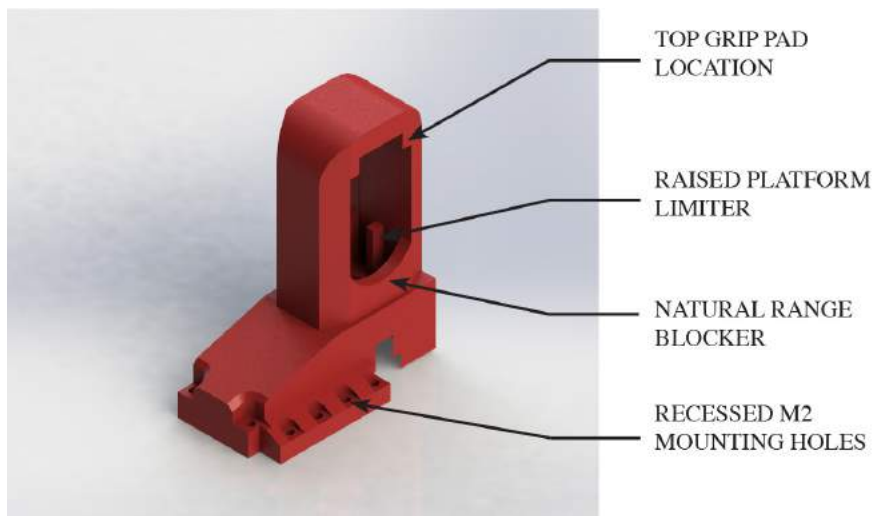


Figure. 4.13: Design of the AX-12A mounting bracket.

The upper half of the mounting bracket has features that match the base of the top gripper pads, and can be seen in Figure 4.12. This allows the pad to press-fit into place and includes an outline of the FSR to be incorporated later. The design of the upper and lower grip pads are discussed further in Section 4.3.2.

The raising platform must be capable of a large enough range of motion to span the gripping of the largest diameter beater, 19 mm, through to the smallest diameter, 12 mm. However, as the bottom gripper pad does not include a thread for the lead rod to interact with, the lead screw cannot rise higher than the face of the raising platform. This limits the range which the lead platform can travel to before the bottom silicone pad interacts with the lead screw. The maximum and minimum set-points of the lead platform are shown below in Figures 4.14 and 4.15.



Figure. 4.14: Maximum position of the lead platform in the gripper sub-system



Figure. 4.15: Minimum position of the lead platform in the gripper sub-system

### 4.3.1 Gripper Material Selection

The gripper sub-system requires a malleable gripping material which permits similar deformation to that of human skin. There are several available materials that have been used in the past such as soft-prosthetics [60][61][62]. However, these generally evaluate the performance of silicones or plastics custom made by the authors and are not easily reproduced.

The hardness of soft materials is measured using a Shore Durometer [63]. Each series of the Shore hardness scale is determined by the indentation which can be caused using a specific spring force and indenter tip on the working face of a material. Resistance from the test sample determines the maximum depth which the indenter will reach, shown in Figure 4.16. A rating of zero correlates to the spring reaching full extension and the indenter reaching a maximum depth. The extension of the indenter remains constant, whilst the diameter of the indenter and the spring force behind it changes for each series [63]. A Shore OO rating typically refers to soft rubbers and elastic gels, while Shore D refers to hard rubbers and semi-rigid plastics, shown below in Figure 4.17 [64].

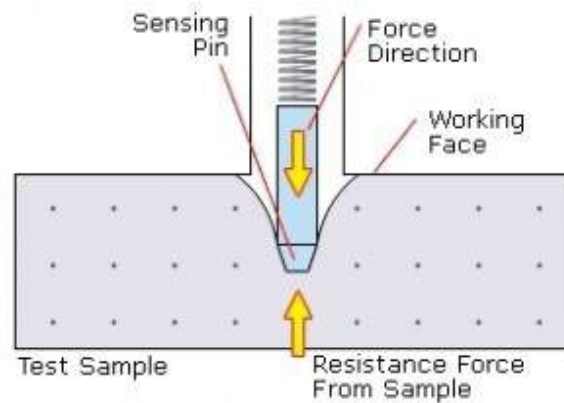


Figure. 4.16: Hardness testing using a Shore Durometer [65].

The human index finger has a Durometer Shore hardness of 33 Shore A [64]. The human hand is not of continuous elasticity, it consists of multiple layers of varying elasticity which vary in depth. The Shore Durometer is intended to test consistent samples and does not account for the contiguous layering of the human hand. The epidermis, dermis and subcutaneous layer have comparable elasticity, whereas the deeper muscle tissue is more rigid [53]. This results in the Shore A reading of the human hand being equivalent to the malleability of a rubber eraser.

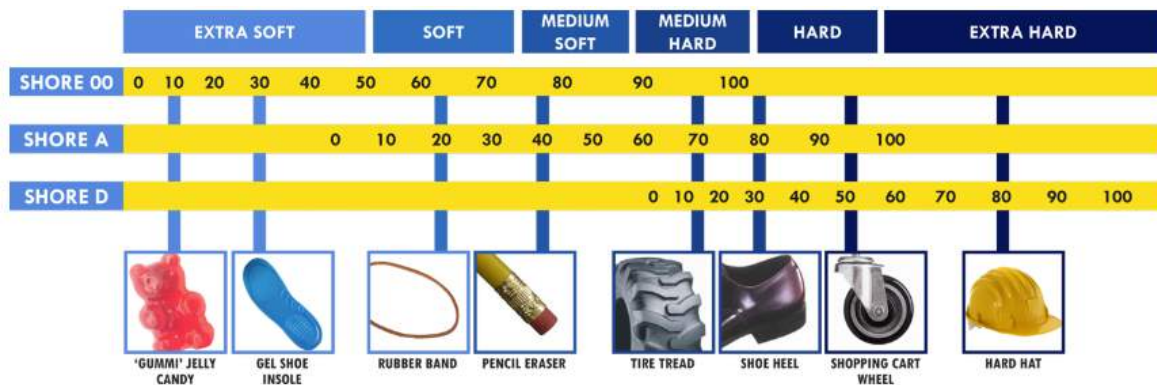


Figure. 4.17: Shore hardness Scale [66].

In-depth testing of the various layers of human skin using a Durometer and an accurate recreation of the multiple layers of said skin would be required to approximate the compressibility of the human hand. Instead, a lower Shore rating can be used to model the malleability of the outermost layers of the human hand.

Mold Star<sup>1</sup> is a platinum-based curing silicone rubber which features relatively low viscosity and is available in a range of shore hardness ranging from 15 to 30. Mold Star 16 has a cure time of 6 minutes and a Shore A hardness of 16. Shore 16 A is a lower hardness than the human finger and allows for greater deformation due to its higher viscosity. This meets the requirement outlined at the start of Section 4.3.1 for a material with greater malleability than human skin.

### 4.3.2 Silicone grip design

The Mold Star 16 silicone mixture requires a mould to form the pads required for the gripper. The design of this mould consists of the negative features of the silicone grip that is desired and would be manufactured from a 3D printed case. The shape of the features required of the silicone will determine the design of the mould. Pouring the silicone mixture into a solid 3D printed mould would require breaking the 3D print to release the silicone once it has hardened. This is due to the silicone mixture adhering to the ABS and requiring peeling away from the plastic to break it free. Instead, the mould can be split in half vertically and secured together using screws to prevent any potential leakage between the halves before hardening.

<sup>1</sup><https://www.smooth-on.com/product-line/mold-star/>

The silicone grips must be designed to afford similar expressivity to a human drummer's grip and create an auditory response equivalent to that of a human strike. The silicone grip will deform to match the face of the beater desired, dispersing the force applied across the face and increasing the grip on the beater. The size of the silicone pads that are to be used should match the width and length of the contact area of the index finger and the thumb.

The lower half of the silicone grip must affix to the lead platform to prevent moving and slippage during play or grip adjustment. To mount the silicone grip to the lead platform, silicone sealant is used due to its adhesion properties to glass and metal surfaces. The silicone sealant is applied to the underside of the bottom pad, matching the features of the raising platform, seen in Figure 4.19. As such, the lower platform cannot be changed easily and the surface which faces the beater must be designed in a way that allows for multiple diameter sticks to be used by the system. This is a trade-off between the ability to easily change out the bottom silicone pad and being able to ensure that it is secured reliably. Ultimately, securing the pad is more important to the function of the gripper sub-system and the trade-off is acceptable.

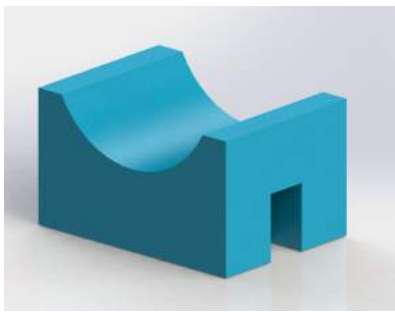


Figure. 4.18: Angled view of the bottom silicone grip pad

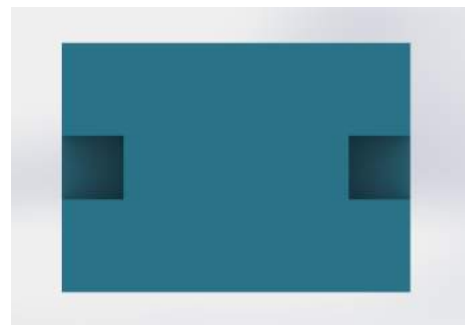


Figure. 4.19: Side view of the bottom silicone grip pad

The bottom silicone pad's face is curved to match the diameter of the largest beater, 19 mm. To be capable of customising the outward angle that the beaters can be played, a flat bottom pad can be implemented.

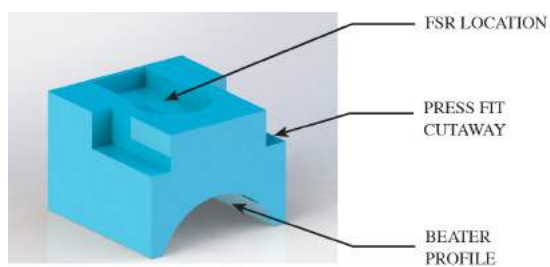


Figure. 4.20: Angled view of the top silicone grip pad

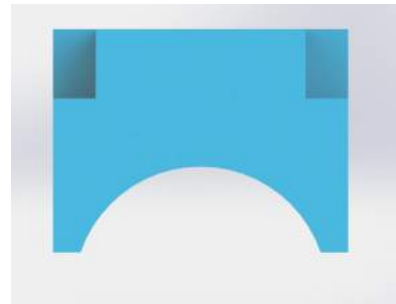


Figure. 4.21: Underside of the bottom silicone grip pad

As mentioned previously, the design of the grip holster includes a cutout for the FSR to be placed into. This is incorporated into the design of the top half of the vertical grip, as well as two features that allow for a press fit into the grip holster. The features of the silicone pad required to fit the FSR are visible in Figure [4.20](#).

The top silicone grip can be easily replaced as it is a press fit and it can be customised to suit any beater. Initial testing with a flat silicone pad gripping a beater resulted in the beater's angle and location drifting over time. The malleability of the human hand and variability of grip allows for looser holds on a beater without sacrificing control. To achieve a similar control over beater location, the face of the top silicone grip can be tailored to the diameter of the beater that is desired. To achieve this, the parametric 3D model for the top silicone mould has an input selection for the different diameter beaters. The altered 3D model will include the features required to press fit as seen in Figure [4.20](#). Upon altering the mould, it can be 3D printed within 30 minutes and filled with the liquid Mold Star 16 mixture. Within one hour of requiring a different diameter grip, it can be fabricated and implemented in the system.

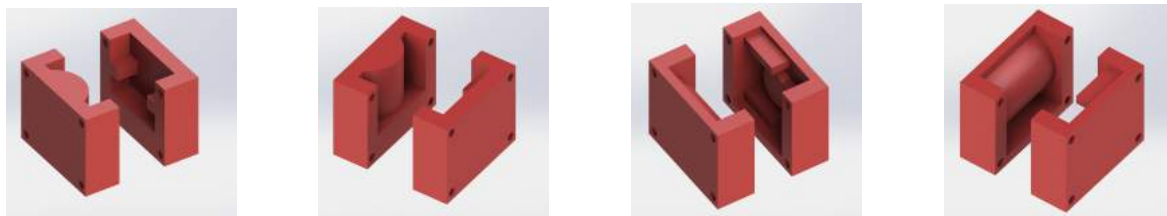


Figure. 4.22: Renders of the index and thumb molds used in this project

The design intention is to have two beaters included, so the design of the corresponding gripper is a mirrored version of the design which has been discussed and is visible in Figure 4.23. As will be discussed further in Section 3.7, the separation of the beaters is greater than the modes of play on the smallest traditional drum skin. To overcome this, the angle of the face of the top gripping pad which contacts the beater can be altered for wider or closer grip positions.

The maximum angle which can be accommodated within the current design of the gripper assembly is  $5^\circ$  in either direction. However, due to the length of the beaters, this angle is multiplied by the radius resulting in a net difference of 45 mm. The smallest separation of the beaters would then be 45 mm, seen in Figure 4.23, within the 55 mm limit of the smallest radius mode on a drum. The widest separation achievable is 135 mm as illustrated in Figure 4.23. This arc length would also allow the system to strike the edge modes of two separate instruments. This is advantageous as it allows the three robotic arms to play across 6 separate instruments simultaneously.

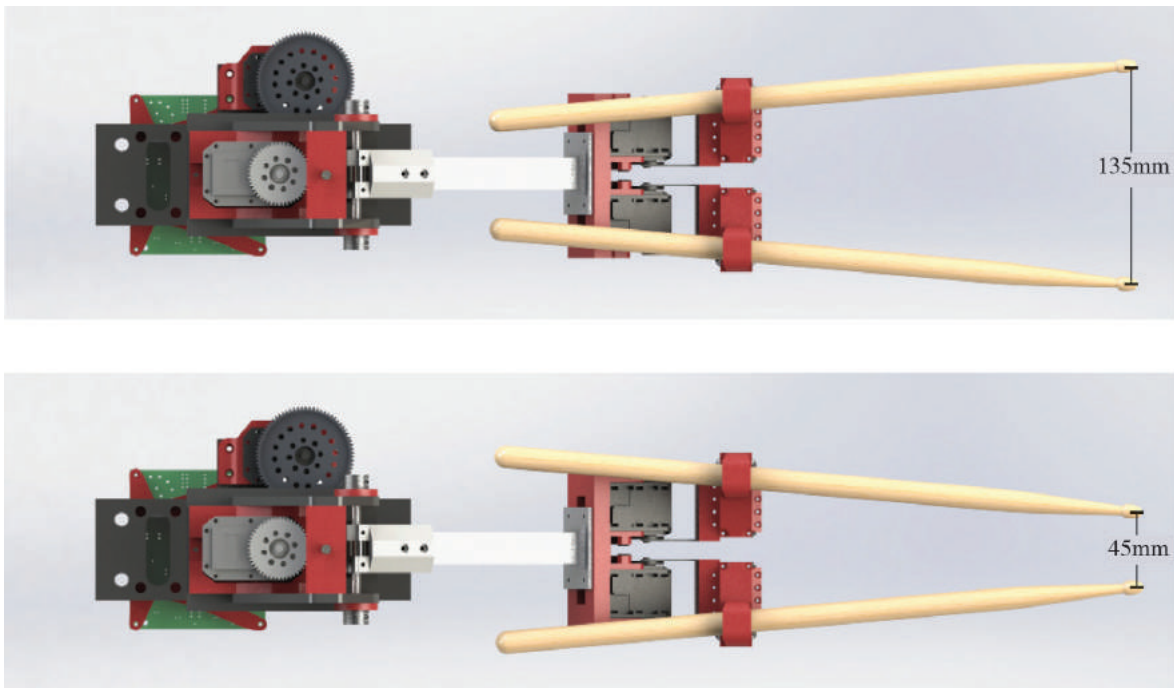


Figure 4.23: Minimum (45 mm) and Maximum (135 mm) grip settings.

As each layer of a 3D model is printed, the vertical resolution of the print is determined by the layer height. The layer height is the minor diameter of the post-compression shape, depicted in Figure 4.24. Each of these layers results in ridges equivalent to the exposed radii, acting to increase the total surface area. These ridges cause imprints upon the liquid silicone mixture when hardening, increasing the surface area of the silicone grip. These features are advantageous as the increased surface area allows for a greater degree of grip upon the beater when they deform and resemble the ridges of human palms discussed in Section 4.1. The highest vertical resolution possible using the 3D printers available is 0.15 mm. This results in a total of 33 features across the face of the silicone pad which grips a 3A drumstick.

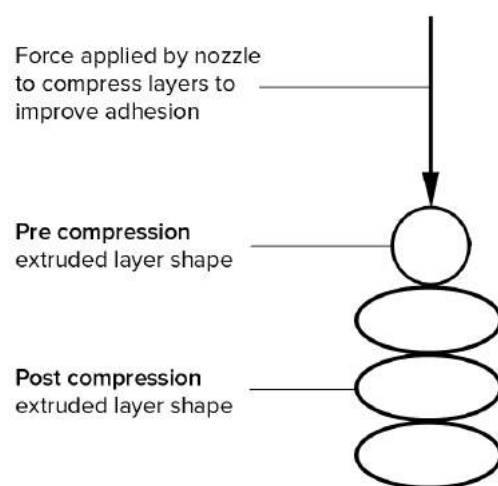


Figure. 4.24: 3D printed layer structure [67].

The drum stick used for testing purposes is the 3A Vic Firth, a stick with a diameter in the middle of the grip sub-system's range (14.8 mm). The design of the gripper meets the requirements outlined at the start of Section 4.1 by being able to vertically grip a wide range of diameter beaters dynamically using customised silicone grips. These grips reduce the potential movement of the stick by being curved to suit the face of the beater desired. The grips also act to increase the total play area of the system and have the ability to play from the smallest drum mode to across two drums. The final design of the left-hand gripper sub-system is shown in Figure 4.25. To achieve a right-hand gripper, this design is mirrored to suit the opposing strike.

## 4.4 Grip Summary

The grip sub-system has been designed to be able to dynamically grip a range of various diameter beaters reliably. The design of the compliant silicone pads and their 3D printed moulds permits fast replacement of components. Additionally, the AX-12A servomotor can vary the pressure applied to the beater used by translating rotational motion to linear with the lead platform. The electronics and software required to power and co-ordinate the operation of the three motion sub-systems and the grip sub-system are discussed below in Chapter's [5](#) and [6](#).

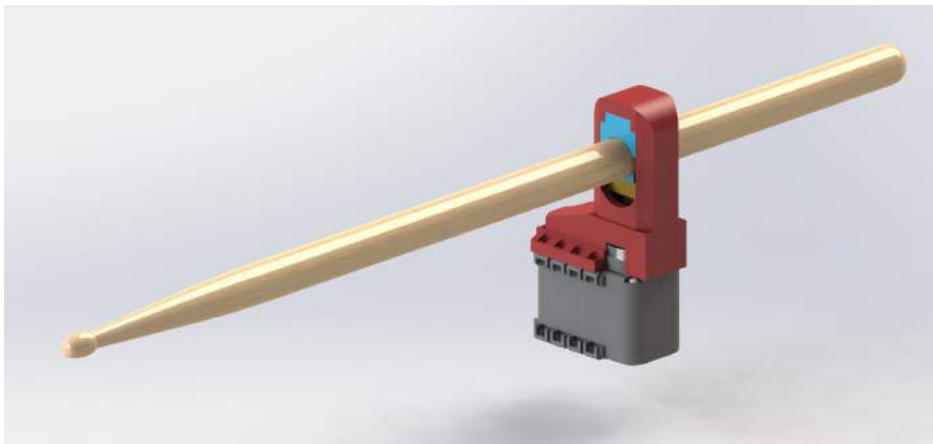


Figure. 4.25: Final design of the Gripper sub-system.

## Chapter 5

# Electronics Design

This chapter describes the design and implementation of both the Mother and Daughter PCBs. These are the communication circuit boards for the overall system and coordinate feedback from the actuators and sensors discussed in Chapter 3.

A number of physical design goals described in Chapter 3 influence the design considerations of the electronics discussed below. These include the overall size of the circuit boards, microcontroller selection and actuator control.

The drumming arm has been designed to span and play across the entirety of a traditional drum kit. Although the individual arm is capable of this, the system should be able to expand further to incorporate more arms, since more drumming arms will allow for additional percussion instruments to be integrated. Doing so will also increase the range of compositions that can be played by allowing identical drumming arms to synchronise together.

The three drumming arms need to be able to communicate with one another in a way that allows for a variety of performance styles, such as playing with one arm spanning the drum-kit, two in parallel or all three in unison. To fulfill this design requirement, the communication topology and power distribution scheme must be capable of connecting to the three arms efficiently. The two communication topologies and power distribution styles considered are parallel and series.

### 5.1 System Communication and Power Topology

A series topology connects the arms by daisy-chaining them together in a continuous link [68]. This has the benefit of being easily expandable to support additional devices past the intended three, allowing for future expansion. Figure 5.1 displays the three arms connected

to a power supply in a series configuration. The position of each arm in this chain is interchangeable due to each requiring input and through-put connectors. This allows for each arm to be used individually without requiring any alterations.

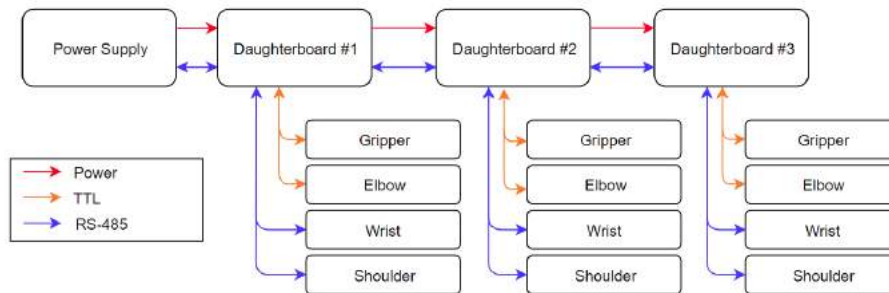


Figure. 5.1: Control Flow Diagram for a serial electronics systems.

In a series configuration, the current required to supply the last device in the chain must flow through the power connectors of each device [68]. If the power traces used are not capable of supporting the maximum current, the traces will begin to dissipate excessive amounts of heat and delaminate themselves from the circuit board [69]. Delamination can cause traces to break away from the solder mask or pads which they are mounted to. Therefore, the power traces and power cables used must be capable of supporting the total current draw of all devices. As each robotic arm requires approximately 15 A (as outlined in Section 5.3.1), the recommended trace width of the power plane for a standard copper thickness exceeds 28 mm for three arms [70]. This width is far greater than can practically be implemented. Therefore, daisy-chained topology is not viable for a high current system as the number of devices that can be connected to the trace width used is limited, cancelling out the benefit of expandability.

An alternative to connecting the arms in series is a parallelisation of the control and power scheme [68]. This requires a method to split the power signal into the three separate arms from a single source. This can be accomplished with a separate control unit that coordinates both the communication and power supply to the individual boards on the arms. By placing the power cables in parallel, only the required current is provided to each board

which in turn reduces the trace requirements of each board to the maximum of 15 A. However, a parallel approach limits the expandability of the system to the number of terminals placed on the central control unit. Figure 5.2 shows the parallelised control scheme with a Motherboard acting as the distribution centre to the boards of each arm.

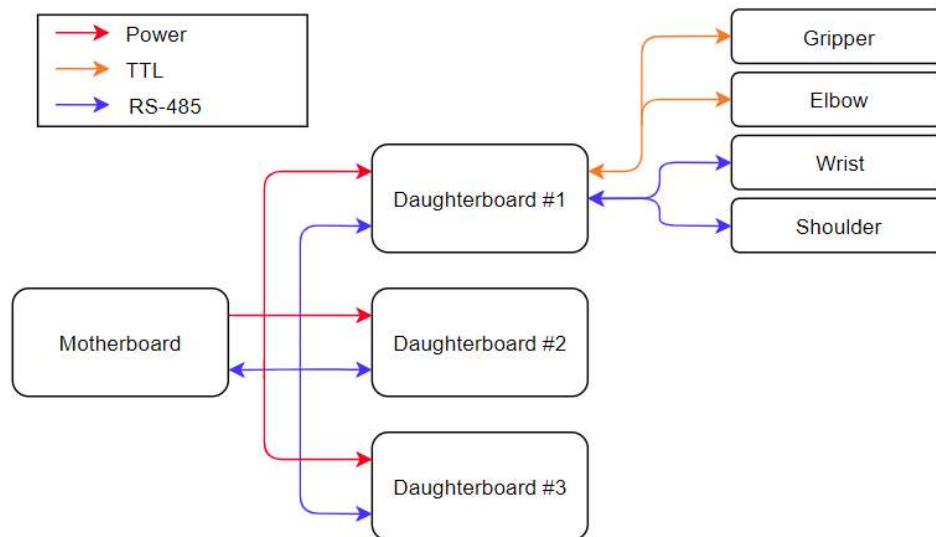


Figure. 5.2: Control Flow Diagram for a parallel electronics system.

To allow for live performances, the Motherboard should be capable of taking an input from a musical controller. The majority of commercial musical controllers have a 5-pin DIN terminal for output signals. The 5-pin DIN connector is a standardised circular connector often used for audio signals and digital signals such as MIDI. While some musical devices offer alternative outputs, such as USB, the MIDI 1.0 electrical specification identifies that the 5-pin DIN connection is the most commonly used [71].

For the arms to be capable of interpreting MIDI from a musical controller, this DIN terminal and circuitry must be included. In a serial topography, each of the daughterboards would require a MIDI-In terminal and MIDI-Thru connection [71]. The MIDI-In connects to the MIDI-Out of the control device, or the through-put of another device in the chain, while the MIDI-thru passes the signal to the next device. This is a cumbersome design as it requires twice the amount of circuitry and connectors per board.

To reduce the number of components required to operate the system, a single MIDI-In could be located on the control board that determines what physical instructions the MIDI signal correlates to. These individual instructions are then relayed to the required arm and sub-system. This hierarchy is shown in Figure 5.2, where the communication type and power re-distribution are displayed.

The Motherboard must be capable of communicating with the Daughterboard over cables to transmit the disseminated instruction signals. The choice of transmission protocol used between the Motherboard and Daughterboards is discussed in Section 5.2.2, while discussion of the Dynamixel transmission protocols occurs in Section 5.3.3.

The parallel approach is chosen for this system as it minimises the current carrying requirement of each robot's boards to the maximum current that a single arm can draw, not the entire network. Additionally, the parallel setup removes the need for two MIDI terminals and accompanying circuitry to be incorporated on each daughterboard.

## 5.2 Motherboard Design

The design requirements of the Motherboard can be broken into five individual areas: Power regulation, communication with the user and the Daughterboard, microcontroller selection, peripheral design and physical size. Each of these sub-sections includes their own set of requirements which must be met.

The power requirements of the Motherboard must be able to take a single input from the power supply and re-distribute this to the three boards in a parallel configuration. This must incorporate setup, operational and voltage regulation safeguards to ensure the stability of the overall system.

The Motherboard must also be capable of communicating with the external user and with the Daughterboard using a suitable microcontroller. Finally, it should include additional peripherals to aid in the incorporation of further sensors and indicate system status.

### 5.2.1 Power

The Motherboard acts as the central hub of the system, having an input from a power supply and splitting this into three separate parallel inputs to the Daughterboards. To prevent the power cables from being plugged in reverse, a blind-mating snap-in terminal is used [72]. This terminal features a plastic clip that is only present on the top orientation of the terminal. The headers that fit the terminals feature a matching plastic hook, preventing the cable from being plugged into the Motherboard and Daughterboards incorrectly.

The highest voltage level required by the Daughterboards must be supplied through the Motherboard as it is the power distribution centre. This voltage level is the operating voltage of the Dynamixel servomotors, which operate between 11 V and 14.8 V. The other sub-system's voltage and current requirements are listed in Table 5.1. The exact power requirements of the Dynamixel servomotors are discussed in further depth in Section 5.3.1, where the decision is made to use a 12 V rail for the input voltage.

Table 5.1: Voltage and current requirements of each sub-system

Sub-System	Minimum Voltage (V)	Maximum Voltage (V)	Current (A)
Shoulder	9	12	2.4
Elbow	10	14.8	4.1
Wrist	9	12	4.8
Gripper	9	12	3.0

The choice of microcontroller and peripherals informs the required logic levels on-board both the Mother and Daughterboard. As discussed in Section 5.2.3, a Teensy 3.5 is selected for the microcontroller.

The Teensy 3.5 can be powered through a USB cable or through an external power source. As the system is intended for pre-programmed use without a USB connection, an external power source is required. As the recommended power supply for the Teensy 3.5 is between 4.5 V and 5.5 V, a supply of 5 V satisfies this requirement and the operating voltage of other ICs on the Motherboard and Daughterboard are therefore also chosen to be 5 V. This simplifies the design to only requiring a 5 V voltage regulator with a sufficient current supply.

Two widely used regulator types available are linear and switching [73]. Linear regulators lower the input voltage by varying an internal resistance in proportion to the input voltage, causing a constant output voltage. This results in a large amount of waste heat and low efficiency when regulating higher voltages.

To regulate a voltage to a lower level in switching regulators, a buck regulator is commonly used [73]. This circuit uses a transistor as a switch that continually connects and disconnects the input voltage to a conductor, resulting in a lower output voltage.

While switching regulators are highly efficient, they require external components such as inductors, diodes and filter capacitors, whereas linear regulators generally require only a low-value bypass capacitor [73]. Additionally, linear regulators have no ripple and low noise, in comparison to higher ripple voltage due to the switching rate of the switching regulator. Therefore, as the device will be powered by supplies plugged into the mains, high efficiency is not as important as low noise and linear regulators are chosen.

The maximum current draw expected can be calculated by adding together the current draw of the Teensy 3.5 and other peripherals that are discussed in sections 5.2.2 and 5.2.4. By adding these together, the approximate current draw expected is 0.3 A.

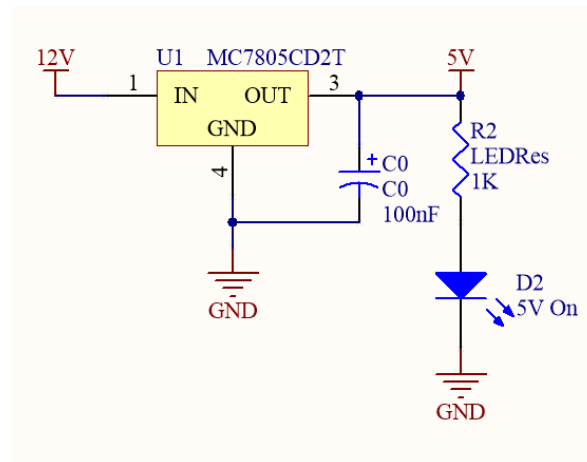


Figure. 5.3: Schematic of the MC7805 5 V regulator aboard the Motherboard and Daughterboard.

The MC7805 linear voltage regulator is selected to lower the input 12 V rail to 5 V to operate the Teensy 3.5 and peripherals as it is capable of a maximum current output of 1 A [74]. Figure 5.3 displays the linear regulator's implementation in a circuit schematic form.

The MC7805 is a simple package that does not require external components. However a bypass capacitor is included to improve transient response and stability and a red LED (D2), is included to indicate a voltage output.

### Reverse Polarity Protection

As the system is intended to be used by a variety of people with varying levels of experience with electronics, the risk of improper setup needs to be reduced. While a blind-mating, snap-in terminal is used as the power connector to prevent improper power connections to the board, this does not prevent the opposing terminals from being plugged in incorrectly.

To protect the circuit from reverse polarity connections, a reverse battery protection circuit is implemented using a P-Channel MOSFET [75]. With the P-Channel MOSFET placed in a forward direction from drain to source, the device will turn on when current of the correct polarity is applied. However, a negative polarity current will fail to power the device, preventing current from flowing further into the circuit. The implementation of this circuit is shown in Figure 5.4

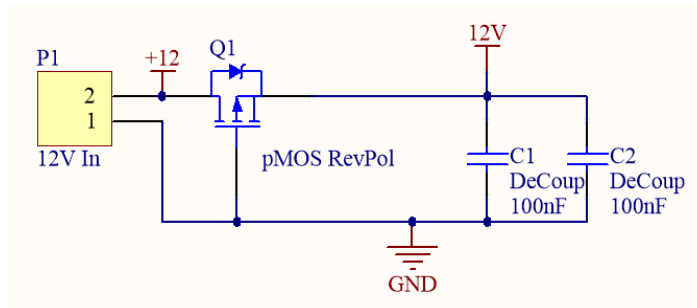


Figure. 5.4: Reverse Polarity Protection Circuit.

Each MOSFET has a body-diode forward voltage, which is the guaranteed voltage drop from the diode of the MOSFET. The value of this voltage drop varies dependant on the specific MOSFET and as such, the MOSFET selected for reverse polarity protection should have a voltage drop lower than 1 V.

The SQJ407EP P-Channel MOSFET is selected as the maximum applied voltage is 20 V and it is capable of sinking 60 A of current [76]. This rating exceeds the requirements that are outlined in Section 5.3.1, and therefore it is capable of supplying both the Motherboard and

Daughterboards. The SQJ407EP has a voltage drop of 0.75 V, which is within the acceptable range of operation for the servomotors. The temperature response of the SQJ407EP for the maximum current draw of 15 A is within the operational area.

## 5.2.2 Communication

Communication is essential to the operation of the overall system and there are several communication topologies that must be incorporated into the design of the Motherboard. The Motherboard should be capable of communication with an external musical controller using MIDI and communicate with the Daughterboard using an appropriate serial communication protocol.

### MIDI

The system is intended to be driven using a MIDI keyboard or another live MIDI-In and therefore a MIDI-In terminal and the ability to process this data into messages that can be interpreted by the microcontroller is necessary. A switch would be advantageous for the user to select between operating on pre-defined routines for playing the instruments or to use an input from a USB connection.

As discussed previously in this chapter, MIDI signals are generally transmitted through 5-pin DIN connectors. The exact layout of a traditional MIDI cable is shown in Table 5.2 and Figure 5.3.

One of the reasons why MIDI is widely used is that a single MIDI link is capable of connecting up to 16 individual devices [77]. If each of these devices introduces a load to the MIDI link, then the reliability of the signals being sent and received decreases. Instead of adding a load to the network, an opto-isolator is used as they introduce no load to the MIDI cable. As shown in Figure 5.5, the anode and cathode pins of the MIDI-In terminal connect to the opto-isolator, producing a single output which connects to the Teensy 3.5 through a toggle switch.

Table 5.2: Standard pin definition of MIDI cables

MIDI Pin Layout	
Pin Number	Designation
1	No Connection
2	Shield
3	No Connection
4	Voltage Reference
5	Data Line

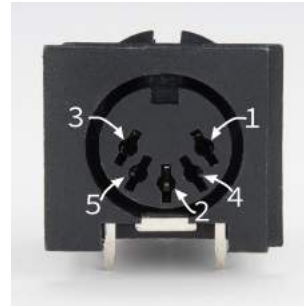


Table 5.3: figure Pin layout of a 5-pin DIN connector [71]

The 6N138 single channel optocoupler is frequently used in modern designs for detection of MIDI signals due to its 60 mA output current and self-contained package [78]. The current is limited to 10 mA by R3 to be compliant with the Teensy I/O pins which are rated to a maximum of 25 mA of input current.

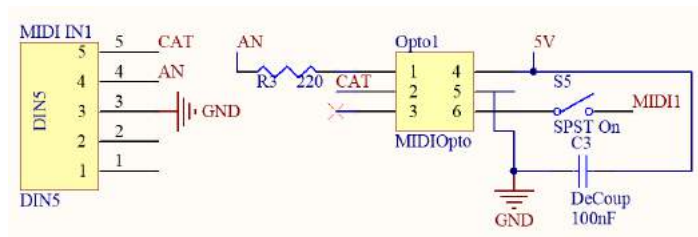


Figure. 5.5: Opto-Isolator Circuit.

### RS485

To communicate between the Motherboard and Daughterboard a communications protocol must be selected.

MIDI communication could be used to co-ordinate between the Mother and Daughterboards. However, as will be discussed in Chapter 6, MIDI transmits messages through three bytes of data. The structure of these packets is pre-defined in the MIDI electrical specifications, which describes the information included in each byte. There are only 4 bits of data that are reserved for system specific information, allowing for up to 16 commands to be programmed [77]. However, these bits are often used as system exclusives, allowing manufacturers of musical controllers to program their own functionality. Additionally, the use of MIDI complicates the software design of the system due to the current capability of MIDI-In from a musical controller. Coding to use MIDI between the Mother and Daughterboard would require re-definition of functions that are used between the Mother and the musical

controller. The overall system design includes three individual robotic arms, with a total of 18 actuators to position. Therefore, MIDI is not an appropriate communication type for this project and does not allow for future expandability.

As mentioned previously, the Dynamixel servomotors communicate using serial communication, sequentially sending data over a defined channel. The Dynamixel servomotors use two different types of serial communication, RS-485 and Half-Duplex Asynchronous Serial. The type used is dependant on the series of servomotor.

RS-485 defines a serial communication protocol that utilises a multi-drop, single-master configuration, transmitting data differentially across two wires [79]. One wire acts as the receive line, and another as the transmission line. RS-485 is a half-duplex serial communication protocol, limited to either receiving or transmitting data, unable to do both simultaneously.

Each device on an RS-485 network is connected in series across a twisted pair of wires. As RS-485 only defines the electrical characteristics of the circuit, each user of this communication type is able to define their own software protocol for packetisation on the software side.

RS-485 is often implemented in a master-slave configuration where the master device initiates all communication in the network. The control hierarchy of the Mother and Daughterboards allows for the implementation of a master-slave arrangement, with the Motherboard acting as the master and Daughterboards as slaves.

RS-485 is capable of data transmission at a rate of up to 10 MBps across a distance of 10 m, or at lower speeds to a range of 1200 m [79]. The maximum length of cable recommended for Half-Duplex Asynchronous Serial communication operating at this data rate is 0.5 m. This limits the potential layout of the system significantly, and therefore Half-Duplex Asynchronous Serial is not the preferred protocol. The maximum data rate the Dynamixel servomotors are capable of is 1 MBps and so the Teensy is configured to operate its serial communication lines at this data rate.

RS-485 uses three-state logic, consisting of reception, transmission and high-impedance mode. Each of the slave devices waits to be addressed in high-impedance mode, with the master device starting communication every time. Once the signal reaches the end of the

twisted pair line, signal reflection occurs which can cause data corruption and instability in messages. To prevent signal reflection, a pair of terminating resistors equal to that of the wire's characteristic impedance are placed at the start and end of the twisted pair line. These resistors are generally  $120\ \Omega$  and their placement is shown in Figure 5.6.

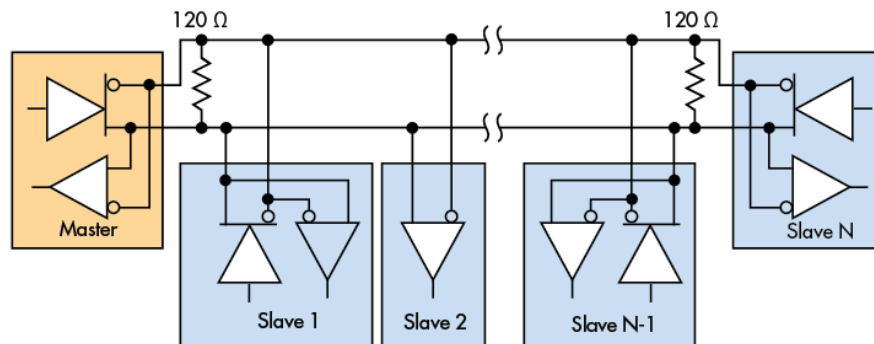


Figure. 5.6: RS-485 Master-Slave topology [80].

RS-485 is selected as the communication type between the Mother and Daughterboard as it supports a custom packetisation scheme which will permit a re-configurable software design without limiting the potential of the system.

A termination resistor can be placed alongside the RS-485 IC which handles the Dynamixel communication and an internal termination resistor within the Dynamixel servomotors impedance matches the system [81]. The Motherboard will have a terminating resistor placed on-board. However, it is unknown which of the three arms will be connected to the end of the twisted pair line. To increase the modularity of the project, each Daughterboard has a termination resistor, which allows any of the three to be the terminating device. This increases the total impedance on the transmission line, increasing the delay in transmission. However, this delay is insignificant given the 1 MBps transmission rate that will be used. R5 in Figure 5.7 was chosen for the termination resistor for the Motherboard as this is equal to the characteristic impedance of Dynamixel servomotor hook-up wire.

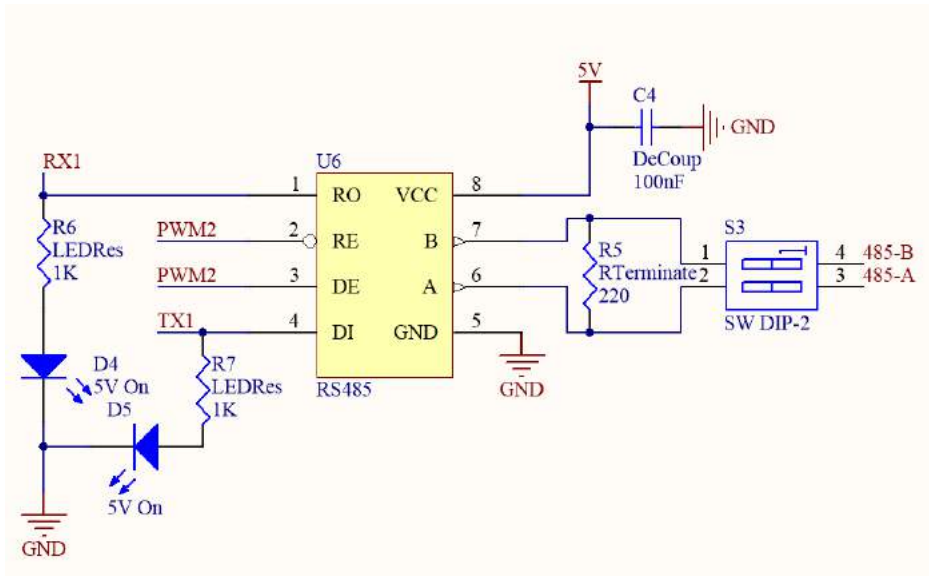


Figure. 5.7: RS-485 Circuit schematic.

The SP3485 is a 5 V tolerant, low power, half-duplex transceiver that meets the electrical specifications of RS-485 [82]. Capable of data rates of up to 10 MBps, this device is selected as the communication IC for both Dynamixel communication and Motherboard to Daughterboard communication.

### 5.2.3 Microcontroller

A microcontroller is necessary to communicate to the Daughterboard and receive instructions over USB or MIDI. The microcontroller selected must be capable of interfacing with the Daughterboards' control systems. This creates a circular loop of microcontroller choice, as both must be capable of interfacing with each other. A solution to this is to use the same microcontroller for both boards, as this only requires familiarisation of protocols for a single microcontroller.

The microcontroller also needs to provide the GPIO functionality for the implementation of sensors and programmable IC's. The clock speed of the processor is generally recommended to be at least 16 times the expected value of the incoming transmission rate [83]. Therefore the clock must have a frequency of at least 16 MHz to accommodate the 1 MHz Dynamixel communication speed. The microcontroller should also provide non-volatile storage so that look-up tables and system data are retained when the system is powered

down.

An individual microcontroller IC requires passive and active circuitry to enable full functionality of the package, such as an oscillator crystal for timing, pull-up resistors and communication modules. This would increase the complexity of the Mother and Daughterboard design. An all-in-one development board, with microcontroller and peripheral support integrated would be advantageous.

Due to the physical size requirements (discussed further in Section 5.2.6), the development package selected should have compact dimensions. A number of development boards which feature the peripheral support and communication topologies required have a large physical size, such as the Jetson, Arduino and Raspberry Pi 3. Conversely, smaller packages which support the communication topologies, often lack the I/O pins required by the external sensors.

The Teensy is a brand of ARM-based microcontroller development board that has processor speeds in excess of 120 MHz, upwards of 25 digital I/O pins, and six serial communication channels [84]. The microcontroller on the Teensy 3.5 is the Kinetis K64, based on the Cortex-M4 ARM architecture [85]. This is a flexible microcontroller framework and allows for a wide range of software libraries to be implemented. As mentioned in Section 5.2, the Teensy is 5 V tolerant.

The Teensy 3.5 has 42 analog & digital I/O pins, enough to support the peripherals discussed in Section 5.2.4 [84]. The pinout of the Teensy 3.5 can be seen in Figure 5.8 and shows the supported signal types for each pin. The multiple communication protocols and data transmission rates outlined in Section 5.2.2 can be handled by the Teensy 3.5 as it has a 180 MHz clock speed.

Native USB support allows instruction signals to be sent directly over a USB connection. The Teensy may be programmed using C++ and is Arduino compatible, making a wide range of libraries available for later implementation.

The Teensy 3.5 also meets the requirements outlined for onboard storage by providing 4 Kb of EEPROM which can retain look-up tables containing dynamic values that would otherwise be lost upon powering down (such as the number of total rotations that a servomotor has completed).

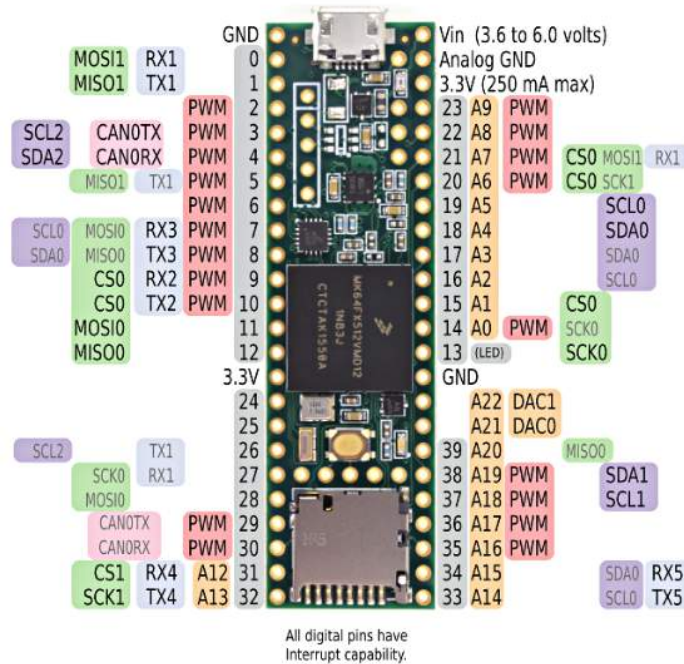


Figure. 5.8: Pinout of the Teensy 3.5 [84].

## 5.2.4 Additional Peripherals

The selection of a Teensy 3.5 provides the required I/O pins for the Daughterboard, however, the Motherboard does not require the same depth of GPIO usage. It would be advantageous for the unused pins to be available for further expansion of the overall system and incorporation of sensors or visual feedback.

### GPIO

To maximise the usability of the Motherboard, additional GPIO pins should be provided to facilitate the addition of external sensors or testing equipment into the project at a later date.

As the Motherboard is primarily for power relay and communication between boards, a large number of I/O pins remain unused on the Teensy 3.5. The remainder of the GPIO pins have been broken out into three separate headers to be used for future testing or external sensor inputs. This is shown in Figure 5.9, with three  $4 \times 2$  headers consisting of the unused GPIO pins.

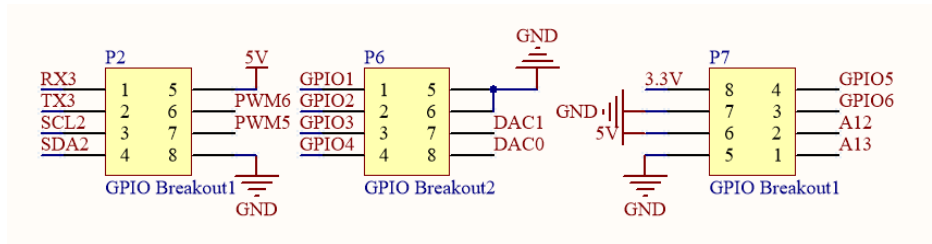


Figure. 5.9: Circuit schematic of broken out GPIO pins on the Motherboard.

### 5.2.5 Status Indicators

As outlined in Chapter [1](#), the system is designed to be capable of operating autonomously and will require an external method of indicating the current status of the Motherboard. This should be done visually to indicate to the operator what the current condition of the system is.

The system is intended for use without a connection from the Teensy 3.5 to a PC, therefore data cannot be conveyed over the serial monitor. As such, external methods of conveying system status are required. LEDs can be used to convey a host of messages to the user of the current status of the system.

A binary number system can be used to efficiently represent status messages with minimal components. For example, 4 LEDs allows for up to 15 individual messages assuming that "no lights" is not used as a status. An example scheme of conditional messages to be implemented on the Mother and Daughterboards is shown in Table [5.4](#).

Table 5.4: Example status indicator scheme

	Motherboard	Daughterboard
1	Arm #1 Connected	Awaiting Input
2	Arm #2 Connected	Currently Playing
3	Arm #3 Connected	USB Connection
4	Custom Designator	Improper Voltage
5	Custom Designator	Overheating
6	Custom Designator	Sensors not connected
7	Custom Designator	Servomotors not connected
...		
15	Custom Designator	Custom Designator

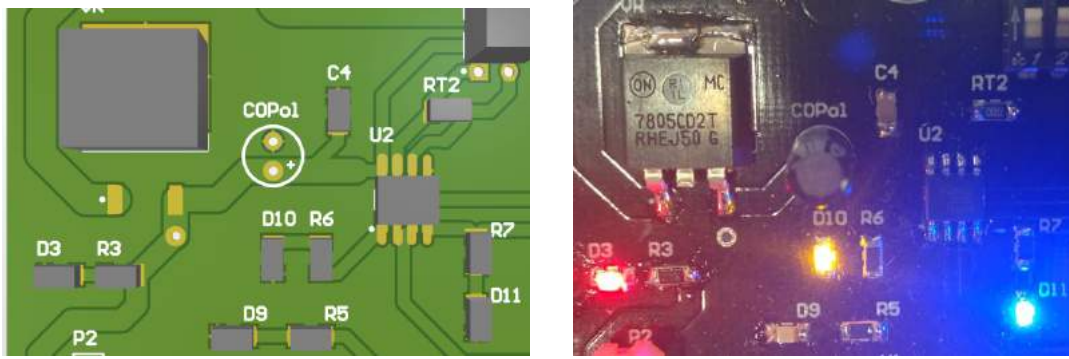


Figure. 5.10: Design of the RS-485 communication LEDs (Left) and the implementation of communication LEDs (Right)

To visually indicate when the Motherboard is communicating with the Daughterboards, or when the Daughterboards are communicating with the servomotors, indicator LEDs are attached to the RX and TX lines of the serial communication ports. Blue and yellow LEDs are used to distinguish between RS-485 transmission and reception respectively. D10 and D11 of Figure 5.10 are the reception and transmission LEDs of the Motherboard.

## 5.2.6 Physical Design

The size requirements of the Motherboard are for the PCB to be as discrete as possible and to allow for external mounting. Additionally, the physical terminals for power, RS-485 and MIDI communication should be located in positions which allow for ease of connection.

The final dimensions of the Motherboard are 75 mm × 90 mm and include M3 mounting positions in the four corners of the board. The location of the power output and communication terminals is at the top of the board to allow for cables to easily be plugged in, as seen in Figure 5.11. As mentioned in Section 5.3.1, the trace width determines the current that can flow without causing overheating. The Motherboard must be capable of transferring high current to the Daughterboards. Trace thickness can be calculated based on the copper thickness and the current expected to travel through the trace using Equation 5.1 [70].

$$A(\text{mm}^2) = \frac{I}{(k * (T_{rise})^b)^{\frac{1}{c}}} \quad (5.1)$$

$$A = 0.53 \text{ mm}^2$$

where  $A$  is the area in  $\text{mm}^2$ ,  $I$  is the maximum current expected through the trace,  $T_{\text{Rise}}$  is the allowable rise in temperature above ambient temperature and  $k, b$  and  $c$  are constants derived from the IPC-2221 specifications on trace width calculation [86]. Using equation 5.1, with 15 A as the maximum current flow expected through the high power trace and an acceptable rise in temperature of  $35^\circ\text{C}$ , we calculate a trace area of  $0.53 \text{ mm}^2$ . From this, we calculate the recommended external trace width using Equation 5.2 [70].

$$W(\text{mm}) = k * (T_{\text{rise}})^b * A^c \quad (5.2)$$

$$W = 2.94\text{mm}$$

where  $W$  is the width of the trace required and  $k, b$  and  $c$  are the constants from IPC-2221. With a known cross-sectional area of  $0.53 \text{ mm}^2$  and a temperature rise of  $35^\circ\text{C}$ , 2.94 mm is the trace width required for 15 A of current. A safety margin of 0.5 mm is used on the high power traces of the Mother and Daughterboards, increasing the maximum current capacity to 17 A.

Following microcontroller trace recommendations, the design of the Motherboard runs all traces either horizontally or vertically to minimise cross-talk between planes.

The design of the Motherboard achieves the requirements outlined at the beginning of the chapter by supporting multiple communication topologies, incorporating power protection and regulation circuitry, and selection of an appropriate microcontroller. The final design of the Motherboard is packaged on a small form-factor PCB, including room for expansion through multiple GPIO pins, selectable MIDI-In and visual status indicators for the user.



Figure 5.11: Image of Final Motherboard design.

## 5.3 Daughterboard Design

The design requirements of the Daughterboard are similar to that of the Motherboard in the power requirements, physical size and communication types. However, the Daughterboard must support the near instantaneous current requirements of the actuators and support the external sensors selected in Section 3.9.

### 5.3.1 Power Requirements

As the system uses the Dynamixel servomotors discussed in Section 3.4, the Daughterboard needs to be capable of integrating with the power output terminal of the Motherboard and powering the three different series of servomotor. The robotic arm consists of a total of two AX-12s, three RX-24Fs and an MX-64T servomotor. Figure 5.12 displays the six servomotors and their respective locations to the control diagram. All three servomotors have different voltage ranges as shown in Table 5.5

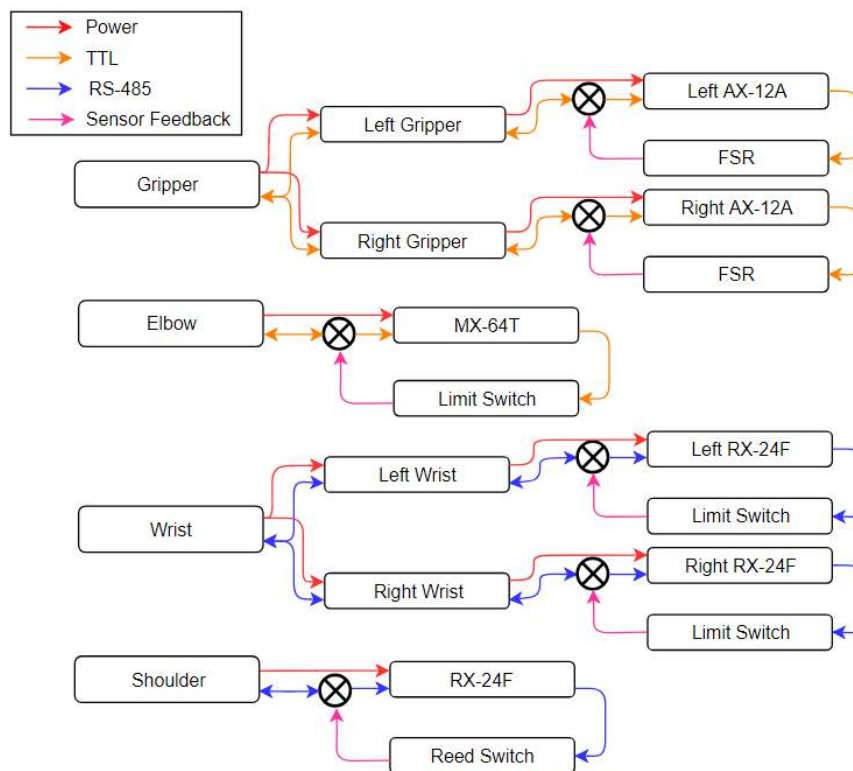


Figure. 5.12: Control flow diagram for the Daughter's sub-systems

The common voltage at which all three series can operate is 12 V. The total power requirement of the servomotors being used on the Daughterboards consists of the individual power draw of the six motors. Servomotors draw a peak current when the torque load on the output shaft causes the output rotational speed of the motor to be zero, stalling the motor. The RX-24 has a peak current draw of 2.4 A at its stall torque, resulting in a current draw of 4.8 A through the wrist servomotors, and 2.4 A through the shoulder servomotor. The AX-12A reaches a peak current of 1.5 A and the MX-64T has a maximum of 4.1 A when operated at 12 V. The resultant current requirement of the servomotors is 14.3 A if every motor operates at stall torque.

Table 5.5: Key Characteristics of the three series of Dynamixel Servomotor

	AX-12A	RX-24F	MX-64T
Weight (g)	53.5	67	135
Stall Torque (N.m)	1.5	2.6	6
Stall Current (A)	1.5	2.4	4.1
Standby Current (mA)	50	50	100
Voltage Minimum (V)	9	9	11.1
Voltage Maximum (V)	12	12	14.8
Recommended Voltage (V)	11.1	11.1	12
Protocol Type	Half Duplex	RS-485	Half Duplex

Assuming a peak draw of the peripheral components of 1 A, the total power supply should be capable of supplying a minimum of 180 W of power. However, the capability of the power supply should be greater than the minimum power draw of the system for reliable operation.

The power supply that is used to power the Motherboard and Daughterboards must be capable of supplying the worst case scenario of 180 W of power to match 15 A current draw at 12 V. We select the Topward 630D DC power supply as it can supply 205 W of power output across three separate outputs, or one single output [87].

The Dynamixel servomotors draw a current that is proportional to the torque which is required to move the servomotor shaft. The servomotor shaft requires the greatest amount of torque when first shifting the load connected to the shaft. The power supply may not be able to switch fast enough to provide the current required by the Daughterboard immediately. When the load on the power supply is suddenly increased by a large amount, the output voltage will momentarily drop. The opposite happens when the load is suddenly disconnected, with the output voltage peaking slightly. Reservoir capacitors can be used to compensate for the sudden increase in current, smoothing the impact of the voltage change. The drop in voltage is commonly referred to as the voltage droop. The maximum allowable voltage droop from the power supply to the Dynamixel servomotors is 0.5 V, as this is still within the minimum voltage range of the servomotors. These requirements lead to the power management discussion presented in Section 5.3.2 below.

### 5.3.2 Power Management

To calculate the size of the reservoir capacitors required, equation 5.3 is used, where  $t_{Switch}$  is the transient response of the power supply,  $I$  is the current and  $V_{droop}$  is the maximum voltage drop allowable [88]. The maximum current expected to be drawn at any given time is 15 A, the voltage droop is 0.5 V and the transient response of the Topward 6303D power supply is 100  $\mu$ s. Therefore, the minimum capacitance required is 3000  $\mu$ F. The reservoir capacitors on the Daughterboard are over-specified to at 6000  $\mu$ F.

$$C = \frac{I * t_{Switch}}{V_{Droop}} \quad (5.3)$$

To minimise the noise introduced by the high power components, the PCB layout is designed to isolate the servomotors from the microcontroller and surrounding peripheral components. This is accomplished by placing the high power servomotor terminals close together and at the top end of the PCB, away from the Teensy.

Due to the high current draw of the servomotors and to reduce ground noise they introduce, a cutout layer separates the servomotors from the rest of the PCB. This isolated layer is connected to the output of the reverse polarity transistor, flooding the plane with charge, increasing the total capacitance. Figure 5.13 displays the connection from Q1, the reverse polarity transistor, to the isolated 12 V plane where C5-10 provide additional capacitance. P4 and P5 are the RS-485 servomotor terminals with two data lines as inputs, whilst P7 and P8 are the Half-Duplex Asynchronous terminals.

The data lines to the servomotor terminals within the 12 V plane connect to the main section of the Daughterboard using jumper switches, allowing the two regions to remain isolated. These jumper switches can be seen in Figure 5.13 as S2 and W1. This allows the data line to the servomotors to be programmed without fear of the servos moving or causing unintentional damage when they are switched off.

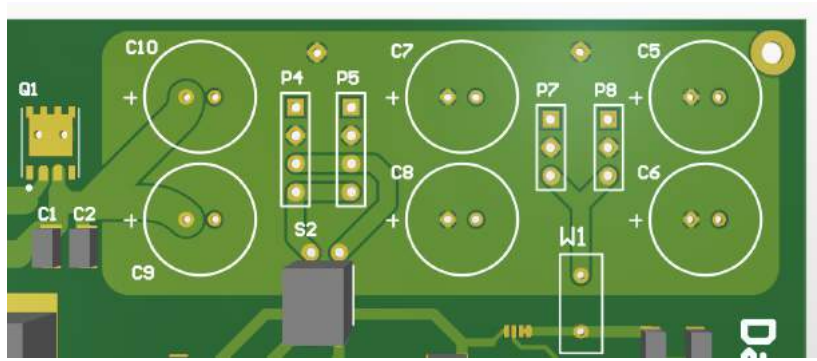


Figure. 5.13: High power section of the Daughterboard PCB

As with the Motherboard's design of traces, the width of the Daughterboard's power management traces are 3 mm wide. Additionally, the microcontroller traces run either horizontally or vertically to minimise cross talk introduced between the top and bottom plane of the PCB.

Section [5.2.1](#) discussed the use of the MC7805 linear regulator for stepping down the voltage from the 12 V rail to a 5 V rail. As the Daughterboard also uses the Teensy 3.5 microcontroller and similar peripherals rated to a 5 V logic level, the same regulator circuitry is used.

Reverse polarity protection is discussed in Section [5.2.1](#). While the final design intention is to have the Motherboard supplying power to all three arms, for testing purposes the arms are powered individually. The issue of improper power supply setup can cause damage to the electronics on-board. The same pMOSFET package is used on the Daughterboard to protect against reverse currents.

As the Daughterboards may be operated individually, they must be able to interface with the Topward power supply. The same power management terminals and voltage regulator as the Motherboard are used due as they operate at a shared voltage. The blind-mating snap-in terminal discussed previously is again used as the power terminal to the Daughterboard.

### 5.3.3 Daughterboard to Dynamixel Communication

The Dynamixel servomotors communicate using RS-485 and Half-Duplex asynchronous serial. Therefore, the Daughterboard needs to be able to communicate using both RS-485 and Half-Duplex Asynchronous Serial. As discussed in Section 5.2.2, the Daughterboard also needs to integrate with the Motherboard to receive commands. This is accomplished by using RS-485 and the aforementioned SP3485 package for communicating with the Motherboard and with the Dynamixel servomotors.

Half-Duplex Asynchronous Serial communication is required for transmitting and receiving information from the AX and MX series Dynamixel servomotors. Half-Duplex Asynchronous Serial communication uses tri-state logic levels to determine whether it is transmitting or receiving data [89]. This consists of two outputs and one input. The outputs are the transmission and Transmit Enable line, whilst the reception line is the input. To transmit data to an AX or MX servomotor, the direction pin must be enabled HIGH, opening the TXD pin for transmission, whilst simultaneously disallowing incoming signals on the RXD line and vice versa. This can be seen in Figure 5.14, where the Direction Port, TXD and RXD lines are tied to Teensy 3.5 output pins. Control of the direction port is set in software.

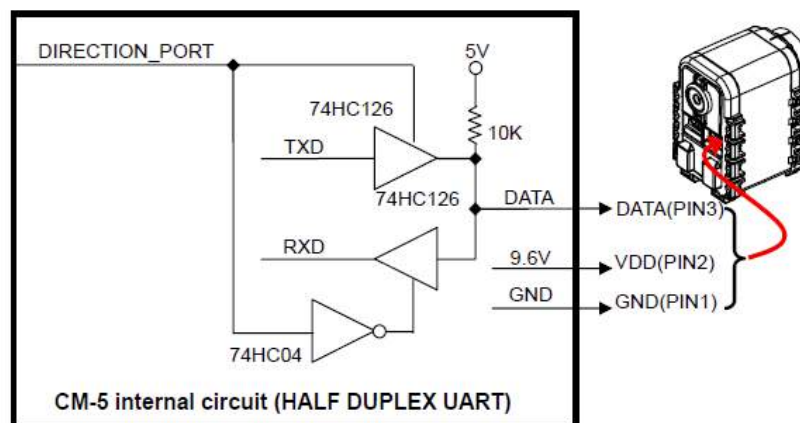


Figure. 5.14: Half-Duplex Asynchronous communication circuitry to support the Dynamixel Servomotor [38]

The SN74LVC2G125DCTR IC is a dual line driven, tri-state buffer capable of Half-Duplex Asynchronous Serial communication [90]. By configuring the two Transmit Enable pins to be the inverse of each other in software, transmission is always disabled when receiving and vice versa.

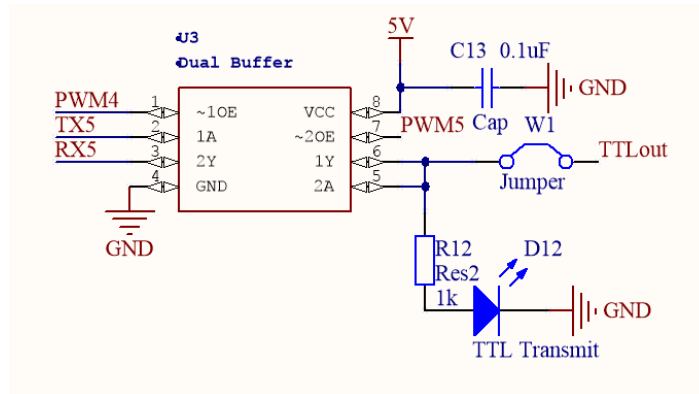


Figure. 5.15: Circuit Schematic of the SN74LVC2G125DCTR package

The Daughterboard requires two RS-485 packages to communicate to the Dynamixel servomotors and the Motherboard. To reduce the chance of improper connection during setup, the Motherboard communication terminal is placed on the left-hand side of the PCB, away from the servomotor terminals.

### 5.3.4 Microcontroller

### 5.3.5 Peripherals

A visual indicator of the system status and especially the presence of a fault is a useful feature. As such, a set of status indicator LEDs are included in the bottom right section of the PCB, as can be seen in Figure [5.16](#).

The Daughterboard must also incorporate the required number of GPIO pins to facilitate external feedback on the status of the servomotors. As discussed in Chapter [3](#), this includes two limit switches for the wrist, one limit switch for the elbow, two force-sensitive resistors (FSR) for the grip and a reed switch for shoulder rotation. The feedback for these sensors will be incorporated to provide safe limits on the servomotor's actions, as shown in Figure [5.12](#).

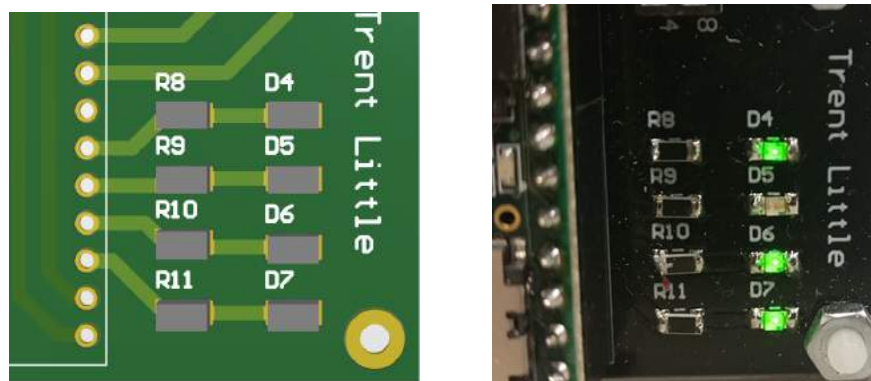


Figure. 5.16: Design of status LEDs (Left) and the implementation of status LEDs to indicate code 11 (Right)

To distinguish between RS-485 and Half-Duplex Asynchronous Serial, blue and yellow LED's represent transmission and reception of RS-485 respectively, whilst an orange LED indicates incoming/outgoing signals on the Half-Duplex Asynchronous Serial data-line. The placement of the orange LED, D12, can be seen in Figure 5.15. The Daughterboard also has the previously mentioned red LED on the 5 V rail.

Each of the Daughterboards is identical and although unique identifiers are assigned in software to differentiate between them, visual distinction is an important characteristic. The three arms are designed to be interchangeable, and as such, any manual identifier should be changeable. To achieve this, a 4-pole, 3-way rotary switch is included to allow the user to select what number each board is assigned. The output of the switch routes through different coloured LEDs (blue, orange, green) to indicate which path is currently selected. This switch can be used in software to determine whether it is Arm #1, #2 or #3. Based on this selection, the microcontroller will determine the actions to carry out; this will be discussed in Chapter 6.

The Motherboard included  $4 \times 2$  header pins breaking out the unused GPIO pins for additional use. The Daughterboard implements similar  $4 \times 2$  header pins, however, these receive feedback from the external sensors described in Chapter 3.

### 5.3.6 Physical Size

The constraints for the physical size of the board are that it must be able to integrate into the chassis of the system. The final dimensions are  $85 \text{ mm} \times 100 \text{ mm}$ , with M3 mounting holes in each of the four corners. A custom 3D printed holster is designed in Chapter 3 to mount the Daughterboard to the chassis effectively.



Figure. 5.17: Image of Final Daughterboard design.

## 5.4 Summary

The Motherboard splits a single power supply input and supplies the three daughterboards in parallel. The Motherboard has been designed to take either USB input or MIDI-In and distribute the resultant physical commands for the servomotors to the Daughterboards at high transmission speed using RS-485. The Daughterboard supports communication to both protocols of the Dynamixel servomotors and incorporates external sensors to provide feedback. Both are designed with visual status indicators, reverse polarity protection and have terminals located on the periphery of the board to allow for ease of use by an external operator.

A Motherboard and multiple Daughterboards have been designed with the communication scheme shown in Figure 5.2 and with the control system of Figure 5.12. Parallelisation of the communication between the Motherboard and Daughterboard allows a master-slave topology to be implemented using the communication protocol RS-485. The software required to communicate between the Motherboard, Daughterboard's and actuators' is discussed and implemented below in Chapter 6.

## Chapter 6

# Software

The signals sent from the Motherboard to the Daughterboard, and from the Daughterboard to the servomotors, are controlled with microcontrollers. The Motherboard microcontroller must co-ordinate communication from the user to the Daughterboard. As discussed in Section [5.2.2](#) the Mother and Daughterboard communicate through RS-485. This requires a control scheme to co-ordinate the transmission and reception of messages.

The Daughterboard co-ordinates communication to the sub-systems of the arms, and the servomotors and sensors they are comprised of. This includes calibration and operation of the two different topologies of Dynamixel servomotors. The software of the Daughterboard must control the Dynamixel actuators of each sub-system and incorporate feedback from internal and external sensors to ensure the system is operating within the recommended limits

This chapter outlines the design and implementation of the embedded software that co-ordinates communication between the Mother and Daughterboard, and the Daughterboard to the individual sub-systems.

### 6.1 Daughterboard Communication to Dynamixel Actuators

As detailed in Section [3.4](#), the Dynamixel servomotors are used as the actuators for the individual sub-systems. The Dynamixel servomotors require software instructions to operate, which are provided by the Daughterboard microcontroller. The format of these instructions is specific to the Dynamixel, requiring a pre-defined instruction packet structure.

The Dynamixel series servomotors are controlled using an on-board microcontroller which communicates to the main controller using a pre-loaded control table loaded into the microcontroller's firmware. This control table consists of multiple data fields that the user can read information from or write instructions to.

The Dynamixel servomotors incorporate internal ID, Baud Rate, present position, voltage, load, and temperature sensors into its operation. The readings of these sensors are stored on the Dynamixel microcontroller and can be polled for in software.

The message format that the Dynamixel servomotors expect to receive is: two Start Bytes, the servomotor ID, length of the command, the instruction given, additional parameters and finally a checksum [38]. The start bytes notify the microcontroller of the beginning of a message. The servomotor ID is programmable from zero to 255 addresses in the daisy chain. The length indicates the total number of parameters in the overall message. The instruction command refers to the pre-loaded control table on the servomotor microcontroller. The parameter bytes store ancillary information if required by the individual instruction. Finally, the checksum determines if the packet was damaged during transmission and is calculated according to the ID, length, instruction, parameters (N) added together and then inverted. The overall packetisation of these messages is shown in Figure 6.1.



Figure. 6.1: Packetisation of Dynamixel instructions

When the Dynamixel has executed the command, a return packet is sent to the controller which is identical aside from the instruction byte being replaced with an error byte. The value of this error byte is representative of the error which has occurred, detailed below in Table 6.1 [38].

An open source library that pre-defines transmission of the unique packetisation structure of the Dynamixel is incorporated into the software of this project [91]. This library pre-defines a number of functions that will be useful for this project, such as move commands and sensor feedback commands. However, the last update to the available libraries was in 2011. Since then, the Dynamixel firmware has been updated, requiring some of the functions be rewritten to match these changes. Additional alterations must be made to the library for it to be compatible with the Teensy 3.5 and support both communication topologies of the servomotors.

Table 6.1: Dynamixel Error Codes

Bit	Name	Definition
7	0	Successful
6	Instruction Error	An undefined instruction was received by the servomotor microcontroller
5	Overload Error	The load applied to the servomotor shaft exceeds the hardware limit
4	Checksum Error	Checksum of the transmitted instruction packet is incorrect
3	Range Error	Transmitted move command exceeds the servomotor's limits
2	Overheating Error	Internal temperature of the servomotor exceeds the operating temperature limits
1	Angle Limit Error	Goal location of the command is set outside of the angular limits defined
0	Input Voltage Error	Voltage applied to the servomotor is outside of the operating range

The methods included in the Dynamixel library simplify the aforementioned communication protocol into a functional programming based library. This allows the user to call on methods such as `Dynamixel.readLoad(ID)` that sends the packets required and returns the value of the load which is currently applied to the shaft of the servomotor.

The library used a tristate buffer that included an internal inverter to provide a high and low response from a single pin. However, the buffer selected in Section [5.3.3](#) for controlling the Dynamixels in this project does not include inverting features. The library was thus changed to provide an inverted signal to an adjacent pin on the Teensy, manually providing the inverted signal to disable the receiver/transmitter and vice versa.

To make the library used for the half-duplex communication suitable for RS-485 requires changes to the functions to support two separate transmission and reception pins. This involves altering each method to write to both data pins of the servomotors in tandem.

The time required to transmit an instruction to the servomotor is less than the time required to carry out said instruction. If a delay is not included between sending each command, using either Half-Duplex or RS-485, the command may become corrupted. This is caused by the controller sending the start of a new command before the previous command has been executed and returned. Without a delay, erroneous operation of the servomotors occurred and the instructions were being properly transmitted around 50% of the time.

The time required to transmit and receive each instruction is evaluated to determine the minimum delay required before risking data corruption. The operation with the longest write/read time is the “move position” command, as when a new position instruction is received before the initial command is completed it will over-ride the initial and move to the new location. The delay required for this function is approximately 8 ms, therefore the delay implemented between functions calls is set to this 8 ms maximum.

Table 6.2: Execution time of various Dynamixel methods

Instruction	Time (ms)
move()	8
turn()	5
torqueStatus()	2
setVoltageLimit()	1
setMaxTorque()	1
setEndless()	1
readTemperature()	1
readPosition()	1
readLoad()	2

Power to the actuators was discussed in Section 5.3.1, where a 12 V power rail was selected. However, this does not prevent a higher or lower voltage from being connected by the user. Based on the voltage ranges of the individual Dynamixel servomotors discussed in Section 3.4, the maximum deviation from the set voltage is 1 V either side of the 12 V set point.

`setVoltageLimit()` is a method provided by the library used and defines the maximum and minimum operating voltage that the actuator will operate within. If the voltage provided is outside of the operating limits, the servomotor microcontroller generates an interrupt that disrupts the power to the servomotor. This prevents operation of the servomotors when the voltage is outside of the 11 V to 13 V limit. The values `lowerVoltageLimit` and `upperVoltageLimit` are the arguments provided to the `setVoltageLimit()` function, with the packetisation scheme shown below in Listing 15.

```

1 int DynamixelClass485::setVoltageLimit(unsigned char ID, unsigned char
  lowerVoltageLimit, unsigned char upperVoltageLimit){
2   Checksum = ~(ID + Length + Write Data Instruction + Set Voltage Limit +
  lowerVoltageLimit + upperVoltageLimit)&0xFF;
3   switchCom(Direction_Pin , TX); // Set Direction pin to Transmission mode
4   sendData(0xFF); // Start Byte
5   sendData(0xFF); // Start Byte
6   sendData(ID); // ID Packet
7   sendData(Length); // Length Packet
8   sendData(Write Data Instruction); // Instruction Type
9   sendData(Set Voltage Limit); // Parameter 1
10  sendData(lowerVoltageLimit); // Parameter 2
11  sendData(upperVoltageLimit); // Parameter 3
12  sendData(Checksum); // Checksum
13  delayus(TX delay); // Transmission Delay
14  switchCom(Direction_Pin ,Rx_MODE); // Set Direction pin to Reception mode
15 return (read_error()); // Return error packet

```

Listing 6.1: Voltage Limit Function

To transmit the upper and lower voltage boundaries for Dynamixel operation, a total of nine packets of data must be sent to the servomotor. The use of the Dynamixel library reduces the amount of code that must be written to perform commands by wrapping this inside the `setVoltageLimit()` function.

As discussed in Section 5.2.2, the Dynamixel servomotors operate at a baud rate of 1,000,000 bps. This value is set using the baud rate registers of the servomotor microcontroller.

As previously mentioned, a command sent to the Dynamixel servomotor uses a unique ID to select a specific servomotor. The servomotor IDs are from 0-5, in the order of the shoulder, elbow, wrist actuators, and grip actuators. A base of 10 is added to the ID to distinguish between additional arms e.g. the third arm's shoulder servomotor ID would be 30, seen in Table 6.3. The three arms used in this project occupy the range of 0 to 36 of the 255 available ID settings of the Dynamixel servomotors. Expansion of this naming convention would allow for a further 22 sets of addressable arms.

Table 6.3: Dynamixel ID allocation for each arm

	Arm #1	Arm #2	Arm #3
Shoulder	0	10	20
Elbow	1	11	21
Wrist #1	2	12	22
Wrist #2	3	13	23
Grip #1	4	14	24
Grip #2	5	15	25

## 6.2 Sub-System Calibration

### 6.2.1 Shoulder

The shoulder is designed to accomplish striking of a horizontal drum kit within a  $300^\circ$  range. The RX-24F has a range of  $0^\circ - 300^\circ$  of controllable motion, using a 10-bit register to store the position. This results in a controllable range of 0 to 1023 in software. However, it can also operate in continuous mode to provide  $360^\circ$  of rotation. When operating in continuous rotation, no positional feedback is available from the servomotor. This project uses the controllable range of  $0^\circ$  to  $300^\circ$ , as this provides the required arc length for operation described in Section 3.3 and provides positional feedback.

The addressable limits of the shoulder are between  $0^\circ$  and  $300^\circ$ . However, it was observed that movement to either of these positions can result in rotation into the dead-band of operation between  $300^\circ$  and  $360^\circ$  due to the momentum of the arm, shown in Figure 6.2. When the shoulder servomotor enters the dead-band region, it will attempt to re-adjust itself to either of the operating limits. If the shoulder completes a full rotation, the cables which are braided through the once inch pipe rotate as well. This causes twisting of the cables as the terminals which they are connected to remain stationary. Three rotations is the maximum rotation which the system can undergo before twisting to a point of potential damage. The servomotor cannot detect if it has entered or exited the dead-band region, resulting in complete rotations being undetectable without external feedback.

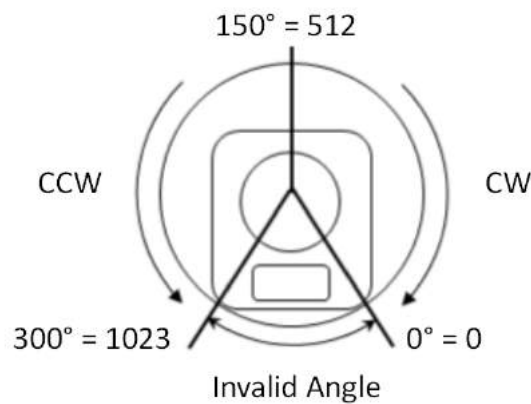


Figure 6.2: RX-24F Area of Operation [39].

A potential solution to this would be to implement a physical limit to the overall shoulder sub-system to prevent further rotation. However, this can potentially damage the shaft of the servomotor due to the momentum of the load causing significant strain.

To monitor the total number of rotations, a reed switch is used. This sensor was selected in Section 5.2.4 to provide external feedback due to its simplistic design, only requiring a magnet to trigger a signal. A neodymium magnet is placed in the underside of the elbow platform. If the shoulder completes a full rotation, the magnet closes the reed switch, sending a signal to the Teensy 3.5. EEPROM storage on the Teensy is used to store the current completed number of rotations, allowing the memory to be preserved after the system is powered down.

This is implemented by tying the reed switch value to an interrupt routine within the operation code of the Teensy. When the value read from the reed switch is detected as a falling edge, the `shoulderInterrupt()` interrupt is entered. However, the reed switch lacks positional information of whether the shoulder is moving clockwise or counter-clockwise. To provide orientation feedback, when the reed switch is triggered, the system checks the orientation of the load register on the Dynamixel. As discussed later in this Chapter, the load register retains information on the current orientation and the total load on the servomotor shaft.

```

1 void shoulderInterrupt(){
2   if(debounce>100 && timerFlag == false){
3     debounce = 0;
4     timerFlag = true;
5     Serial.println("Shoulder in DeadZone");
6     shoulderDirection = Dynamixel.readLoad(1);
7
8     if(2048>shoulderDirection>1023){
9       redirectPosition = 0; // Should re-direct to 0 based on CCW load value
10    }
11    else if(0<shoulderDirection<1024){
12      redirectPosition = 1023; // Should re-direct to 0 based on CW load value
13    }
14    else{
15      Serial.println("Shoulder could not define direction");
16      redirectPosition = currentGoal;
17    }
18    previousPosition = currentGoal; // Save previous goal location
19    Dynamixel485.move(shoulderServoArm1, redirectPosition); //Re-direct within
    operating limits
20    delay(100);
21    Dynamixel485.move(shoulderServoArm1, previousPosition); //Move to previous
    goal location
22    timerFlag = false; // Reset limiter flag
23  } }

```

Listing 6.2: Reed Switch Interrupt Code

The timer `deBounce` and Boolean `timerFlag`, shown on Line [2](#), prevent the shoulder interrupt code from being triggered multiple times. Once the shoulder interrupt is entered, the timer variable and the `timerFlag` are reset, preventing the loop from being entered before re-positioning has occurred. The value read from the shoulder servomotor's load register, `shoulderDirection`, determines the current orientation of the servomotor's rotation and sets the reset position, `redirectPosition`, accordingly. If the value of the load register is outside of the clockwise or counter-clockwise load ranges, the goal position is set as the last position the servomotor was instructed to move to and a warning is printed to the serial monitor. The shoulder is then instructed to return to within the operating range to the position it entered the dead-band from and resumes operation, returning to its previous goal position and the Boolean flag is reset. This prevents cables from becoming twisted and potentially being damaged by ensuring the arm won't complete more than one complete rotation in most cases.

## 6.2.2 Elbow

The elbow was designed in Section [3.6](#) to span a minimum range of  $50^\circ$ . However, the physical design actually permits up to  $80^\circ$  of rotation. The range of the MX-64T is from  $0^\circ$  to  $360^\circ$ . In software, positional control is accomplished with a 12-bit register, 0 to 4095 individually addressable positions, shown in Figure [6.3](#). A single  $360^\circ$  rotation of the MX-64T equates to an angle of  $65^\circ$ , this is less than the  $72^\circ$  range the physical design is capable of. Therefore, multiple rotations of the MX-64T are required to utilise the full potential of the elbow sub-system.

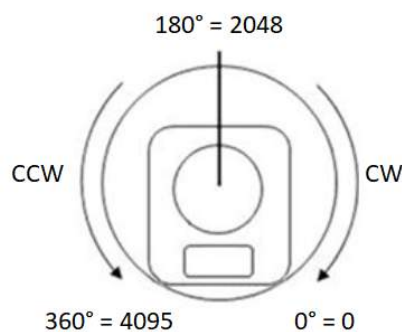


Figure 6.3: MX-64T Area of Operation [\[40\]](#).

The MX-64T is capable of three modes of operation, continuous, joint and multi-turn. Joint mode allows control across a single rotation. Continuous operation was described previously and lacks positional feedback from the servomotor. Multi-turn mode keeps track of the total number of rotations in the clockwise or counter-clockwise direction using a 4-bit register and two's complement. The most significant bit indicates the direction and the three remaining bits track the number of rotations completed. The MX-64T can rotate seven times in either direction, increasing the controllable range to -28,672 to 28,672 positions. Zero is the lower limit of the MX-64T's operable range and 4400 is the upper limit before the aluminium arm contacts the worm gear's shaft.

As detailed in Section 3.6, a limit switch provides positional feedback on the lower limit of the elbow. To calibrate the MX-64T, it is rotated continuously downwards until a signal is received from the limit switch, indicating that the arm has reached the lower limit. This value is then stored in the Teensy 3.5's EEPROM register as the lower limit. The upper limit can be calculated as the total range remains constant.

The operation of the MX-64T is limited to within the calibrated positions by using the `constrain()` method. `constrain()` limits the range of values that can be assigned to a variable, in the case of the elbow sub-system, this is the motor movement variable. The lower limit calculated using the limit switch is used as the absolute lowest position that can be passed to the elbow sub-system, as seen in Listing 6.3

```
1 constrain(int elbowPosition, int lowerLimit, int upperLimit){
2     if(elbowPosition < lowerLimit){
3         elbowPosition = lowerLimit;
4     }
5     if(elbowPosition > upperLimit){
6         elbowPosition = upperLimit;
7     }
8 }
```

Listing 6.3: Reed Switch Interrupt Code

If the value assigned to `elbowPosition` is lower than the minimum value, then it is re-assigned the value of the lower limit. This prevents the elbow from operating outside the known limits of the system.

### 6.2.3 Wrist

As previously discussed in Section 3.8, limit switches are implemented as part of the natural range blockers to detect the lower limit of the wrist servomotors. Given a lower limit at the point of triggering the limit switch and a known range, the upper limit can be calculated. The wrist utilises the same functionality of `constrain()` to prevent movement outside of this set range post-calibration.

These switches are prone to switch bouncing. When the switch is toggled, the contacts move to complete the connection. As the contacts move, there can be a physical oscillation before they settle, resulting in the switch being opened and closed multiple times. When using a hardware interrupt to detect the status of the limit switch, such oscillations could cause the interrupt loop to occur multiple times.

Switch de-bouncing in software prevents the calibration routine from running multiple times. A timer detects how much time has elapsed between the switch closing and the next trigger. During testing, the time required for the limit switch signal to settle was found to be 100 ms. Therefore, the minimum time between limit switch interrupt loops is set at 200 ms using the debounce variable seen below in Listing 6.4.

Calibration only occurs once in the setup of the wrists, but moving through the full range of the wrist will trigger the hardware interrupt. To prevent multiple calibrations of the wrist, a Boolean flag is set during calibration that causes future interrupt requests to be ignored (shown in Listing 6.4).

```

1 void wrist1calibrate() {
2   if (debounce > 200 && wrist1calibrate == false) {
3     wrist1position = Dynamixel485.readPosition(wristServo1);
4     wrist1upperLimit = wrist1position; // Set upper limit
5     wrist1lowerLimit = wrist1position - wrist1range; // Set lower limit
6     constrain(wrist1goalPos, wrist1lowerLimit, wrist2upperLimit);
7     wrist1calibrate = true;
8     debounce = 0; // Reset debounce timer // Reset entry conditions
9     Serial.println("Wrist 1 Calibrated");
10  } }

```

Listing 6.4: Reed Switch Interrupt Code

The current position of the wrist actuator is read and informs the upper limit, after which the lower limit is calculated using the physical range limit of the wrist design. The range of motion of the wrist is constrained with the `constrain()` method and the calibration flag is set preventing the loop from being entered if the limit switch is triggered during play.

## 6.2.4 Gripper

The gripper utilises FSRs to provide feedback to the system as the AX-12A motors operate in continuous mode and are incapable of providing positional feedback. As the grip on the beater changes, the value detected from the FSRs varies between 50 and 900 when holding the beater. A greater number indicates a looser grip, with the maximum value indicating that no pressure is applied.

During testing, it was found that the beater can dislodge itself in sessions of extended play at loose grip settings. An adjustment routine is required that lets the user re-position the beater or replace the beater with equal or smaller diameter beaters. The adjustment routine of the grip actuator starts with the corresponding wrist actuator and elbow actuator moving to a mid-position to make placement of the beaters easier for the user, shown below in Listing 6.5. Continuous rotation of the grip actuator is enabled using the library function `setEndless()` and the actuator is instructed to rotate in the orientation specified within the function `turn()`. The Boolean `calibrateFlag1` is used to monitor the status of the FSR sensor during calibration. If the value detected on the FSR is greater than the upper threshold of 900 for a period of longer than 250 ms, the grip actuator is stopped with the `setEndless()` function. The Boolean monitoring calibration is then set to true, exiting the while loop and printing a statement to the serial monitor, shown below in Listing 6.5.

```
1 void grip1Adjustment() {
2   Dynamixel485.move(wrist1, wristMid1);
3   Dynamixel.move(elbow, elbowMid);
4   Dynamixel.setEndless(grip1, ON);
5   Dynamixel.turn(grip1, unwind, maxSpeed);
6   fsr1timer = 0;
7   while(calibrateFlag1 == false){
8     if(fsr1value > 900 && fsr1timer > 250){
9       Dynamixel.setEndless(grip1, OFF);
10      calibrateFlag1 = true;
11    }else if(fsr1value < 900){
12      fsr1timer = 0;
13    } }
14   Serial.println("Maximum FSR Position");
15 }
```

Listing 6.5: Grip1 Calibrate Code

The gripper is capable of holding beaters of various diameters. If the grip sub-system were holding the minimum diameter beater before calibration, the distance between the lead platform and the top grip pad would not be large enough to insert the maximum diameter beater. Therefore, a method is required to move the lead platform to the minimum position.

The minimum position which the lead platform can move to corresponds to the maximum beater diameter that can be gripped. During testing, the load on the grip actuator's shaft would surpass 25% only when the lead platform was pushed against the minimum position of the AX-12A bracket. This load value is used to inform the conditional statement within the beater change method, seen below in Listing 6.6. Once the load on the servomotor shaft is greater than 25%, rotation of the actuator is stopped and a message is sent to the serial monitor directing the user to place a beater into the gripper. A delay of four seconds is used to allow the user to place a beater into the gripping area. After this delay, the While loop is exited by setting the conditional flag `beater1flag` to true and the actuator is instructed to wind until the FSR value indicates pressure.

```

1 void beater1change () {
2   Dynamixel485.move(wrist1 ,wristMid1);
3   Dynamixel.move(elbow , elbowMid);
4   Dynamixel.setEndless(grip1 ,ON);
5   Dynamixel.turn(grip1 , unwind , maxSpeed);
6   while(beater1flag == false){
7     grip1Load = Dynamixel.readLoad(grip1);
8     if(grip1Load > 255){
9       Dynamixel.setEndless(grip1 , OFF);
10      Serial.println("Please place beater into Grip 1");
11      delay(4000);
12      beater1flag = true;
13    }
14  }
15  Dynamixel.setEndless(grip1 ,ON);
16  Dynamixel.turn(grip1 , wind , maxSpeed);
17  timer1 = 0;
18  while(beater1flag == true){
19    if(fsr1Value < fsrMax){
20      Dynamixel.setEndless(grip1 , OFF);
21      beater1flag == false;
22    } else if(timer1 > 4000){
23      Serial.println("No beater detected");
24      Dynamixel.setEndless(grip1 ,OFF);
25      beater1flag == false;
26    }
27  }
28 }

```

Listing 6.6: Grip1 Larger beater code

`timer1` is used to track the total time that the lead platform has been rotating for. Testing the time taken to wind from the minimum to maximum position was approximately four seconds. If the total time spent unwinding exceeds four seconds, then the minimum beater diameter has been surpassed and the lead platform is at risk of un-threading. Therefore, if `timer1` exceeds four seconds, rotation of the grip actuator is halted.

### 6.3 Calibration routine

Sections 6.2.2 through 6.2.4 discussed the implementation of individual calibration sub-routines. Calibration starts with the wrist, followed by the elbow, shoulder and then the grip sub-system. When the system is powered down, the wrist actuators fall due to gravity and rest perpendicular to the ground.

If the elbow or shoulder is calibrated before the wrist this can cause the beaters to knock into surrounding equipment. As such, the wrists are calibrated first, moving them upward from their resting position to reduce the chances of them interacting with the surroundings. Following this, the elbow raises to its maximum position and the shoulder calibrates itself. The elbow is moved upward to prevent the arm from contacting anything within the environment. Finally, as discussed in Section 6.2.1, the shoulder, elbow and wrist sub-systems return to their neutral mid-point for grip calibration and placement of beaters.

The total time required to complete the calibration routine is approximately 16 seconds, dominated by the time required to place the beaters into the grip sub-system.

### 6.4 Internal feedback

As discussed at the beginning of Chapter 6, the Dynamixel servomotors have a set of pre-defined registers stored on the microcontroller. These registers form a control table of 50 commands which can be accessed through software. 24 of these registers are non-volatile and remember their saved value after being powered down. The remaining 26 registers are stored in volatile memory, resetting to a known value when a loss of power occurs. The non-volatile registers allow characteristics such as baud rate, ID and maximum torque to be read and written to, seen in Figure 6.4, while the volatile registers provide feedback on the servomotors status using internal sensors.

Table 6.4: Dynamixel Control Table [40].

Storage Area	Address (HEX)	Name	Description	Access	Initial Value (HEX)
E E P R O M	0 (0x00)	Model Number (L)	Lowest byte of model number	R	24 (0x18)
	1 (0x01)	Model Number (H)	Highest byte of model number	R	0 (0x00)
	2 (0x02)	Version of Firmware	Firmware Information	R	-
	3 (0x03)	ID	ID of Actuator	RW	1 (0x01)
	4 (0x04)	Baud Rate	Baud Rate of Actuator	RW	34 (0x22)
...	...	...	...	...	
R A M	46 (0x2E)	Moving	Lowest byte of	R	0 (0x00)
	47 (0x2F)	Lock	Lock of Actuator	RW	0 (0x00)
	48 (0x30)	Punch (L)	Highest byte of punch	RW	32 (0x20)
	49 (0x31)	Punch (H)	Highest byte of punch	RW	0 (0x00)

The initial value of the non-volatile registers, shown in Figure 6.4, sets the threshold values within the corresponding volatile register that provides feedback to it. For example, the maximum temperature of the RX-24F servomotor is 80°, and the internal limit temperature is set to a value of 80°. If the volatile register containing the current temperature is greater than 80°, a hardware shutdown is implemented by the servomotor. A hardware shutdown requires the servomotor to be powered down and restarted before it will continue operation.

Having the servomotor stop operation and require powering down before continuing operation is inefficient and leads to a loss of functionality for the overall system. A software interrupt would allow the system to detect the value of the volatile registers which pose a threat to the overall operation and monitor their value to ensure they remain within the hardware limits.

### 6.4.1 Temperature and load protections

The Dynamixel servomotors have an operating temperature that ranges from -5 °C to 70 °C for the AX-12A and up to 80 °C for the RX-24F and MX-64T. As discussed in Section 3.4, the load on the servomotor shaft determines the current drawn from the power supply and in turn, the temperature of the servomotor. Operation at, or near, the stall current will cause the servomotor to overheat and shut down. This is a hardware level shutdown, ceasing operation to the servomotor until the servomotor has been completely powered down.

Operating the servomotor at close to the maximum temperature threshold for extended periods of time can cause irreparable damage to the servomotor even in the absence of a hardware shutdown being triggered, drastically decreasing its lifespan and maximum output torque.

The limits that can be set within the on-board microcontroller include temperature, highest and lowest voltage and angular position limits. A software interrupt or warning before the servomotor reaches this value would be advantageous and should continue interrupting until the temperature has decreased below the set threshold, preventing potential damage to the servomotor.

The threshold temperature for the servomotors is chosen to be 10 °C less than their hardware limit. This is selected due to the temperatures detected during testing, discussed in Section 7.1, being 30 °C greater than internal temperatures at the temperature threshold. However, the difference between internal and external temperature readings lessens with lower internal temperatures. At 10 °C less than the maximum, the external temperature detected was approximately 88 °C.

The load on the shaft is returned as a 16-bit packet, with five bits blank, ten bits indicating the magnitude of the load and the one bit indicating the direction of the load on the shaft, seen in Table 6.5. A zero indicates a counter-clockwise load, while a 1 indicates a clockwise load. This results in the value of the load returned ranging from 0-1023 for counter-clockwise loads, and 1024-2047 for clockwise loads. This is converted into a percentage and used to indicate whether the load on the shaft is greater than the recommended 25% threshold for extended operation.

Table 6.5: Load register of the Dynamixel servomotor [40].

Bit	15-11	10	9	8	7	6	5	4	3	2	1	0
Value	0	Load Direction	Data (Load Ratio)									

The function `servoStatus()` polls for values in the volatile registers to monitor the status of the servomotor. The two registers integral to ensuring the servomotors stay within safe operating ranges are temperature and load.

`servoStatus()` first uses a switch statement to compare the ID provided against two separate case blocks to determine the communication type of the servomotor to be polled, seen below in Listing 6.7. As the MX series and AX series operate on the same communication protocol, but possess different temperature ranges, a flag indicates whether it is an AX series servomotor. If the ID does not match one of these case blocks, a message is sent to the Serial monitor indicating that an incorrect ID was provided.

```

1 int servoStatus(int servoID){
2     switch(servoID){           // Runs servo ID number against known definitions
3         for arm1
4         case 0:                // Shoulder ID indicates RX-24F, 2.
5             servoType = 2;
6             break;
7         ...
8         case 5:                // Cases 4 & 5 trigger a flag indicating AX-12A
9             status.
10            axFlag = true;
11            servoType = 1;
12            break;
13        default:
14            Serial.println("Incorrect ID");
15            break;
16    }

```

Listing 6.7: `servoStatus()` servo identification

Once the series of the servomotor is known, a second switch statement polls the appropriate commands depending on whether the servomotor is RS-485 compliant or is Half-Duplex asynchronous serial. These two case blocks are identical except for the handle of the library which is used. This is due to the servomotors using slightly different pin instantiations, but retaining a consistent packetisation scheme.

The load acting on the servomotor is polled first to establish whether it is operating within an acceptable range. The register value returned is 11 bits long, the first 10 indicate the current load on the shaft from 0-1023 and the 11<sup>th</sup> is the orientation bit. If the orientation bit is one, the shaft is rotating clockwise and a zero denotes counter-clockwise rotation. The difference the 11<sup>th</sup> bit makes is deducted and the load percentage can be determined, seen in Listing 6.8. If the load is lower than the threshold of 25%, only the percentage is returned and operation continues. If the load is higher than 25% then warning messages are written to the terminal indicating that overheating is a possibility if operation is continued.

```

1 load1 =Dynamixel.readLoad(servoID); // Polls the Load of the servomotor being
  checked
2 if(load1>1024){
3     load1 = load1 - 1023; // Orientation determination
4 }
5     if(load1>256){ // If load is greater than 25%, a
  warning is provided through serial
6         load1 = ((load1/1024)*100);
7         Serial.println("Current Load exceeds recommended 25%");
8         Serial.print("Load: ");
9         Serial.print(load1);
10    }

```

Listing 6.8: servoStatus() Load Identification

After polling for the current load acting on the shaft, `servoStatus()` compares the current temperature to determine whether the servomotor is under the lower limit, between the lower and upper limit, or higher than the upper limit. This range changes based on the series of the servomotor as mentioned previously.

The Boolean `axFlag` seen in Listing [6.7](#) is used to determine whether an AX-12A or MX-64T is being polled using `servoStatus()` and informs the temperature range used. If the servomotor temperature is within 5 °C of the aforementioned 10 °C threshold, a message is printed to the serial monitor alerting the user of the current temperature. However, if the internal temperature is greater than 10 °C from the maximum temperature, then the servomotor ceases operation until the temperature has decreased to below the lower limit, seen below in Listing [6.9](#).

```

1 if(temp1>65 && temp1<70 && axFlag==false){ // Determine whether the MX-64T
  is within temperature threshold
2     Serial.println("Current temperature exceeds recommended MX-64T operating
  range");
3 }else if(temp1>70 && axFlag==false){ // If the temperature exceeds the software
  threshold ..
4     while(tempFlag == false){ // force an interrupt until temperature has
  decreased adequately.
5         temp1 = Dynamixel.readTemperature(servoID);
6         Serial.println("MX-64T servomotor exceeds upper temperature threshold");
7         if(temp1<65){
8             tempFlag = true;
9             Serial.println("MX-64T temperature decreased");
10        }else {
11            delay(500);
12        }
13    }

```

Listing 6.9: MX64-T Temperature Identification

The values of the variables used in this method are reset once `servoStatus()` completes, and the servomotor ID is returned.

`servoStatus()` takes approximately 3 ms to poll a single servomotor for their temperature and load. During a drum roll, a 6 ms delay to poll both servomotors will significantly impact the strike rate that is achievable. However, temperature testing of the wrist servomotors (discussed further in Section [7.3.5](#)) indicated that their operating temperature during a sustained drum roll is less than their threshold temperature.

### 6.4.2 Instrument Calibration

When a Dynamixel servomotor is powered on, the position of the servomotor can be manually adjusted as there is no current goal position stored in its volatile register. After being provided a goal position, the servomotor shaft will remain fixed until the next position is provided. This would require calibrating the locations of the percussion instruments through continual "Guess & Check" position adjustments until the exact location was found. However, the `torqueEnable()` function interrupts the signal from the power supply to the servomotor shaft, allowing manual positioning of the arm. Although the power is disconnected from the servomotor shaft, the internal sensors retain functionality, providing positional feedback.

The `percussionCalibrate()` function disables the torque to the wrist, elbow and shoulder servomotors allowing each one to be manually positioned to the desired location, seen below in Lines 2:5 of Listing [6.10](#). It then prompts the user to enter the total number of positions to be stored in a look-up table for reference during play. A For loop is used to iterate through the required positions, directing the user to move the arm until the beaters are in the desired position and use the serial monitor to indicate they are. The position of each servomotor is polled and stored in a look-up table for use later during play, seen in Lines 15:18 of Listing [6.10](#).

```

1 void percussionCalibrate () {
2   Dynamixel485.torqueEnable(shoulderServo , OFF);
3   Dynamixel.torqueEnable(elbowServo , OFF);
4   Dynamixel485.torqueEnable(wrist1 , OFF);
5   Dynamixel485.torqueEnable(wrist2 , OFF);
6   Serial.println("Enter number of positions to calibrate");
7   if(Serial.available() > 0){
8     arrayReq = Serial.parseInt();
9   }
10  int servoPositions[arrayReq][4];
11  for(int i = 0; i < arrayReq; i++){
12    Serial.println("Move the arm until the beaters are in position");
13    Serial.println("Press the Enter Key when ready");
14    if(Serial.available() > 0){
15      servoPositions[i][1]=Dynamixel485.readPosition(shoulderServo);
16      servoPositions[i][2]=Dynamixel.readPosition(elbowServo);
17      servoPositions[i][3]=Dynamixel485.readPosition(wrist1);
18      servoPositions[i][4]=Dynamixel485.readPosition(wrist2);
19    }
20  }
21 }

```

Listing 6.10: Position Calibration Routine

This process is required for each individual configuration of a drum kit. A pre-generated look-up table is stored on the Daughterboard during testing in Chapter 7 to avoid repetitious calibration.

### 6.4.3 Movement

The elbow and shoulder sub-systems' ranges allow multiple heights of drums to be incorporated. The positioning of the wrist sub-system affects whether the arm potentially damages itself or the surrounding environment when changing between instruments.

When moving between positions vertically or by panning, the wrists move from their current position to a raised position to reduce the risk of damage. The function `moveArm()`, seen below in Listing 6.11, sends a command to the wrist actuators to move to  $10^\circ$  above the desired location to prevent the beaters from bumping the edges of the instruments and causing potential dislodgement. An angle of  $10^\circ$  correlates to a shift of 92 mm, clearing the tips of the beaters from the instruments. Following the wrists raising, the elbow and shoulder sub-systems travel to the position stored in the look-up table.

```

1 int moveArm(int drumPos){
2   wrist1travelPos = servoPositions[drumPos][3] + 30;
3   wrist2travelPos = servoPositions[drumPos][4] - 30;
4   Dynamixel485.move(wrist1 , wrist1travelPos);
5   Dynamixel485.move(wrist2 , wrist2travelPos);
6   Dynamixel485.move(shoulderServo , servoPositions [drumPos][1]);
7   Dynamixel.move(elbowServo , servoPositions [drumPos][2]);
8 }

```

Listing 6.11: moveArm() Snare drum use case

## 6.5 System Operation

For the overall system to provide functionality which is valuable to an external user, the operation of each sub-system must be integrated. This involves the calibration of the individual actuators and connecting the operation of the sub-systems to larger functions that can take a unique drum position as input and output a strike with the desired qualities.

### 6.5.1 Strike method written for custom use

Chapter 2 identified four basic drum stroke types: full, down, up and tap. The essential characteristics of a drum stroke are the start position, end position and the force behind the stroke. The force varies depending on the style of composition played. The location of the drum skin determines the start position, while the end position and range is dependent on the stroke type.

Testing in Section 7.3.2 indicated that the minimum angle required to achieve a drum stroke was  $1^\circ$ . This correlates to a value of 10 within the Dynamixel servomotor's position register. To achieve a maximum sound level, the angle required was  $10^\circ$ , or 100 in register value. The four stroke types defined in Chapter 2 have custom ranges which determine the start and end position of the beater, shown in Listing 6.12.

```

1 int strokeType[4][2] = {
2   {100, 100}, // Full Stroke
3   {100, 10},  // Down Stroke
4   {10, 100},  // Up Stroke
5   {10, 10}   // Tap Stroke
6 };

```

Listing 6.12: 2D Array used for stroke types

A full stroke requires the goal position set on the Dynamixel servomotor to change by 100, resulting in the maximum sound level stroke.

The time required for the stick to move and make contact with the skin depends on the distance from the starting position of the stick and the drum. This distance varies with each loudness, drum position and elbow position. One approach would be to implement a variable delay which factors in the velocity of the command and the range required, calculating the optimal delay to contact the drum. Utilising this approach requires the delay to be calculated for every position, range and velocity which the wrist actuator strikes. This is incredibly complex due to the number of variables and the individual range of each of these variables. The result of the delay being too short results in the beater not contacting the instrument and too long a delay introduces artefacts in the sonic response of the membrane. These artefacts are the result of the beater bouncing on the drum membrane, discussed in Section 7.3.4, and introduce potentially unwanted noise into the drum stroke.

An alternative to specifying the delay between wrist movements would be to poll the position of the wrist servomotor and compare this to the known instrument position. When the two values are equal, the wrist then moves to a range specified by the drum stroke type. This removes the need for a delay and results in the strike of the drum being as fast as possible, given the velocity.

The `strike()` function requires the drum position specified earlier during Section 6.4.2, the velocity of the strike and the stroke type. The function uses a Boolean, `strikeTracker`, to keep track of which wrist last struck the drum and alternates between them dependant on its value. The functional flow of `strike()` can be broken into five blocks based on the inputs (`drumPos`, `velocity`, `stroke`) and the current value of `strikeTracker`, shown below in Figure 6.4.

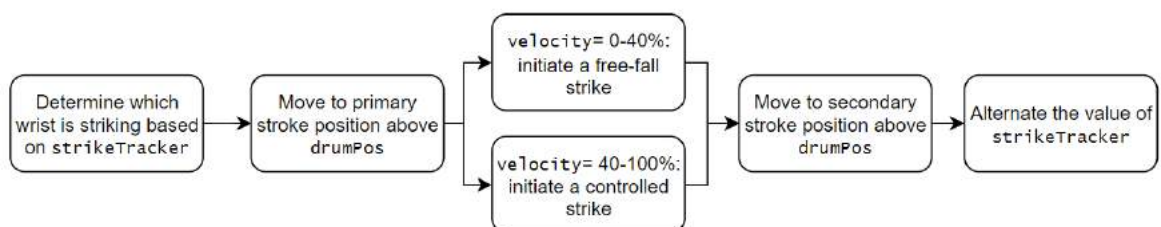


Figure. 6.4: Control flow diagram for the strike function.

The range of the beater from the drum position is determined using the stroke type and values defined in Listing 6.12. After calculating the start position, the corresponding wrist actuator is instructed to move there. The aforementioned comparison of current and desired position is used to determine whether the wrist actuator has reached the instructed position. Once the wrist is in position above the drum, the velocity specified determines the speed and therefore the loudness of the strike. When the velocity setting of the drum strike is lower than 40% the beater comes into sustained contact with the drum skin, resulting in multiple strikes, further discussed in Section 7.3.2. Therefore, if the velocity is lower than 40% (400 in servomotor position) the wrist actuator disables the voltage from the shaft, causing a free-fall strike. An investigation into the effect that range and velocity have on the sound level of the strike is discussed in Section 7.3.2. This discussion helps to inform the values provided to the `strike()` function.

```

1 int strike(int drumPos, int velocity, int stroke){
2   if(strikeTracker == false){           // Used to alternate wrist strikes
3     wrist1pos = servoPositions[drumPos][3]+strokeType[stroke][1];
4     Dynamixel485.move(wrist1, wrist1pos); // Move the wrist actuator down
5     while(posFlag == false){
6       readPos = Dynamixel485.readPosition(wrist1);
7       if(readPos==wrist1Pos){          // Compare actual position to desired position
8         if(velocity < 400){            // Lower than 40% is a free-fall strike
9           Dynamixel485.torqueEnable(wrist1, OFF);
10          posFlag = true;               // Exit down-strike loop
11        }else if(velocity >=400){
12          Dynamixel485.moveSpeed(wrist1, servoPositions[drumPos][3], velocity;
13          posFlag = true;
14        }
15      }
16    }
17    ...

```

Listing 6.13: Strike function for one wrist actuator

As soon as the instruction to move the wrist to strike the drum has been given, the Boolean `posFlag` negates the while condition and the next while loop matching the current value of the Boolean starts, seen in Listing 6.14. Once the current position of the actuator meets the position stored in the look-up table, the torque to the shaft is re-enabled regardless of whether a free-fall strike was used or not. If the torque was still enabled, then the command is essentially ignored. After making contact with the instrument, the actuator moves to the range specified by the previous stroke type, using the second position stored in the 2D array, at max speed.

```

1  while(posFlag == true){ // Immediately enter movement-up loop
2      readPos = Dynamixel485.readPosition(wrist1);
3      if(readPos==servoPositions[drumPos][3]){ // Wait until drum has been hit
4          Dynamixel.torqueEnable(wrist1,ON); // Re-enable shaft torque
5          wrist1pos = servoPositions[drumPos][3]+strokeType[stroke][2];
6          Dynamixel485.moveSpeed(wrist1,wrist1pos,maxSpeed); // Move up
7          posFlag = false; // Reset flag for next strike function
8      }
9  }
10  strikeTracker = true; // Alternate striking actuator
11  }
12  ...

```

Listing 6.14: Strike function for one wrist actuator

Listings [6.13](#) and [6.14](#) detail the motion of one wrist actuator and describes half of the overall `strike()` functionality. The remaining half includes the code required for the opposing wrist actuator, utilised when the Boolean `strikeTracker` is equal to `true`, after being set at the end of Listing [6.14](#).

## 6.6 Motherboard communication

The Motherboard must be capable of interpreting the MIDI packets sent from the user. This can be done using the inbuilt functionality of the USB MIDI library, which disseminates the content of a MIDI message into corresponding message functions [\[92\]](#). From here, it is a matter of using case blocks to determine the mapping of individual notes to the drum positions stored on the arms, shown in Listing [6.15](#).

```

1  int NoteOn(byte Channel, byte Note, byte, Velocity){
2      switch(Note){
3          case 38: // Acoustic Snare Drum
4              arm1.strike(snare, velocity);
5              break;
6          case 41: // Low Floor Tom
7              arm2.strike(LFtom, velocity);
8              break;
9          case 51: // Ride Cymbal
10             arm3.strike(rideCymbal, velocity);
11             ...

```

Listing 6.15: Example MIDI Note On Handling function

This function assumes that the drums used and their assigned locations are pre-defined for each arm. Future implementation of the Motherboard software would include feedback from the Arms as to the drum type which have been calibrated using the `calibrate()` function.

The Motherboard communicates to the Daughterboard through Serial communication using RS-485. This is accomplished using functions relating to the Serial Port library of the Teensy. The Daughterboards detect transmissions from the Motherboard by continuously checking if data is available on the Serial line. The Boolean `charCheck` is used to identify whether the message has ended in a new-line character which will end the Serial read loop.

```
1 void serialEvent() {
2   while (Serial.available() && charCheck == false) {
3     char dataIn = (char)Serial.read(); // Reads message sent from
4     outputString += dataIn;          // Enters Serial data into a string
5     if (dataIn == '\n') {           // If a new-line character is detected, exit loop
6       charCheck = true;
7     }
8   }
9 }
```

Listing 6.16: Reading of Serial messages from the Motherboard to the Daughterboard

The characters received in the function `serialEvent` are read in the main loop on the Daughterboard, where the information in `outputString` is disseminated to the related functions.

Due to time limitations, the implementation of a comprehensive serial communication protocol between the Mother and Daughterboard was not developed. Future work would improve upon the framework developed and integrate more extensive links between the operation of the Daughterboard and requests from the Motherboard.

## 6.7 Summary

The Motherboard is capable of receiving and deciphering MIDI signals from an external source and has the functionality required to transmit Serial messages to the Daughterboard in place. While further work is required for the Daughterboard to receive complex messages from the Motherboard, a framework has been established that allows for simple reception of messages over serial.

The software design of the Daughterboard is capable of accurately controlling the two different communication topology actuators and integrates external feedback from sensors to ensure operation within the safe limits of the system. Additionally, the operation of the overall system is achieved using abstracted functions which only require the identifier of the drum to be struck, velocity and type of stroke. This removes the need to understand

the operation of the Dynamixel actuators or their libraries, allowing ease of use by the user. Load and temperature monitoring routines aid in decreasing the chances of servomotor burnout and act to increase the total lifespan of the actuators.

The calibration routine identifies the safe operating limits of the four sub-systems, implements relative positioning through feedback for three of the sub-systems, coordinates replacement of beaters and calibrates grip strength. The functions described in this Chapter are used to calibrate and control the actuators during testing and evaluation of the overall system, discussed below in Chapter [7](#).



# Chapter 7

## Results

As specified in Chapter [1](#) and Chapter [2](#), the goal of this project is to design a system capable of playing a traditional drum kit at rates similar to or better than those of a human drummer and for an extended period of time. In order to determine whether these specifications were met, a series of experiments were designed to measure the beat rate, the range of motion of the sub-systems, determine the thermal profile of the actuators and evaluate the operation of the overall system. This chapter outlines the form of these experiments, the results that were obtained and how they might indicate a limiting of the performance of the drumming system.

### 7.1 Shoulder

The shoulder sub-system was tested to characterise its range of motion, travelling time, speed and expected operational duration. The requirements of the shoulder were established in Section [3.3](#). These requirements are based on the minimum functionality that a shoulder should possess to be capable of playing a traditional drum kit at the pace of a contemporary piece.

#### 7.1.1 Range of Motion

The shoulder was designed to utilise the 300° range of the RX-24F servomotor and pan across a range of 2640 mm, or 285.4°. This range would satisfactorily play across a traditional drum kit when horizontally laid out. The range of motion must be evaluated to ascertain whether the shoulder is capable of panning this range and the resolution it can achieve.

The individual instruments were laid out in a semi-circle around the system. The shoulder is then positioned between the maximum and minimum position required and the current position was recorded. With the beaters positioned at the middle of the ride and crash cymbals, the actual angle required to play across a complete drum kit is  $250^\circ$ , shown below in Figure 7.1.

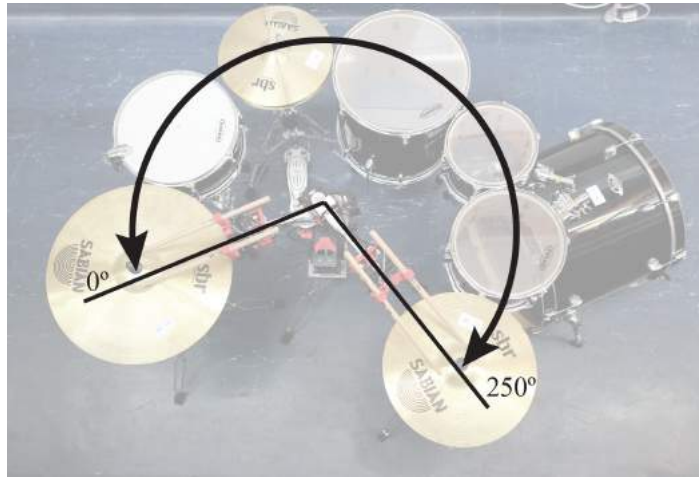


Figure. 7.1: Maximum and minimum range of the shoulder sub-system.

To evaluate the characteristics of the shoulder sub-system, the RX-24F was instructed to move between the maximum and minimum set points while the internal temperature and travel time were being recorded. This test continued until either the servomotor reached a steady-state temperature, or it exceeded the maximum temperature threshold.

The resolution required of the shoulder sub-system is defined in Section 3.4 as 10 mm so that the shoulder could accurately position beaters over smaller drum modes. The RX-24F is capable of a resolution of  $0.29^\circ$ , resulting in an arc length of 2.68 mm. However, the backlash angle introduced between the drive and driven gear of the shoulder sub-system results in a difference of 5.03 mm in the placement of the beater tips when approaching from either direction. This reduces the resolution to 7.71 mm depending on the direction that the shoulder positions itself from, detailed below in Table 7.1.

Table 7.1: Characteristics of the shoulder sub-system

	Required	Design	Actual
Range ( $^\circ$ )	285.4	300	250
Resolution (mm)	10	2.68	7.71

### 7.1.2 Operation of the Shoulder

The shoulder sub-system determines the range of instruments that can be played and the speed with which they can be played. The desired operational time of the shoulder was outlined in Chapter 3 to be at least one hour, with a characteristic settling temperature less than the temperature threshold of the servomotor. To establish how long the shoulder could reliably operate, the speed of the shoulder has to be evaluated.

This was performed by instructing the shoulder servomotor to move between the minimum and maximum set points of  $0^\circ$  and  $300^\circ$  at 100% speed and recording the time and current value of the internal temperature register.

The Dynamixel servomotors dissipate heat through vents located adjacent to the motor. During testing it was found that the external package temperature of the RX-24F exceeded the temperature thresholds, resulting in the servomotor's performance slowing and eventually burning out. A thermal imaging camera was used to accurately measure the external package temperature. The FLIR T400 infrared camera is capable of measuring temperatures up to  $1200^\circ\text{C}$  with an accuracy of  $\pm 2\%$  and was used to capture the external package's temperature profile [93]. Further testing revealed the external package temperature was more than  $30^\circ\text{C}$  hotter than the indicated internal temperature of  $80^\circ\text{C}$ . This influences the operational temperature limits previously defined in Section 6.2.1. The external temperature recorded after operating the shoulder for approximately five minutes, with an internal reading of  $80^\circ\text{C}$  is shown in Figure 7.2 as being  $112^\circ\text{C}$ . The ambient temperature was recorded as  $20^\circ\text{C}$  with a  $2^\circ\text{C}$  deviation during the testing period.



Figure. 7.2: Maximum recorded temperature of the RX-24F Package.

The temperature difference between the internal sensor and external readings is caused by the motor package being visible through the exterior grating used for passive heat dissipation of the motor. This results in the peak external temperature being greater than that of the internal sensor located on the PCB, situated away from the motor.

As the internal temperature defines the thermal shut down point of the servomotor, the servomotor continues operation despite being in excess of the temperature threshold. The sustained current draw and temperature resulted in the delamination of the wires powering the servomotor and a breakdown of the lubrication on the internal bearings, further increasing the torque required to shift the arm. The RX-24F shoulder servomotor was replaced once during testing due to these effects.

During evaluation of the shoulder, it was found that the torque required to shift the arm from a static position was approximately 80% of what the RX-24F could supply. The servomotor draws large currents to initially move the weight of the arm. There is additional strain in this movement caused by the misalignment of gear faces discussed in Section 3.4, and from the system suffering from real-world efficiency losses. The RX-24F shoulder servomotor uses as much torque as is required to move the load of the arm. This caused the current draw of the servomotor to be in excess of what is recommended for extended operation of the servomotor and heats up the servomotor past the temperature threshold after only 3 minutes of operation (shown in Figure 7.3).

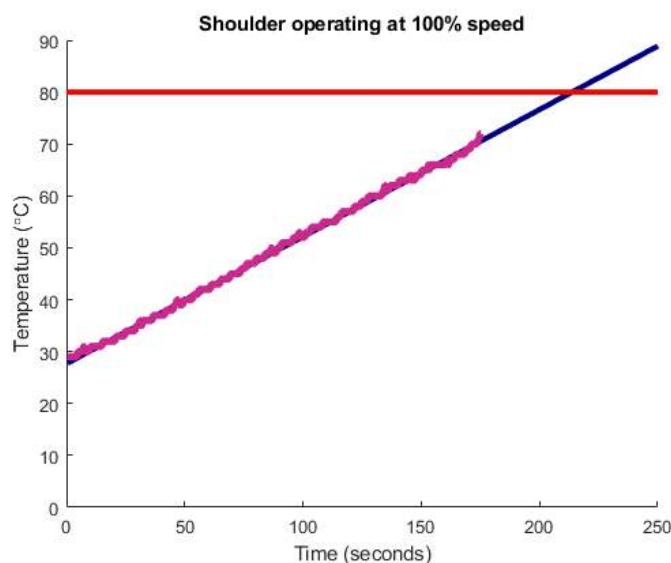


Figure. 7.3: Temperature of shoulder servomotor operating at 100% speed.

Although the servomotor operation was evaluated at 100% speed, a lower speed will draw a comparable amount of current as it must accelerate from zero to the set speed under the same torque conditions. However, the initial torque is similar, the deceleration at the end of the movement is lower as the overall speed is lower. This results in an increase of operating time, shown below in Figure 7.4, but the servomotor still fails to level out to a stable operating temperature below the temperature thresholds.

The `torqueEnable()` method, discussed in Section 6.4.2, was written in response to the need to control the current which the RX-24F draws. The recommended torque applied to the shaft for sustained operation is 25%. The speed of the servomotor set in software will only be achieved by the servomotor if the load acting on the shaft is less than 25%. A trade-off in speed and operating time to the torque, and the effect of the torque setting, was evaluated to establish which approach met the shoulder sub-system's requirements. A comparison between the servomotor operating at 25% speed with no torque limit, and at 100% speed with a 25% torque limit shows that the torque limit results in a settling temperature of 62°, seen in Figure 7.4. This is below the threshold of the RX-24F and remained stable after 10 minutes of operation at this temperature. However, operating at 20% with no torque limit results in crossing the temperature threshold after 25 minutes.

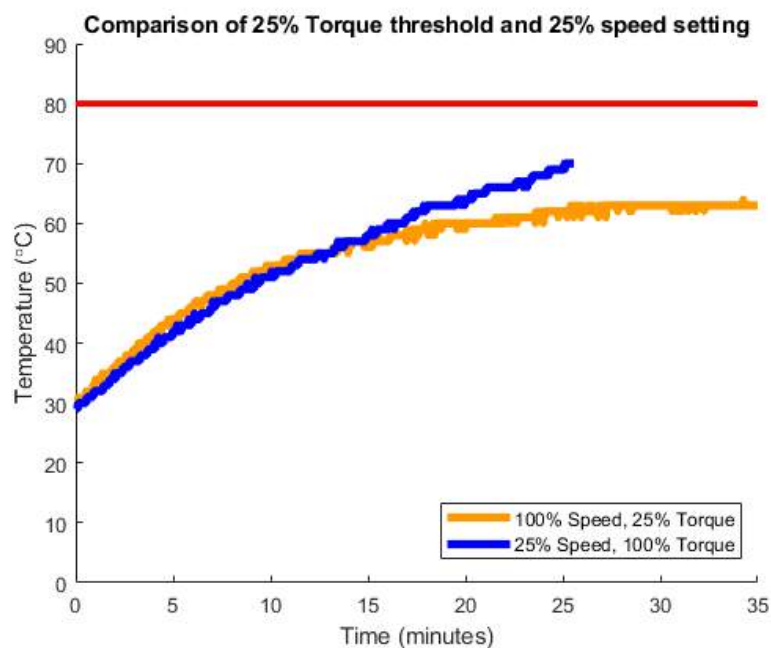


Figure. 7.4: Temperature response of the shoulder servomotor operating at the maximum recommended torque and lower speed.

While the recommended torque limit of the servomotor is stated as being 25%, the operation at values greater than this are evaluated to establish whether this is accurate when operating the shoulder sub-system. To test this, the servomotor was instructed to pan from  $0^\circ$  to  $300^\circ$  in intervals of  $60^\circ$  (or 550 mm of arc length). The test was performed ten times for each torque setting and the time required to rotate for each distance was averaged and plotted, shown in Figure 7.5.

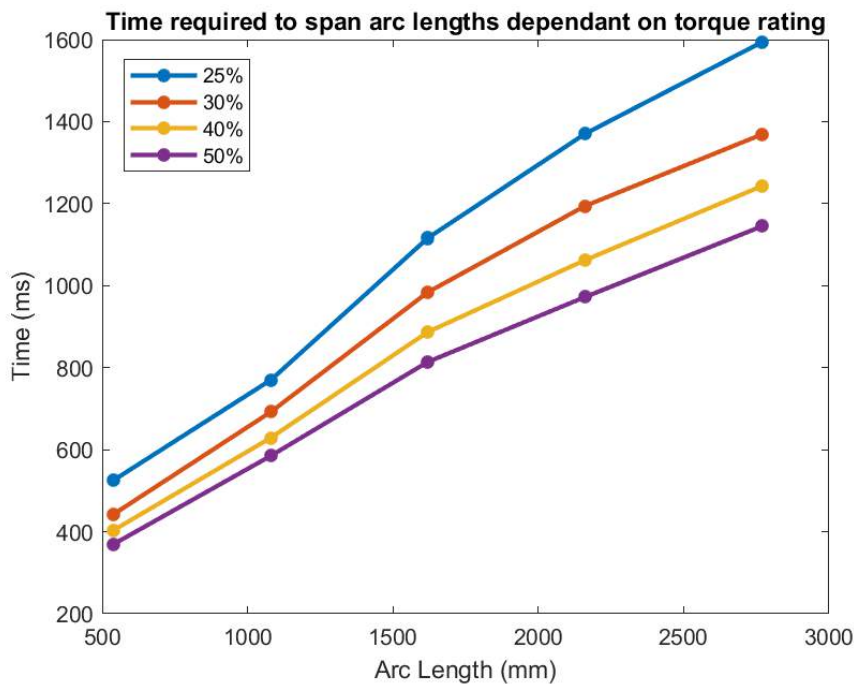


Figure. 7.5: Evaluation of the Torque setting and its impact on the shoulder sub-system.

The relationship between each torque and the relevant response time is relatively linear, as expected, the 50% torque setting provides the lowest panning time for each interval. However, the increase in current and operational life expectancy must also be measured to determine whether the temperature exceeds the thresholds during an extended performance. To evaluate this, the servomotor was operated at increasing torque limits ranging between 25% and 50% while being recorded under similar conditions to previous speed and torque tests. The resultant increase in temperatures were graphed against time and are shown in Figure 7.6. Torque thresholds greater than 30% result in the servomotor's temperature being greater than the temperature threshold, whereas a setting of 30% has a stable operating temperature of  $66^\circ\text{C}$ .

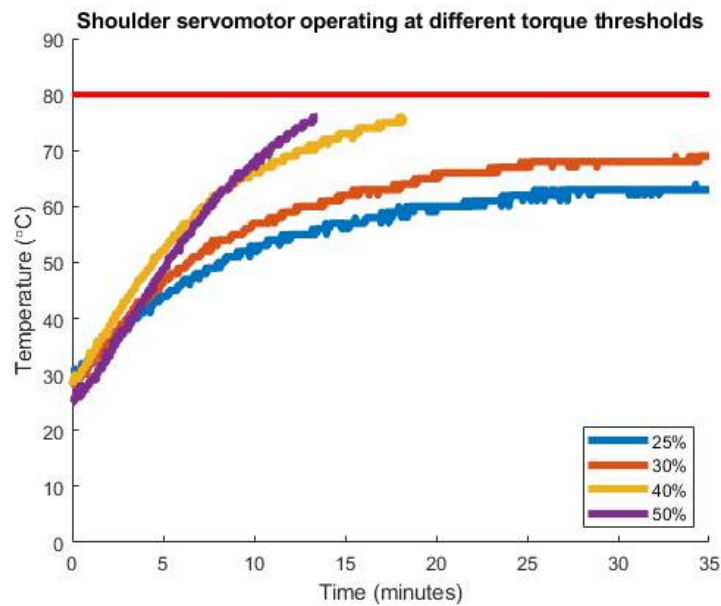


Figure. 7.6: Temperature response of the shoulder servomotor operating at the torque levels above the recommended value.

The speed of the arm when the torque is limited is dependant on the load acting upon the shaft. The panning time of the shoulder sub-system was evaluated for both torque limit and speed control to determine the relationship between the maximum torque and the equivalent speed which the servomotor travels. To evaluate this, the same 60 °C panning positions and time were recorded for values of servomotor speed between 20% and 100%, and for torque values ranging between 25% and 50%, shown in Figure 7.7.

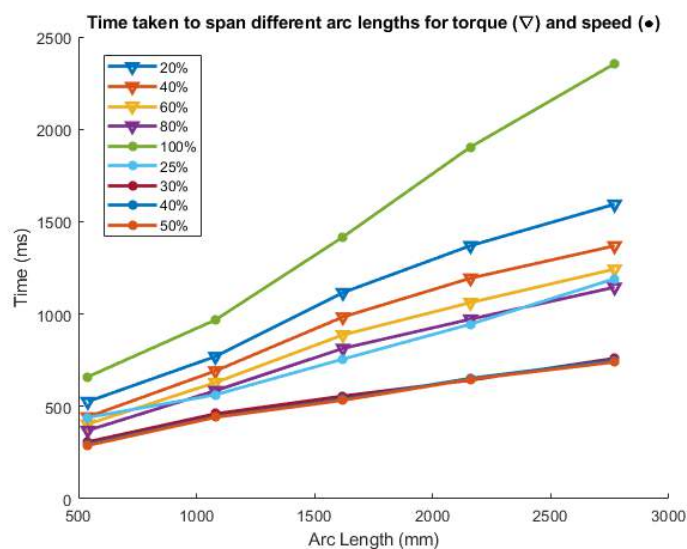


Figure. 7.7: Evaluation of the Torque and Speed settings of the shoulder sub-system.

There were no significant gains in travel time between the speed settings of 60% and 100%, with a variance of 15 ms at maximum. This implies that the force provided by accelerating to 60% will shift the arm to its maximum speed. A torque setting of 50% is approximately equivalent to 40% speed. This results in a panning time of 1.1 seconds for the entire shoulder. However, Figure 7.6 shows a limit of 50% decreases the operation time significantly. 30% torque has a stable operating temperature and a total panning time of 1.25 seconds. This is greater than the outlined requirement but provides consistent operation.

The external temperature operating at 30% torque was recorded with the infrared camera as peaking at 68.6 °C after 35 minutes of operation, shown in Figure 7.8.



Figure. 7.8: External temperature of the shoulder sub-system at 30% torque limiting after 35 minutes.

### 7.1.3 Shoulder Summary

The travel time of the shoulder sub-system is greater than what was desired, however, the placement of the instruments which the drum plays makes a large contribution to the panning time. In a worst case scenario where the shoulder has to pan from the maximum to minimum position, the panning time is 1.3 seconds. A reasonable set up of the drum kit would involve the most used components being at the middle of the shoulder's range, decreasing the time required to shift to 0.69 seconds. The shoulder sub-system is therefore capable of meeting the outlined requirements of the range of motion, resolution and operation time.

## 7.2 Elbow

The requirements of the elbow were that it should be capable of altering the heights with which the beaters can strike to a wide enough range so that it can play across a traditional drum kit. Therefore the range of motion, resolution, travel time and operational expectancy were evaluated to determine if the elbow sub-system met these requirements.

### 7.2.1 Range of Motion

The elbow was designed to have a range of motion of approximately  $75^\circ$ , providing an arc length of 700 mm for the wrist to pan across. This would allow the system to play across a traditional drum kit with ease. The range of motion must be evaluated to ascertain whether the elbow is capable of panning this range and the resultant resolution. The maximum and minimum set points that the elbow was capable of achieving are shown in Figure 7.9

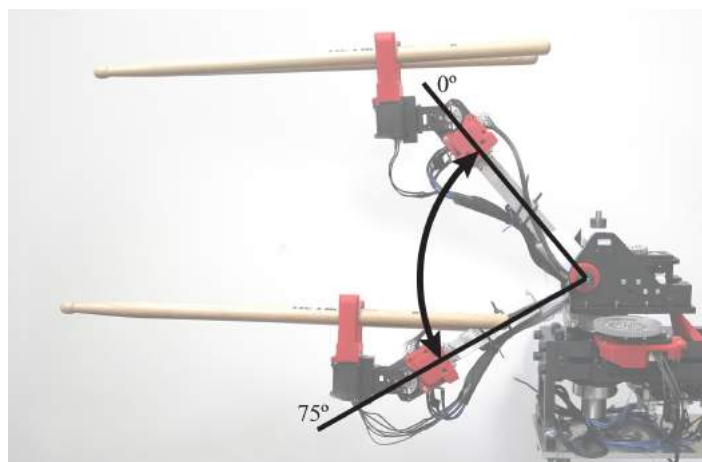


Figure. 7.9: Maximum and minimum range of the elbow sub-system.

The MX-64T servomotor that drives the elbow was instructed to travel between the two position extremes at maximum speed, the current temperature, position and time taken between the two points was recorded. The test continued until the servomotor reached the temperature threshold, at which point images were captured of the elbow sub-system's external temperature profile. The results of this characterisation are displayed in Table 7.2 below.

Table 7.2: Characteristics of the Elbow sub-system

	Required	Design	Actual
Range of Motion (°)	45	75.6	75
Resolution (mm)	2.68	0.157	1.08

The resolution which the elbow can achieve is limited by the backlash angle between the worm screw and worm wheel which introduces a  $0.1^\circ$  difference between operating in each direction. This results in the resolution increasing to 1.08 mm. However, this is still beneath the required threshold.

### 7.2.2 Operation of the Elbow

The minimum operating time desired for the elbow sub-system was outlined in Section 3.5 as being at least one hour. To establish how long the MX-64T could reliably operate, the load and temperature characteristics of the elbow were evaluated.

This was accomplished by instructing the MX-64T to continuously move between its maximum and minimum positions and measuring the current load, position and temperature of the internal registers. Operation of the servomotor was ceased once a steady-state temperature had been reached, or the temperature exceeded the threshold. Once the servomotor was powered down, the external temperature profile was captured with the infrared camera and the data was plotted. The resultant load profile for the elbow sub-system in upward and downward motion is displayed in Figure 7.10. The elbow sub-system is capable of panning a range of  $75^\circ$  in 1.1 seconds, which exceeds the range desired in Section 3.6 of  $45^\circ$  in 0.76 seconds.

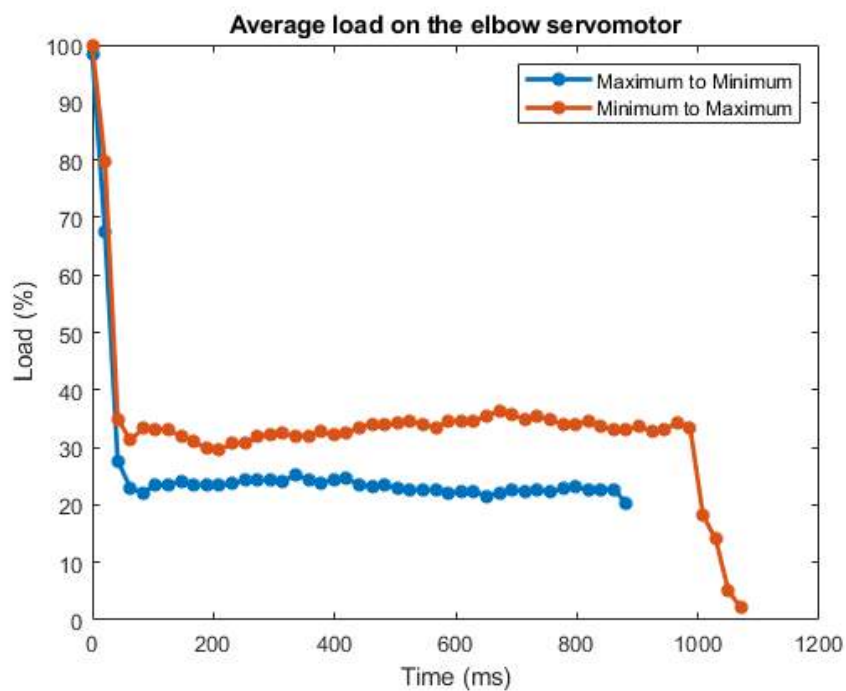


Figure. 7.10: Resultant load acting on the elbow sub-system servomotor shaft during upward and downward motion.

Operation of the servomotor moving upward places a continuous load of approximately 33% on the servomotor shaft. This is greater than the recommended load, indicating that the temperature characteristic may be outside the temperature thresholds. The upward motion requires 10% more torque from the servomotor to move. This is due to the servomotor and worm gear configuration working against gravity, requiring more torque and time to rotate upward. The result of the elbow sub-system's temperature recordings is shown below in Figure [7.11](#). The ambient temperature when testing the elbow sub-system was recorded as 19°, however, testing with the MX-64T prior to continuous operation caused the internal measurement to be higher than the ambient.

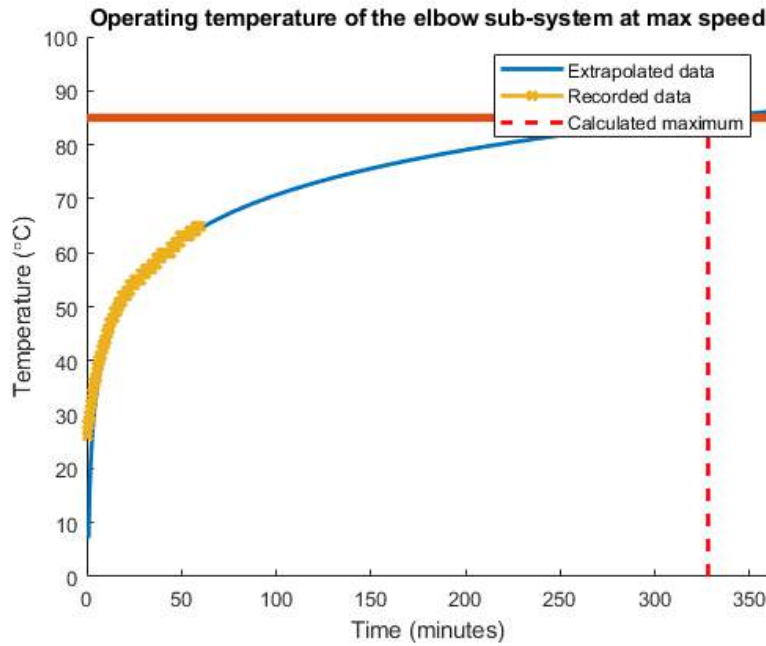


Figure. 7.11: Internal temperature of the elbow sub-system servomotor during continuous operation.

Operation of the MX-64T was ceased after continuously moving for the minimum desired time frame outlined in 3.6. A logarithmic relationship was inferred from the data recorded and the projected time which the elbow would exceed the threshold temperature was 340 minutes, or over 5 hours of operation. The external temperature profile indicates that the peak temperature of the elbow sub-system after an hour of operation peaked at  $60.9\text{ }^{\circ}\text{C}$ , shown below in Figure 7.12a, while the temperature of the worm wheel reached a peak of  $48.8\text{ }^{\circ}\text{C}$ , shown in Figure 7.12b.

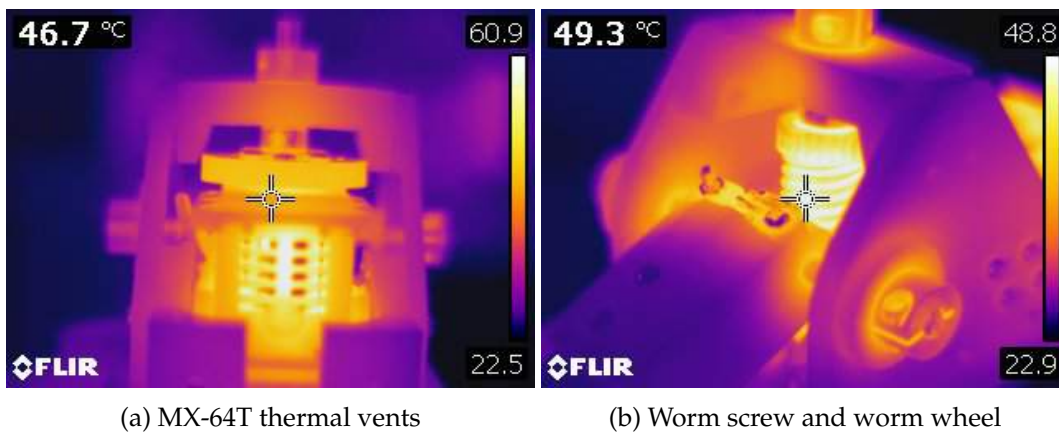


Figure. 7.12: Thermal profile of the elbow sub-system after operating for 60 minutes

### 7.2.3 Elbow Summary

While the elbow sub-system was predicted to cross the temperature threshold after 5 hours of operation, it should be noted that the continual movement between minimum and maximum is unrepresentative of normal operation. For the elbow to need to rotate constantly, would mean we have a significantly un-optimised drum setup. This would require the most commonly struck instruments to be located at significantly different heights which the wrists would not be able to reach without fully extending the elbow sub-system repeatedly. The travel time is lower than what was required, providing an additional 30° of range within the outlined requirement of one second. Although backlash decreases the total resolution, precise control is still achievable. Overall, the elbow sub-system meets the outlined requirements of travel time, resolution, range of motion and operation time.

## 7.3 Wrist

The motion of the RX-24F wrist servomotors defines the speed and range of the beaters and the characteristics of striking an instrument. The wrist requirements centre on being able to provide varying loudness of strikes, a high beat rate and being able to operate for extended periods of time. The functionality of the overall system heavily depends on the performance of the wrist sub-system.

### 7.3.1 Range of Motion

The design of the wrist limits the rotation of the RX-24F actuators from their 300° range of motion down to 210° using the natural range blockers. This range allows the wrist to play across varying heights of equipment in conjunction with the elbow. The range of motion must be evaluated to determine whether the design of the wrist provides the required range and precision required, as outlined in Section 3.8.

The wrist servomotor was moved between its maximum and minimum set points and the current position registered on the servomotor shaft and the angle between the beaters and the central servomotor shaft were recorded. The maximum and minimum positions and the achieved angle of 210° are shown below, superimposed on top of one another, in Figure 7.13.

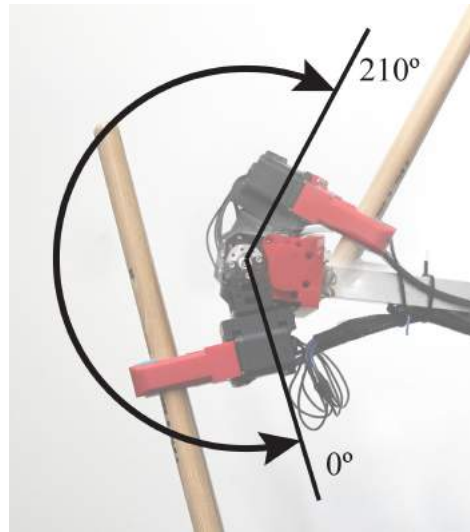


Figure. 7.13: Maximum and minimum range of the wrist sub-system.

The wrist actuators were instructed to move between the range required to achieve the maximum beat rate, and subsequently the range required to achieve the maximum loudness. The exact ranges of these two settings are discussed further in Sections [7.3.4](#) and [7.3.2](#), but are needed here to characterise the wrist sub-system.

The resolution required of the wrist was defined by the expected minimum distance required to effectively strike the instruments. As discussed previously, the RX-24F has a resolution of  $0.29^\circ$  and can achieve a controllable arc length of 1.56 mm. The wrist is the only directly driven sub-system of the overall design, meaning that there is no backlash angle on its operation.

Table 7.3: Characteristics of the Wrist sub-system

	Required	Design	Actual
Range ( $^\circ$ )	45	210	210
Resolution (mm)	2	1.56	1.56
Strike Rate (BPM)	1200	3000	3114
Loudness (dB)	100	-	106

The thermal profile of the wrist sub-system is evaluated further in Section [7.3.5](#) below, but the resultant characteristic temperature found during testing the wrist servomotors is less than the temperature threshold. The operation time of the wrists is as long as the lubrication of the internal bearings is maintained, or for as long as the system is required to operate before servomotor burnout.

### 7.3.2 Sound Pressure Level

The minimum sound level required of the wrist strike is 80 dB, with potential sound levels greater than this being advantageous but also potentially damaging, as outlined in Section 3.7. Therefore, the maximum sound level which the sub-system is capable of striking with must be evaluated to forewarn the user of the risks that operating the wrist can have and recommended exposure times.

Each instrument in the drum kit is used for different notes and sound level responses. The loudness which is achievable across the instruments must be evaluated to establish which instrument presents the largest potential threat to the hearing of the user.

To perform this evaluation, a single wrist actuator was instructed to strike the surface of the instrument and immediately return to the starting position after the instrument was struck. The sound level produced by the strike was measured using the Tenma Sound Level Metre 72-947 [94]. The human ear can perceive changes in noise level of approximately 3 dB, with a change in 10 dB correlating to twice the perceived loudness. The Tenma sound level metre is accurate to  $\pm 1.4$  dB which is below the detectable ranges most humans perceive. Three different types of instrument were evaluated with a consistent speed and range strike to determine which produced the loudest sound level. The practice pad, snare drum and ride cymbal were used due to their three distinct properties of energy absorption and sound response, shown in Figure 7.14. The practice pad is a commonly used training module for drummers that features a responsive but quiet surface that allows rebounding of beaters without the accompanying sound level generated by traditional drums.

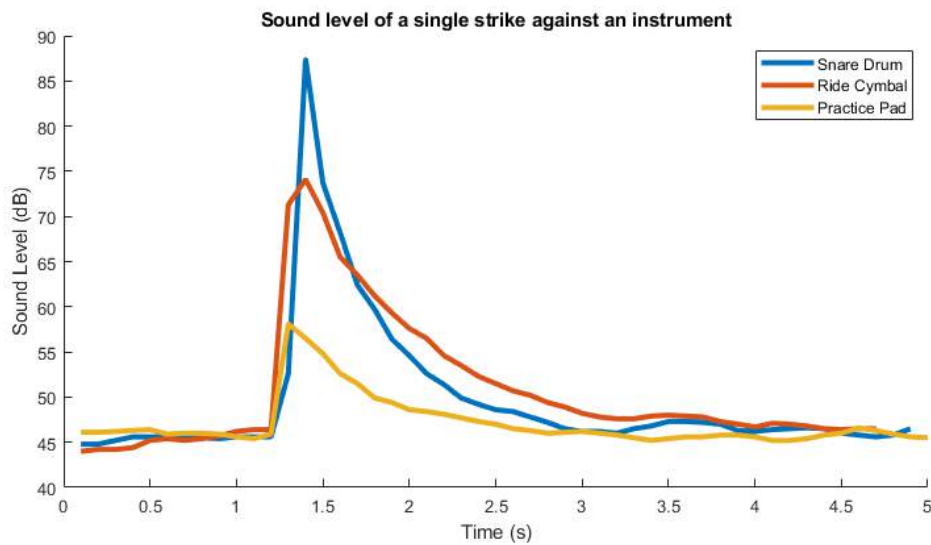


Figure. 7.14: Sound level variance of an identical strike across three instruments.

The same energy is introduced to each system, however, a cymbal disperses the energy over a longer period of time, producing a sustained sound. The material of the practice pad absorbs the majority of the energy and the snare drum disperses it rapidly based on the tension of the membrane. The snare drum has a lower settling time and greater peak to the sound level registered with a single strike. Therefore, the snare drum was selected as the testing instrument.

There are several properties that can be altered when striking percussion instruments that have an effect on the sound level produced. These include, but are not limited to, the position on the instrument, the force behind the strike, the range leading up to the strike and the angle of attack.

The position struck on the instrument is dependant on the instrument and not the system and so it was not evaluated. The attack angle was discussed in Chapter 2 as having little impact on the musical expressivity of a professional drummer's performance as it is most often the angle which the individual drummer finds comfortable to play for long periods with.

Three separate approaches were used to model the variance in sound level: varying the range, varying the speed and letting the stick freely fall at different ranges. Each of these characteristics provided a different amount of force behind the strike and a varying sound level profile.

To evaluate the impact that changing the range has on the strike, the wrist actuator was set to a constant speed and had the central angle between the drum and the start position of the strike changed. This test was repeated ten times and the average sound level of the strikes for each angle are shown below in Figure 7.15. The maximum difference in variance between each recorded sound level was approximately 2 dB, below the perceptible range of humans.

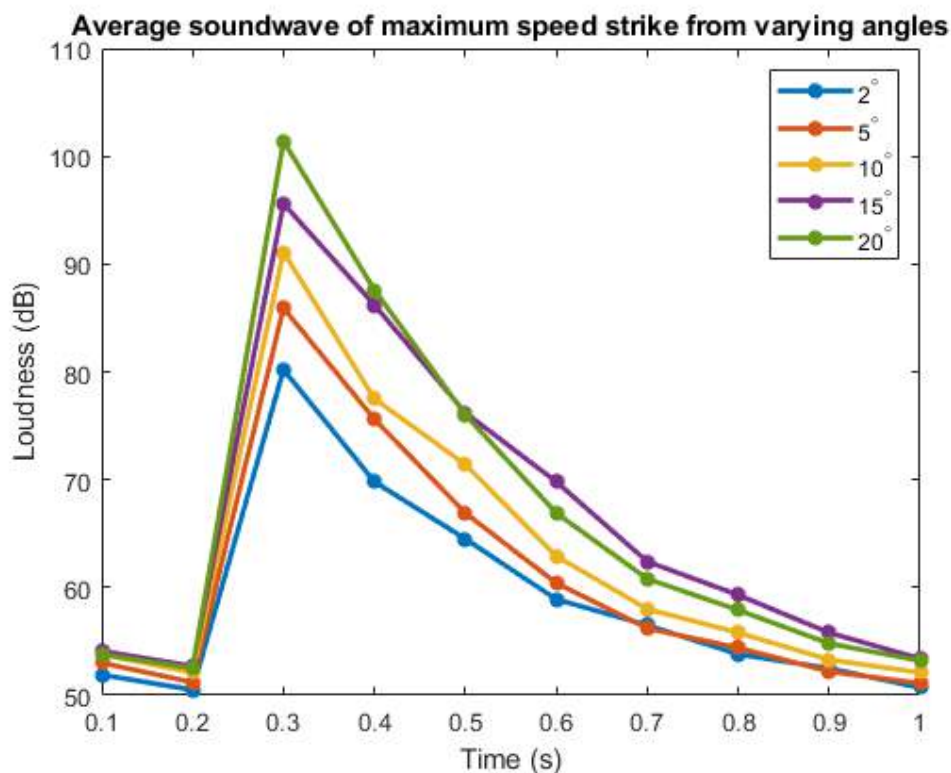


Figure. 7.15: Sound level variance of altering the range for a single strike of a snare drum.

The difference between each variation in angle follows a linear trend, with an increase of 5 dB per increase of  $5^\circ$  up to a maximum of 101.4 dB. The minimum sound level achievable when varying the strike angle and travelling at the maximum velocity is 80.2 dB. Operation at this sound level has a recommended exposure time of 25 hours making it suitable for extended use [50].

The lowest sound level achievable still falls within the range of sound levels that can be considered potentially hazardous or irritatingly loud. A lower operating speed was investigated to determine the impact that velocity has on the sound level of a strike and whether a lower level strike could be achieved.

The velocity variance test was set up in a similar manner to the range tests, with a sound level meter and 10 tests being conducted and averaged. It was observed that speeds lower than 40% made sustained contact with the drum skin, resulting in multiple strikes. Therefore the lowest speed was limited to 40% during testing. The resultant sound levels of a varied velocity are displayed below in Figure 7.16.

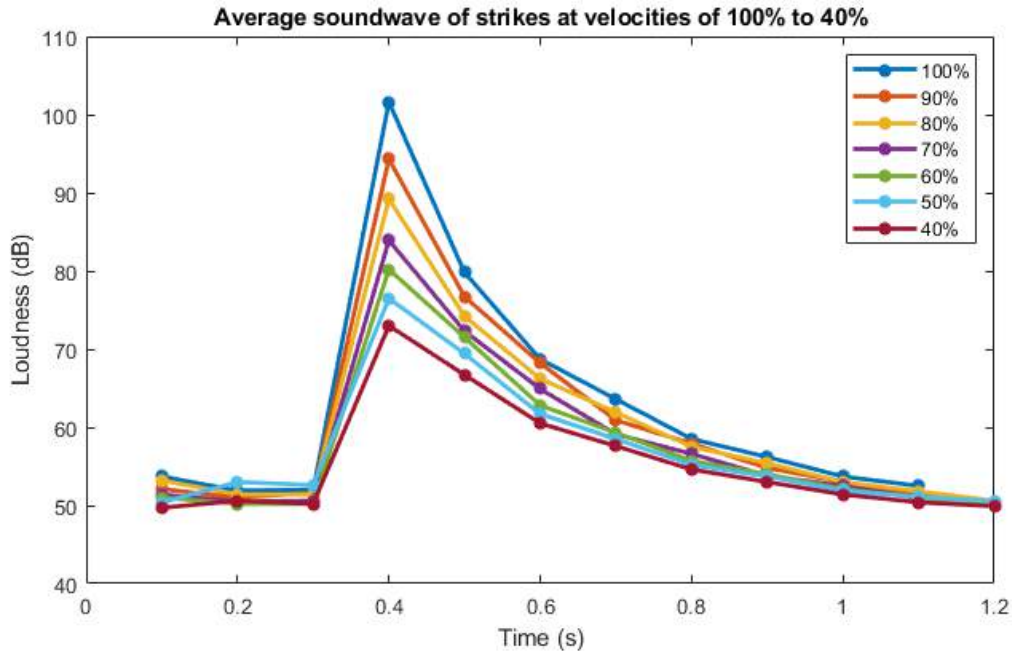


Figure. 7.16: Sound level variance of altering the velocity for a single strike of a snare drum.

As with the variance in range, the relationship between velocity and resultant loudness of the strike is a linear 4 dB for velocities of 70%. Above this velocity, the increase between loudness is approximately 7 dB for every 10% gain. This is attributed to the silicone pads gripping the beater deforming more at higher velocities, resulting in additional energy being added to the system. The lowest sound level recorded was 73 dB using the lowest velocity of 40%. This is below the potentially hazardous range of sounds or the irritating band of noise. Free-fall striking removes the velocity from the strike and completely depends on gravity to provide the force behind a strike.

To evaluate this, the servomotor was set to an angle above the skin of the snare drum, whereupon the torque of the shaft is disengaged, allowing the beaters to free-fall. The resultant sound level was recorded using the sound level meter and the average response is shown below in Figure 7.17.

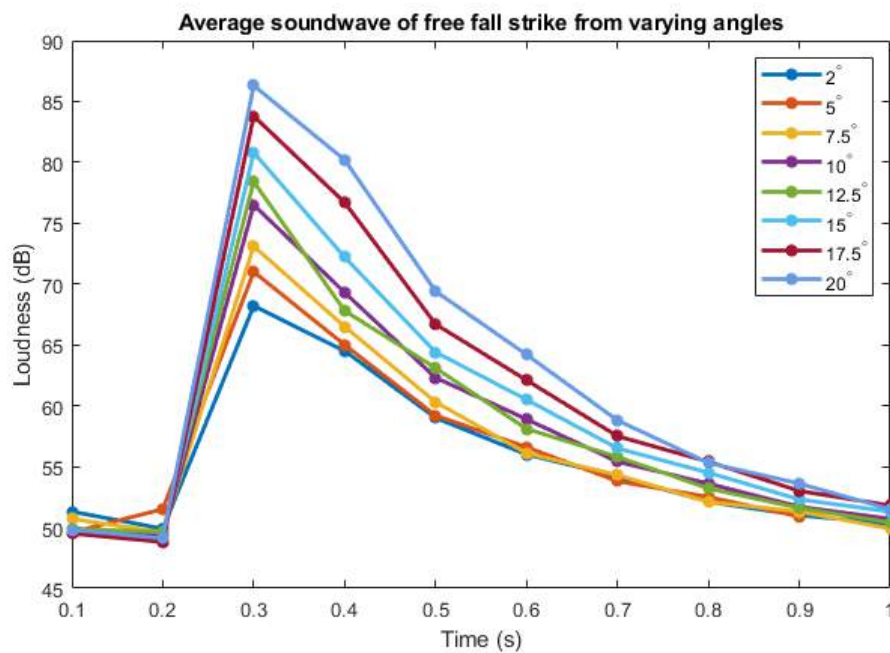


Figure. 7.17: Sound level variance of altering the range for a free falling strike of a snare drum.

The relationship of the sound level to the increase in angle remained approximately consistent for all angles tested, with an increase of 3 dB, or approximately twice as loud per angle. While the maximum sound level achievable with free-fall striking is less than that of the range or velocity varied strike (86.3 dB), the minimum sound level is 68.2 dB. This sound level is comparable to the loudness of the average conversation or low music levels.

### 7.3.3 Audio Analysis

While audio waveforms provide clear distinction to notes when listening to them, identifying a peak can be difficult in the time domain if the resonant noise of a strike is present in the amplitude of the signal. Additionally, the modes of the instrument being struck introduce different frequency artefacts that make distinguishing the strike difficult when analysed in the frequency domain.

Transient noises such as doors opening or power supplies switching, introduce artefacts and impulses to an audio recording. These artefacts are not representative of the signal to be analysed and increase the difficulty in detecting the true waveform of the signal. An alternative to audio analysis is measuring the vibration of the object which is struck. Contact

microphones mount directly to the surface of the object that is being recorded, using the piezoelectric effect to transfer mechanical stress through vibration to a voltage which can be measured.

Contact microphones are insensitive to vibrations through the air, providing an isolated measuring system for the recording of percussive strikes. To observe the analog response of the drum membrane, the contact microphone shown in Figure 7.18, was mounted to the head of the drum.



Figure. 7.18: A standard piezoelectric contact microphone [95].

When a percussion instrument is struck, energy is transferred from the beater to the surface of the instrument, resulting in sound being generated. The characteristics and material of the instrument determine the dispersion of the energy. Cymbals introduce a large amount of noise as the metal vibrates, dissipating the energy introduced during a strike. Drums disperse the energy over a shorter period of time due to the taut membrane.

To evaluate the noise introduced by vibration of the instrument, the single strike amplitude of three different percussion instruments was recorded using a contact microphone. The instruments tested are again the snare drum, ride cymbal and a practice pad. The resultant waveform of the single strikes are plotted and presented below in Figure 7.19.

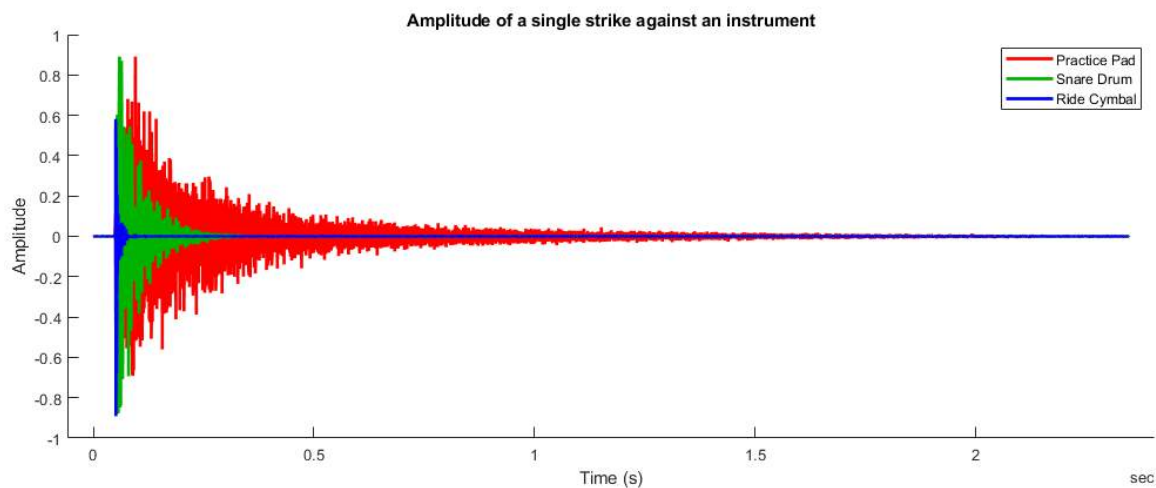


Figure. 7.19: Amplitude of a single strike across various percussion instruments.

The practice pad has the smallest settling time due to the material of the pad absorbing the strike and dispersing it through the increased thickness of the striking layer, as opposed to radiating through the membrane of a drum or thin metal disc of the cymbal. The settling time of the practice pad is 23 ms, compared with the snare drum's 240 ms or the ride cymbal's 1 second settling time. Therefore, to detect the strike rate the practice pad was used as a lower settling time allows strikes to be more easily detected.

### 7.3.4 Strike Rate

The strike rate of the wrist sub-system determines the tempo of music which the overall system can play. Chapter 2 noted that the fastest professional drummer was capable of approximately 1200 BPM, or 20 Hz strike rate. Performance at, or above this threshold would allow the wrist sub-system to play the majority of contemporary music performed by professional drummers. Strike rates greater than this would facilitate the composition and performance of new forms of music which cannot be performed in a live setting by professional drummers.

Although the individual strikes can be heard in the audio recording, identification of the peaks via observation of the raw waveform is increasingly difficult at higher strike rates as the previous response has not reached its settling point.

The Savitzky-Golay filter is a digital filter that is applied to a waveform in the time domain for the purpose of smoothing. This filter is widely used to identify trends in a signal without distorting the original waveform by a significant amount [96] [97].

This filter determines a polynomial relationship which can be applied to a sub-set of data specified by the window length, smoothing the amplitude of data points within the window by an amount proportional to its difference from the applied polynomial

The window length was determined by evaluating the effective window which a single strike was measured across when striking the practice pad. Using a sampling frequency of 44.1 kHz, a common analog recording frequency, a total of 3388 samples occur across this time. The rise time of the first peak detected on a strike of the practice pad is 7.8 ms with a total of 345 samples being taken, shown in Figure 7.20.

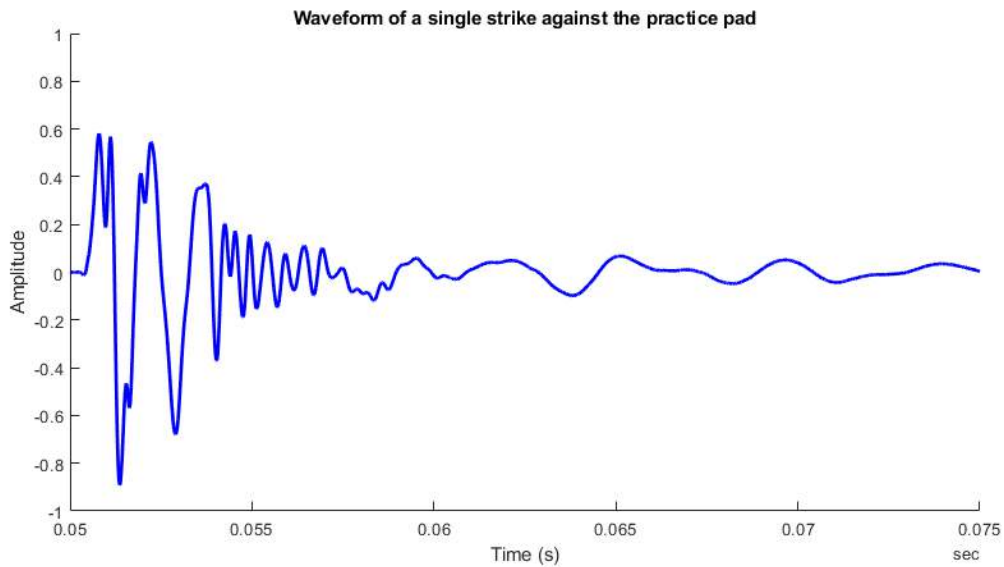


Figure. 7.20: Evaluation of the practice pad's response to a single strike.

The maximum window length was determined to be one-third of the total number of samples across an individual peak as this would result in three polynomial curves being fitted to the waveform, providing a reliable indication of a peak.

The strike rate of an individual actuator and of the two wrist actuators in unison are tested to determine the maximum operating characteristics of the wrist. To evaluate the maximum strike rate of a single actuator, the strike method discussed in Section 6.2.3 was

used. The range which the wrist moves between each strike is fine-tuned to find the maximum strike rate, recorded with the contact microphone. The minimum range which permitted the wrist enough time to strike was  $2^\circ$ , resulting in the waveform in Figure 7.21 below.

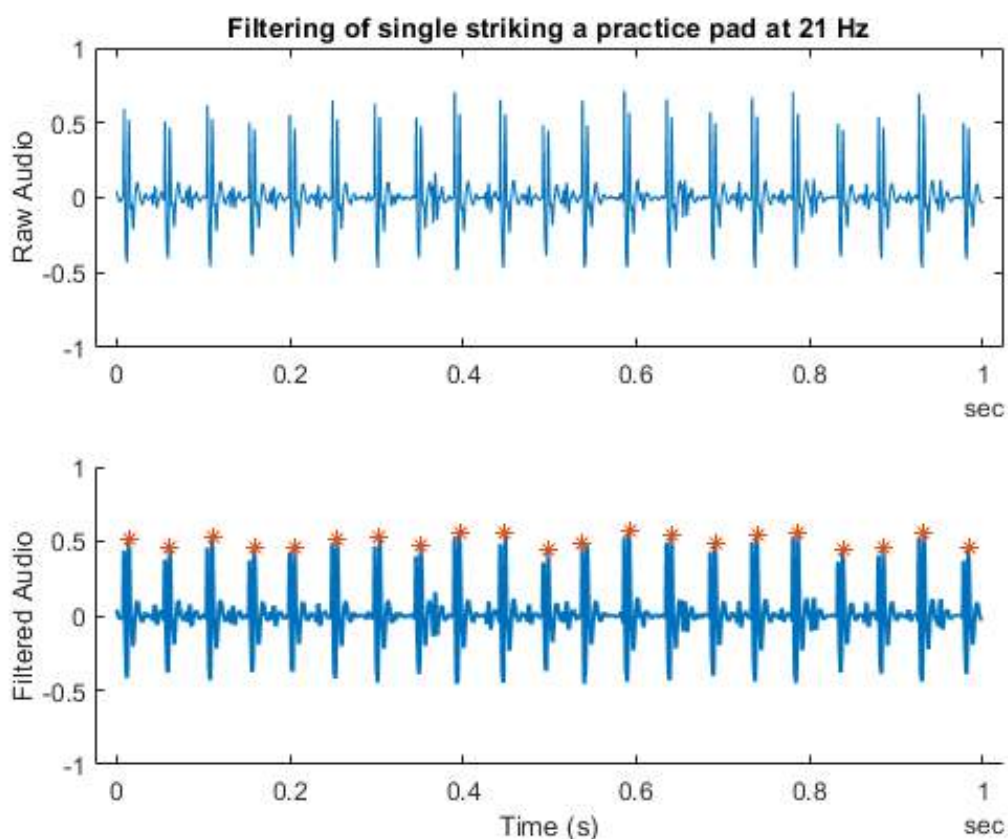


Figure. 7.21: Maximum controllable strike rate of a single actuator.

The maximum strike rate was 21 Hz, or 1260 BPM utilising a single beater against the practice pad. The clarity of the waveform indicates a lack of bouncing occurring in striking the practice pad. The strike rate of a single actuator meets the minimum requirements of the wrist sub-system operating by itself.

Incorporating the bounce of the beater into the strike rate resulted in a waveform with more artefacts present, as the consistency of the secondary strike amplitude was unpredictable. This results in primary and secondary strikes with varying sound levels due to the location of the beater changing post-strike. The cause for this is the flex of the silicone grip introducing further movement in the beaters. The amplitude of the strikes was inconsistent with the operation of the beater, resulting in the waveform shown in Figure 7.22

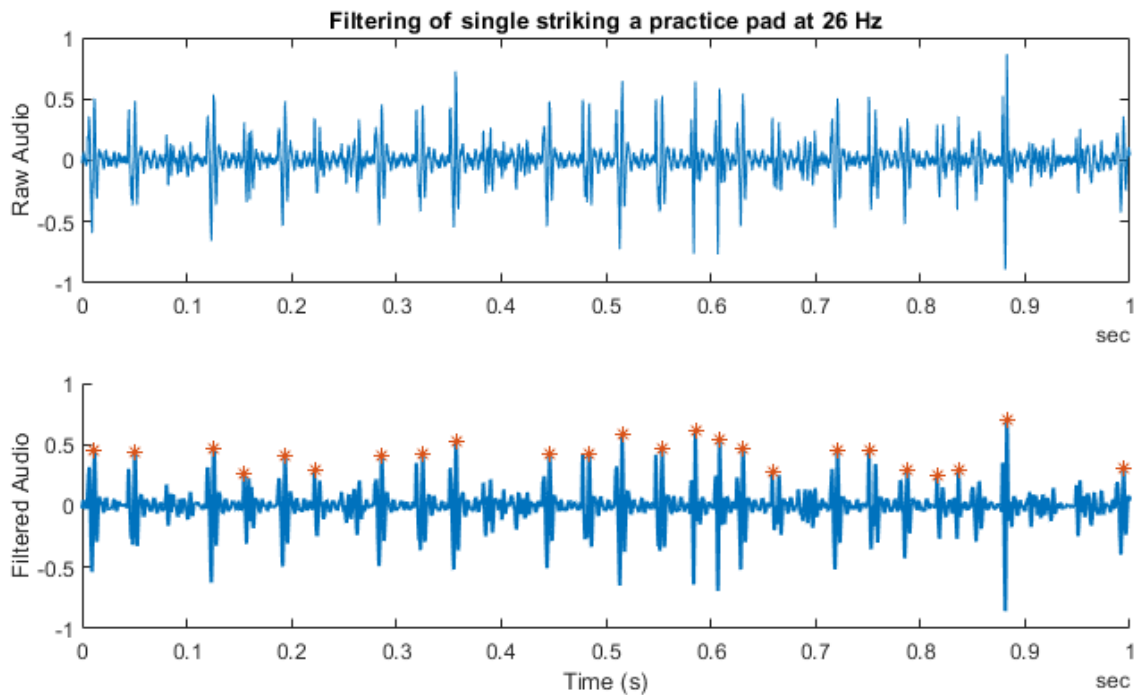


Figure 7.22: Maximum strike rate of a single actuator utilising bounce of the stick.

The maximum achievable strike rate is greater than that of the controlled strike, however, this comes at a cost to the sound level of the strike and the predictability of the amplitude.

To evaluate the performance of both wrist actuators striking the practice pad, they are instructed to operate out of phase with each other such that one beater is striking whilst the other is returning to the start position. The resultant waveform contains a large amount of noise as the maximum frequency which the practice pad can be struck before overstepping the settling time is 44 Hz. At higher frequencies, identification of resolvable single strikes becomes difficult due to overlapping strike signals with decaying signals. Savitzky-Golay filtering identifies the underlying waveform of the raw waveform being evaluated, shown in Figure [7.23](#).

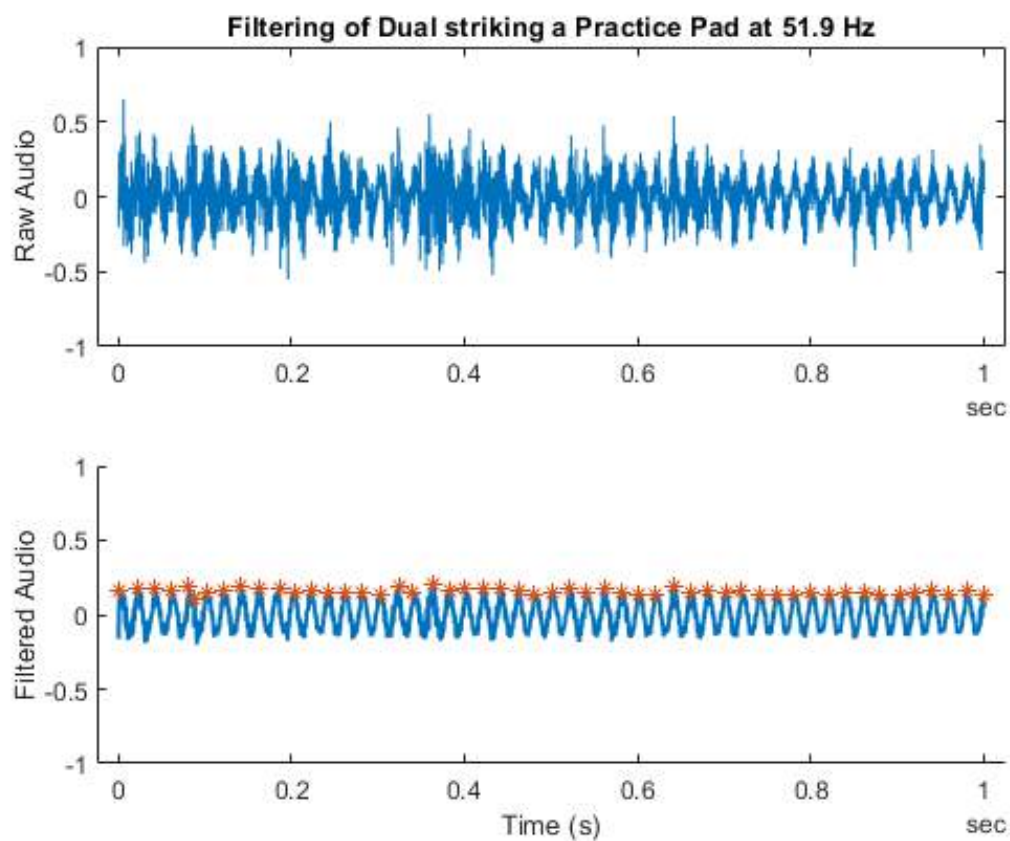


Figure. 7.23: Maximum strike rate of dual actuators.

The maximum strike rate that can be achieved utilising both actuators is 51.9 Hz. This incorporates the resultant bounce of the sticks against the practice pad. However, the resultant operation of the wrist at this frequency produces a waveform with almost indistinguishable peaks using the naked eye and inconsistent peak amplitudes. The settling time of existing drums and cymbals is too high to take advantage of the maximum speed the system is capable of. If an instrument possessed a sharper settling time than the practice pad this would present a new avenue for musical expressivity with this system.

### 7.3.5 Operation of the Wrist

Once the ranges and speeds required to achieve the maximum sound level and the maximum strike rate were known, the thermal characteristics of the wrist sub-system were evaluated.

The wrist sub-system is the only sub-system which will be required to operate almost continuously while playing a musical piece. Therefore, the temperature characteristic of the wrist when operating at the maximum strike rate or maximum sound level must be below the temperature threshold of the RX-24F.

To evaluate this, two individual tests were conducted with the wrist servomotors, one with them continuously striking the drum at maximum loudness and one with them continuously playing at the maximum strike rate. During these tests, the internal temperature and time elapsed since the start of the test were recorded. Once the internal temperature of the servomotors reached a stable temperature for longer than 10 minutes the test concluded. The resultant temperature curve for the two tests is displayed in Figure 7.24. The ambient temperature was recorded as 22° while testing the wrist servomotors and deviated by 1° between testing the maximum strike rate and the maximum sound level.

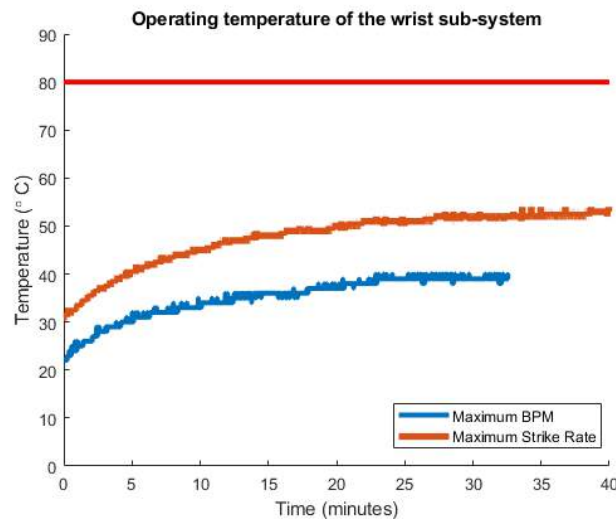


Figure. 7.24: Temperature characteristic to operation of the wrist sub-system as maximum strike rate and maximum speed.

Operating at the maximum sound level had a slightly higher settling temperature of 52°, compared to that of the maximum strike rate which settled at 39°. This is a result of the wrist servomotors travelling a larger range when achieving a greater sound level and having a greater momentum behind the movement of the servomotor shaft. However, the operation at both settings resulted in a stable temperature after 30 minutes of operation. This indicates that the wrist sub-system is capable of meeting the long operational performance requirements.

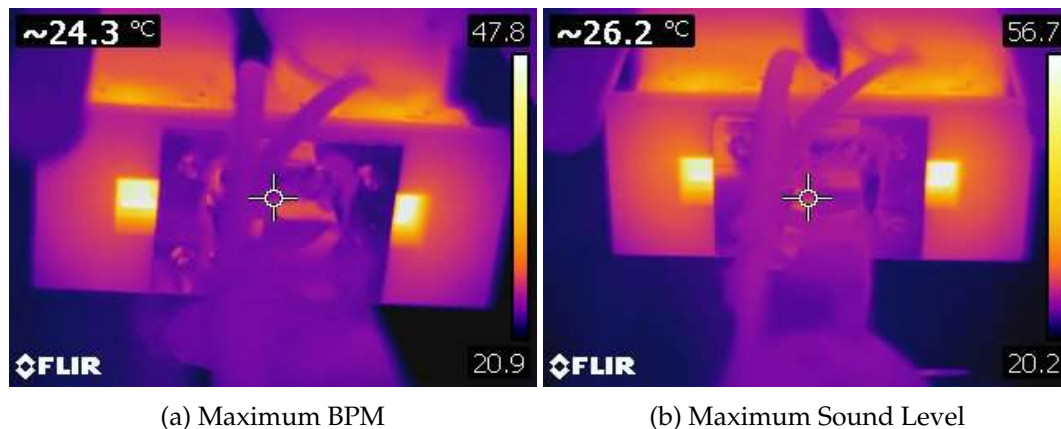


Figure. 7.25: Thermal profile of the wrist sub-system after operating for 30 minutes

The external temperature profile of the wrist sub-system was recorded with the infrared camera through the RX-24F thermal vents discussed in Section 3.8. The temperature difference between the reported internal and measured external package varies by 8 °C for the maximum strike rate and 4 °C for the maximum sound level. This difference is due to the aforementioned motor package being visible through the external package and the internal sensor measuring the temperature inside.

### 7.3.6 Wrist Summary

The wrist is capable of varying the loudness of a single strike between 68.2 dB and 106 dB using a variety of striking techniques. The resolution and range of the gripper exceed what was required, allowing the wrist to play across a variety of instrument heights. The steady-state temperature at both the maximum strike rate and the maximum beat rate is within the temperature thresholds of the actuators, allowing for extended play time. Overall, the wrist sub-system meets the requirements outlined in Section 3.7.

## 7.4 Gripper

The grip sub-system determines the amount of force with which the beaters are held in place. The expressivity of a strike is dependant on the force which the beater contacts the instrument with. This varies for different levels of pressure placed on the beater, as discussed in [4.3.2](#)

### 7.4.1 Range of Motion

The grip sub-system applies pressure to beaters of various diameters by raising and lowering the lead platform. One rotation of the AX-12A actuator is equivalent to moving one thread on the threaded platform, or a linear distance of 0.5 mm.

To evaluate the range of the grip sub-system, the AX-12A actuators rotate to the minimum position which the design allows for. Upon reaching this position, the actuators raise the lead platform until the maximum position where the threaded rod still contacts the internal thread of the platform. The time required to move from the minimum to maximum and the total displacement of the platform was recorded. The maximum and minimum positions of the grip sub-system are displayed below in [Figure 7.26](#).

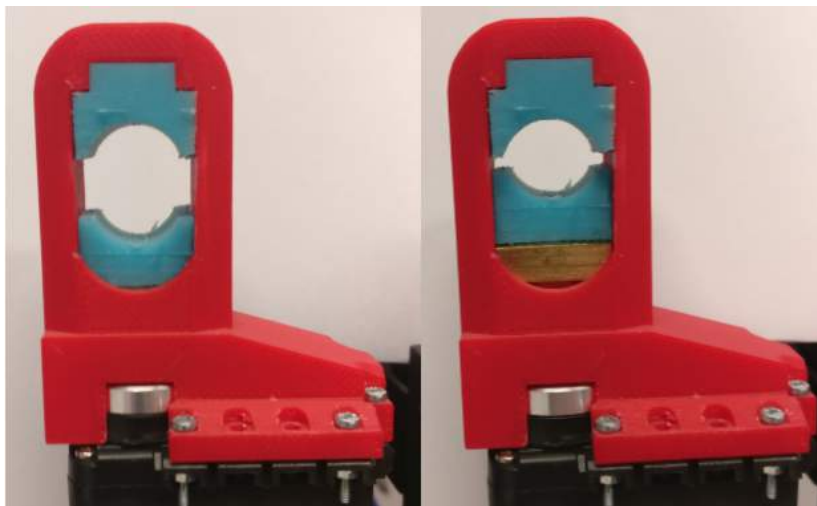


Figure. 7.26: Minimum and Maximum positions of the lead platform of the gripper sub-assembly.

The lead platform can move a total range of 8 mm from inside the AX-12A bracket. At the minimum position, beaters with a 19 mm diameter can be placed and secured by the platform. At a maximum position, a beater of 12.4 mm can be gripped. The travel time of the system is 1 s between the minimum and maximum grip positioning at maximum speed. A total of 0.5 mm deformation was recorded in the top and bottom silicone grip pads. The FSR sensor was incorporated into the design of the gripper to provide feedback to the force applied to the beater which is being held. The resolution of the grip sub-system is determined by the FSR value. The speed of the AX-12A can be adjusted from a minimum of 0.036 mm per second to a maximum of 0.5 mm per second.

### 7.4.2 Effect of grip variation

The grip placed upon the beater determines the response characteristics of striking the instrument. The range which the sensor provides must be evaluated to determine grip settings for the sub-system. This was accomplished by raising the lead platform from the minimum pressure value read by the FSR to the maximum value, at which point the platform is then lowered back to the minimum. The current time and value of the FSR sensor was recorded and the resultant grip curve is shown below in Figure 7.27.

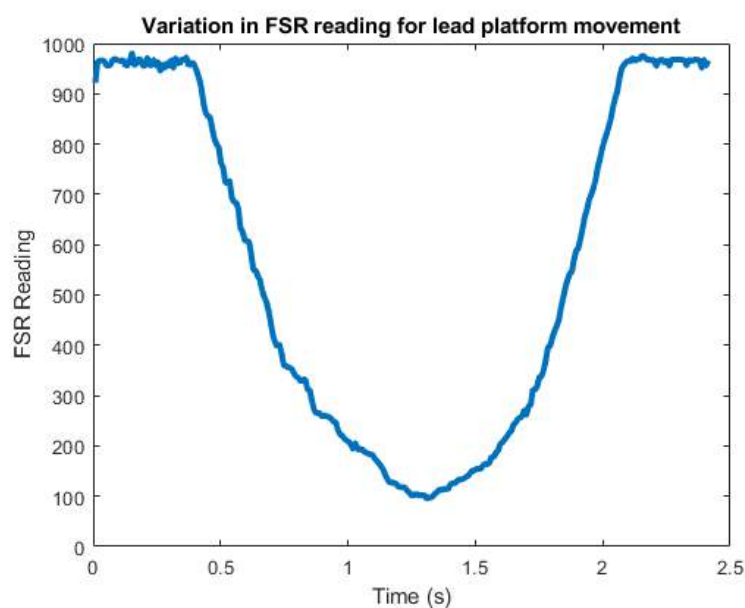


Figure. 7.27: Effect of grip actuator rotation on the FSR reading.

The movement of the platform is linear, changing the value of the FSR consistently while increasing and decreasing the pressure applied to the beater.

To evaluate the effect which the level of grip has on the strike response of the beater, six individual levels of grip were chosen based on a percentage value of the sensor value from the FSR. These values vary from 100% to 0% in steps of 20%. The wrist sub-system moves to strike the surface of a snare drum and disengages the torque on the servomotor shaft allowing it to move freely after making contact with the surface. The waveform of the initial strike and bounce of the drum stick was recorded using the piezoelectric contact microphone. The responses of each grip setting were plotted and are displayed below in Figure 7.28.

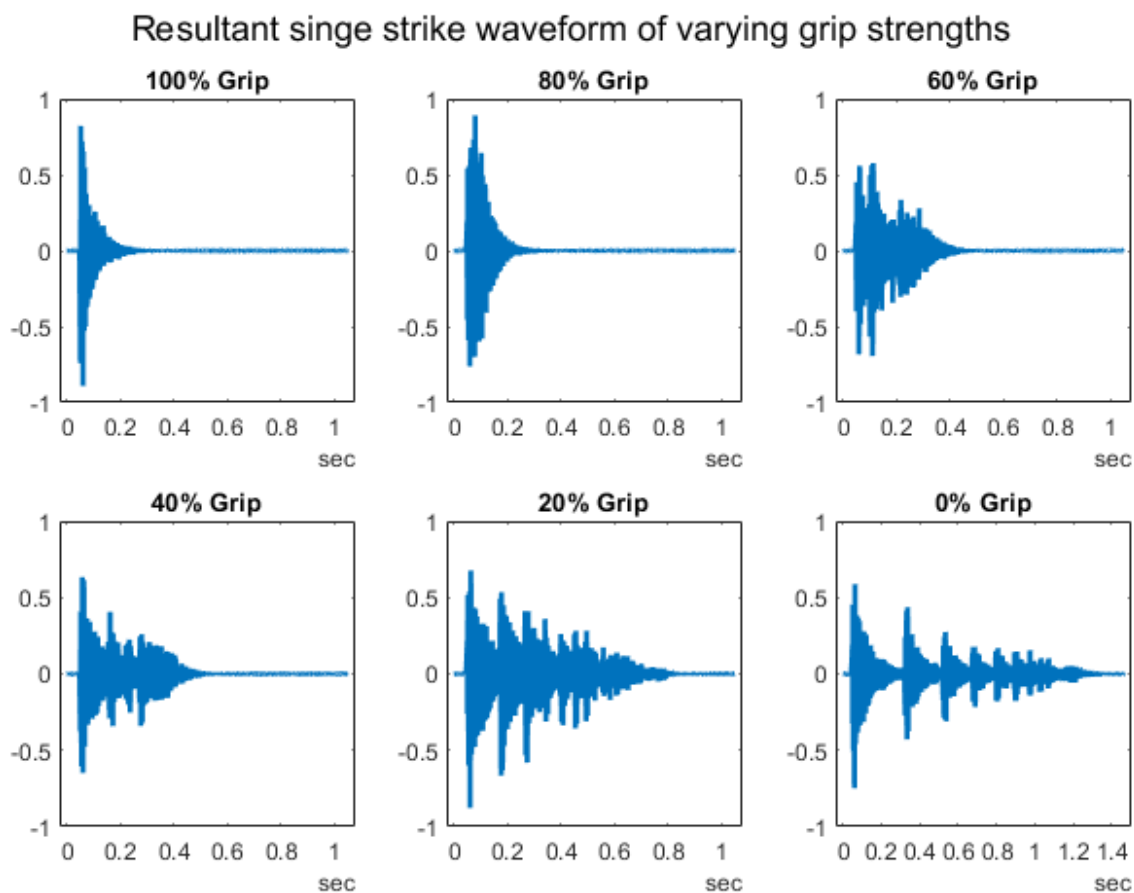


Figure. 7.28: Effect of grip setting on the response of the beater.

As the grip decreases on the beater, the number of additional strikes increases, indicating that the grip has an impact on the level of resultant deflection post-striking. A grip of 0% permits an additional eight strikes after the initial impact. At this setting, the stick is essentially free to move and flex the silicone grip. The same number of strikes are visible in the 20% grip setting, however, they are within a smaller frame of time. This indicates an equal level of energy placed in the strike and the effect a decrease in flex due to grip has on the waveform. As the grip increases, the resultant energy dispersion occurs in a smaller and smaller time frame, with a succinct single peak strike at 100% grip.

The relationship between the grip strength and the number of resultant strikes would indicate that it could be used to increase the overall strike rate of the system. However, the instruments available were unable to clearly distinguish peaks from current high-speed operation and evaluation of similar frequency waveforms would be unreliable.

### 7.4.3 Operation of the Gripper

Variation in the grip of a professional drummer seldom occurs and there is currently no established framework which influences the choice of grip in this system. The predominant use of the grippers is in the initial calibration of the system and use of varying beater diameters. Grip variation during play was not explored during evaluation of the system, and a thermal profile was unnecessary due to the minimal operating time which the AX-12A's are being used for.

## 7.5 System Overview

### 7.5.1 Noise Characterisation

Once the maximum and minimum ranges of motion for each sub-system were defined, the overall mechanical noise introduced by the robot was identified. The ambient noise recorded in the testing environment was measured as 47.2 dB, with a peak of 49.6 dB. This is comparable to the average air-conditioned room, with a generally continuous noise profile and low frequency intermittent noise. The continuous sinusoidal noise throughout Figure 7.29 is the hum of the Topward power supply which powers the system.

Table 7.4: Recorded sound level of ambient and system noise

	Average Sound Level (dB)	Maximum Sound Level (dB)
Ambient Noise	47.2	49.6
Shoulder	53.2	54.7
Gripper	53.4	54.5
Wrists at Max BPM	47.1	48.7
Wrists at Max Loudness	48.1	50.4
Elbow	54.5	56.2
Overall System	56.9	61.8

The profile of the sound level from the wrist sub-system operating at maximum strike rate and maximum sound level settings deviate from the average noise level of the ambient room by  $\pm 0.8$  dB. This is low enough to retain the fidelity of a drum strike if a microphone is used to record the drum's performance, as the wrist will be the most active sub-system when playing a composition.

The loudest operational noise was recorded when all four sub-systems are engaged, moving at maximum speed between the extreme set points, a worst-case scenario, shown below in Figure 7.29.

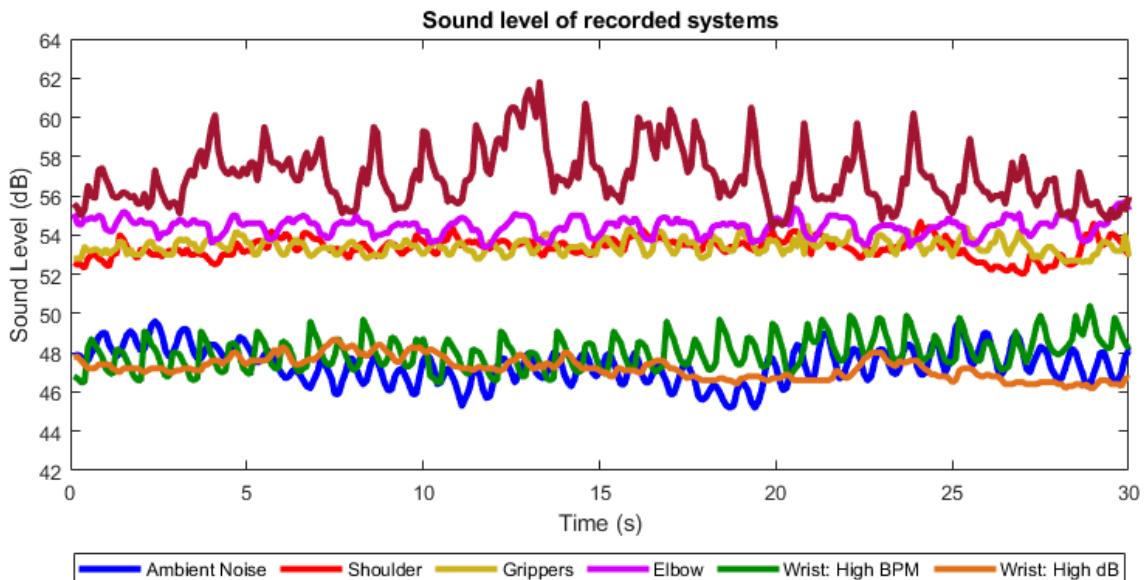


Figure 7.29: Sound level of each sub-system operating individually, together and ambient noise.

The recorded noise displayed a continuously intermittent pattern, resembling the sound level of the loudest sub-system recorded, the elbow sub-system. Superposition can be used to predict the resultant summation of individual sound waves if the waves have a consistent frequency and phase relationship. However, the noise produced by the four sub-systems is incoherent and uncorrelated. The average noise produced by the system operating in the worst-case scenario was recorded as 56.9 dB, with a peak of 61.8 dB.

The minimum sound level produced by a single strike of the wrist, discussed above in Section 7.3.2, was recorded as 68.1 dB. The difference of 6 dB results in an effective 1.5 times louder, two times more sound pressure and 4 times as much acoustic intensity. Therefore, the maximum noise produced by the operation of the sub-systems is low enough to not impact the sonic quality of a live performance. This allows the system to be operated without requiring the instruments to be selectively amplified for smaller performances.

## 7.5.2 Simultaneous Operation

To determine the overall functionality of the system, the three main sub-systems performed a test which required movement comparable to that of a contemporary composition.

The test involved having the system play across a snare drum and a crash cymbal that are set up in two different locations of the shoulder arc and at two different heights. Both wrist actuators had to strike the snare drum and then strike the cymbal at a lower sound level. This test required the elbow, shoulder and wrist sub-systems to move in unison and operate as one functioning system. The resultant waveform is displayed below in Figure 7.30.

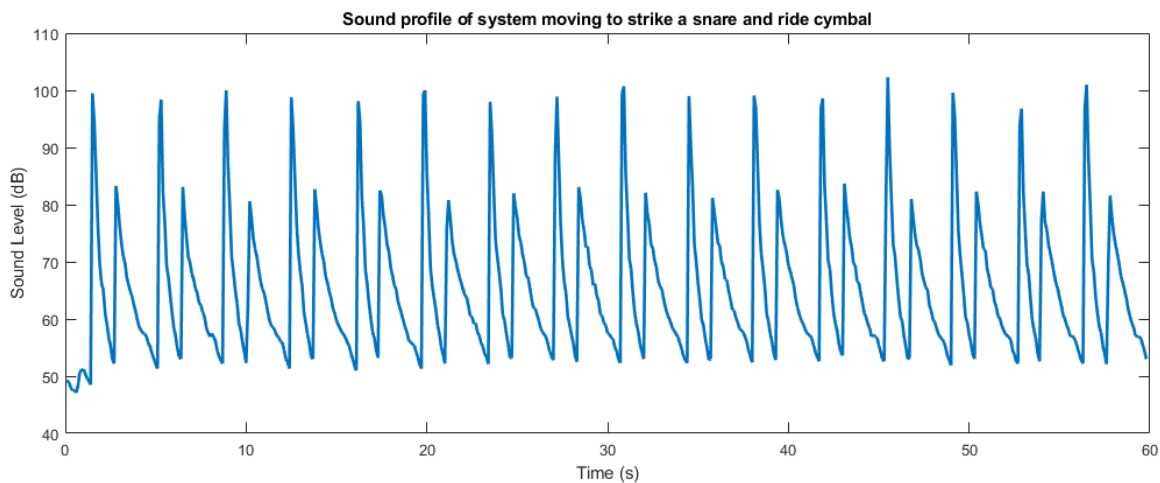


Figure. 7.30: Sound level of the overall system test playing the snare and crash cymbal.

The snare drum produced an average sound level of 98.6 dB with a standard deviation of 3.4 dB, with the crash cymbal having an average sound level of 82 dB and a standard deviation of 2.1 dB.

The variation in sound level is within the acceptable limits of a professional drum player and may be attributed to the backlash in the shoulder sub-system affecting the positioning of the wrist actuators as they strike different locations on the drum. The crash cymbal has a relatively uniform sound profile due to the metal having equivalent noise characteristics if it is struck with the same force, as opposed to the snare drum, whose sonic qualities and decay vary heavily based on position.

## 7.6 Summary

Overall, the system provides the panning range required to play across a horizontal drum kit, the tilting capacity to play across a traditional drum kit and a strike rate more than that achievable by a professional drummer and at a controllable and variable sound level. The system provides additional capacity for expressiveness through the variation of force on the beater, allowing or preventing additional strikes.

Video documentation of a singular arm operating and of the three arms together in a variety of combinations can be retrieved at the following cited links [\[98\]](#) [\[99\]](#) [\[100\]](#) [\[101\]](#) [\[102\]](#) [\[103\]](#) [\[104\]](#).

## Chapter 8

# Conclusion

### 8.1 Summary

Previous mechatronic percussion instruments that spanned across multiple instruments lacked expressivity and modularity. We designed a system that can expressively play across an entire drum kit while successfully mitigating the limitations that were identified in human drummers.

Our mechatronic percussion system consists of four sub-systems whose operation was characterised and overall performance evaluated. Each of these sub-systems is actuated using Dynamixel series servomotors and constructed using a mix of 3D printed ABS, laser cut acrylic and machine milled components. The limitations of each sub-system's design have been minimised through the use of external sensors.

The Motherboard co-ordinates communication from an external user, interpreting MIDI signals into actionable movements sent to each Daughterboard using RS-485. The voltage and current required by the Daughterboards are distributed through the Motherboard to each of the arms in a parallelised configuration.

The Daughterboard includes external sensor functionality and effectively communicates to both the Dynamixel servomotors and Motherboard through a microcontroller. Several safety protocols which incorporate feedback from the external sensors and the Dynamixel actuators are implemented to prevent the arm from damaging itself. The software package on the Daughterboard supports operation of the actuators, using feedback from internal and external sensors to perform system calibration, calibration of drum locations and different drum strokes effectively.

The evaluation of the mechatronic system's performance included characterisation of each sub-system, analysis of drum strokes and variation of grip settings. Steady-state temperature evaluation of the shoulder sub-system indicated that operating using speed settings led to servomotor overheating. Instead, the shoulder must be torque limited with further evaluation indicating safe operating settings and the resultant change in overall performance. With a torque limit in place, the overall system could operate for a minimum of 5 hours before the elbow sub-system failed. However, reasonable operation of the system is projected to allow for continuous operation without heat damage to the components. This allows the system to play for extended periods of time in an installation or live performance setting.

Range of motion evaluation indicates that the system is capable of playing across both a traditional drum kit with no further alterations being required, with the modularity to be positioned and calibrated to a wide variety of custom configurations. While there are configurations that would optimise operation for minimal travel times, any position within the reach of the arm and arc of the shoulder can be played.

The grip sub-system is capable of dynamically varying the pressure applied to a wide range of beaters that are commonly used by professional drummers. The incorporation of compliant silicone pads increases the expressivity of grip placed upon the beater. Additionally, the design of 3D printed moulds for creation of the silicone pads allows the user to implement new beater diameters or alter separation between beaters in short periods of time. The implementation of the grip sub-system permits further investigation into the effect of pressure and compliance on the acoustic qualities of percussion compositions which has not been done before.

Analysis of various striking techniques found that the sound pressure level created by the wrist sub-system could be controlled between 68 dB and 106 dB using two different striking techniques, allowing the system to play a large variety of percussion styles suitable for different settings. An evaluation of noise generated by the overall system indicated that when operating at maximum speed, the level of noise was notably less than the minimum strike loudness that could be produced.

## 8.2 Future Work

Our mechatronic percussion system has some limitations or aspects that could be improved if additional time was available. Future work that could expand upon this project is outlined below:

- The panning speed of the shoulder servomotor from the minimum to maximum set points is lower than the original specifications of the system. The speed of the shoulder could be increased by gearing up the ratio from 1:1. However, this will increase the torque acting on the motor shaft which will potentially slow down the RX-24F servomotor further. Upgrading the current shoulder servomotor to decrease the panning time between instruments would facilitate faster repositioning.
- While the servomotor selected for the gripper is capable of altering the pressure applied to beaters of different diameters, the accuracy of the pressure applied is dependent on the placement of an external sensor with no reliable force feedback relationship. FSRs use a layer of conductive ink to decrease the resistance measured across its connectors. Over time, this ink is prone to breakdown, altering the relationship between force and resistance. Future work could replace the grip sub-system's actuator with a linear actuator which would increase the reliability of operation and reduce the complexity of the design by not requiring a lead screw and platform to apply pressure to the beater.
- The software implemented for the MIDI interpreter on the Motherboard to receive signals from an external source includes use cases for NoteOn functionality. Future work could implement further MIDI functions which affect the wider operation of the arms such as volume and mode of the instrument being struck.
- Three identical arms were constructed that operate using the same software functions. However, to achieve play across a drum kit still requires individual addressing of each arm and the required striking parameters. Future work would integrate the operation of the three arms through use of the Motherboard, to provide one addressable unit. This would allow abstraction of control to a higher level, whereby a MIDI command is all that is required to direct the corresponding arm to the instrument and strike.

- Analysis of the maximum strike rate which could be reliably achieved was inhibited by the settling time of the instrument used. Development of a percussive instrument with a lower settling time, such as a bespoke drum or cymbal with a small diameter, would allow further experimentation with high-speed compositions.
- 3D printed ABS plastic was used to construct several components of the system. Over time these components are subject to wearing down and breaking, requiring re-printing and replacement. Future revisions to the physical design would use materials which are more durable and have greater tensile strength, such as milled aluminium.

### 8.3 Conclusions

A single wrist actuator is capable of reliably playing at a faster strike rate than the fastest recorded human drummer. Two actuators operating in an alternating strike pattern, with incorporation of secondary strikes, can achieve a rate of 2.5 times the human speed. This allows users to experiment with compositions containing high strike rates while preserving the expressive characteristics generally lost from previous robotic or synthetic approaches.

Previous systems have not included a way to hold varying beaters without changes to the design, let alone alter the pressure applied to the beater. Our system can incorporate a wide selection of beater diameters dynamically without requiring modifications prior to use. Additionally, the grip sub-system can apply variable pressure to the entire range of beaters that can be held.

The overall system can play across a traditional drum kit set up in a purely horizontal configuration or in a conventional, vertically staggered system while varying the loudness of strikes between levels that are comparable to office conversation and as high as live rock concerts.

The project achieved its goal of designing and constructing a mechatronic system that exhibits the desirable expressive qualities highlighted through an evaluation of human drummers and previous systems. Additionally, it is capable of playing across a large range of percussion instruments precisely for an extended period of time.

# Bibliography

- [1] J. Murphy, *Expressive musical robots: building, evaluating, and interfacing with an ensemble of mechatronic instruments: a thesis submitted to the Victoria University of Wellington in fulfilment of the requirements for the degree of Doctor of Philosophy*. PhD thesis, Massey University, 2014.
- [2] J. Long, J. W. Murphy, A. Kapur, and D. A. Carnegie, "A methodology for evaluating robotic striking mechanisms for musical contexts.," in *NIME*, pp. 404–407, 2015.
- [3] N. Collins and J. d'Escriván, *The Cambridge companion to electronic music*. Cambridge University Press, 2017.
- [4] S. Fujii and T. Moritani, "Rise rate and timing variability of surface electromyographic activity during rhythmic drumming movements in the world's fastest drummer," *Journal of Electromyography and Kinesiology*, vol. 22, no. 1, pp. 60–66, 2012.
- [5] T. D. Rossing, "Science of percussion instruments," 2001.
- [6] R. Toulson, C. C. Crigny, P. Robinson, and P. Richardson, "The perception and importance of drum tuning in live performance and music production," *The Journal on the Art of Record Production*, no. 4, 2009.
- [7] G. Nicholls, *The Drum Book: A history of the rock drum kit*. Rowman & Littlefield, 2008.
- [8] A. Wagner, *Analysis of drumbeats: interaction between drummer, drumstick and instrument*. PhD thesis, Kunglia Tekniska Högskolan, 2006.
- [9] S. E. Millender Jr, J. M. Bradman, and J. William 'Billy' L, "Method and apparatus for optimizing sound output characteristics of a drum," June 28 2011. US Patent 7,968,780.
- [10] J. A. Bilmes, "Techniques to foster drum machine expressivity," in *ICMC*, vol. 93, pp. 276–283, 1993.
- [11] C. J. Hasser and M. R. Cutkosky, "System identification of the human hand grasping a haptic knob," in *haptics*, p. 180, IEEE, 2002.
- [12] J. A. Lento, "Drum glove," Nov. 2 2004. US Patent 6,810,531.

- [13] "Drum physics, pt. 2: A primer on the two grip-styles." <http://hyper-drum.blogspot.com/2014/08/drum-physics-pt-2-primer-on-two-grip.html>, 2014.
- [14] S. DiGiovanni, "Drum for striking upwardly and method therefor," May 5 2009. US Patent 7,528,312.
- [15] S. Dahl, "Striking movements: A survey of motion analysis of percussionists," *Acoustical science and technology*, vol. 32, no. 5, pp. 168–173, 2011.
- [16] C. Eduardo and F. Kumor, *Drum circle: a guide to world percussion*. Alfred Music Publishing, 2001.
- [17] G. Anderson, "Drummer ali smashes guinness world record in memory of 7 year-old cousin cariss." <https://www.belfastlive.co.uk/incoming/drummer-ali-smashes-guinness-world-12135205/>, 2016.
- [18] J. Bell, "British champion drummer breaks second world record with 12-hour drum roll in dartford." [https://www.newshopper.co.uk/news/dartford\\_swanley/12956594.British\\_champion\\_drummer\\_breaks\\_second\\_world\\_record\\_with\\_12\\_hour\\_drum\\_roll\\_in\\_Dartford/](https://www.newshopper.co.uk/news/dartford_swanley/12956594.British_champion_drummer_breaks_second_world_record_with_12_hour_drum_roll_in_Dartford/), 2015.
- [19] W. Balliett, *American musicians: fifty-six portraits in jazz*. Oxford University Press, USA, 1986.
- [20] D. Grohl, "Dave grohl - play (official video)." <https://www.youtube.com/watch?v=e05H80-k0mY>.
- [21] E. M.-B. Speed, "Maneuvering around the kit with combos (full drumeo lesson). 2016," *Youtube-opetusvideo. Viitattu*, vol. 29, 2017.
- [22] H. Honing and W. B. De Haas, "Swing once more: Relating timing and tempo in expert jazz drumming," *Music Perception: An Interdisciplinary Journal*, vol. 25, no. 5, pp. 471–476, 2008.
- [23] G. N. Tamlyn, *The Big Beat: Origins and development of snare backbeat and other accompanimental rhythms in Rock'n'Roll*. PhD thesis, University of Liverpool England, 1998.
- [24] J. D. Knowles and D. Hewitt, "Performance recordivity: studio music in a live context," 2012.

- [25] M. Brain and L. Looper, "How electromagnets work," *HowStuffWorks. HowStuffWorks.com*, 1 Apr. 2000. Web. 30 Sept. 2014.; <http://science.howstuffworks.com/electromagnet.htm>, 2000.
- [26] A. Kapur, M. Darling, J. W. Murphy, J. Hochenbaum, D. Diakopoulos, and T. Trimpin, "The karmetik notomoton: A new breed of musical robot for teaching and performance.," in *NIME*, pp. 228–231, 2011.
- [27] A. Kapur and M. Darling, "Building musical robots for the machine orchestra," in *Proceedings of the IEEE International Conference on Intelligent Robots and Systems*, pp. 25–30, Citeseer, 2010.
- [28] G. Weinberg, S. Driscoll, and T. Thatcher, "Jam'aa-a middle eastern percussion ensemble for human and robotic players.," in *ICMC*, 2006.
- [29] J. Long, J. W. Murphy, A. Kapur, and D. A. Carnegie, "A methodology for evaluating robotic striking mechanisms for musical contexts.," in *NIME*, pp. 404–407, 2015.
- [30] J. Murphy, D. A. Carnegie, and A. Kapur, "Little drummer bot: Building, testing, and interfacing with a new expressive mechatronic drum system," in *Proceedings of the International Computer Music Conference. ICMC*, 2014.
- [31] A. Davies and A. Crosby, "Compressorhead: the robot band and its transmedia story-world," in *International Workshop in Cultural Robotics*, pp. 175–189, Springer, 2015.
- [32] W. Commons, "Platin drums classic set 2216 amber fade." [https://commons.wikimedia.org/wiki/File:Platin\\_Drums\\_PTCL2016\\_AF.jpg](https://commons.wikimedia.org/wiki/File:Platin_Drums_PTCL2016_AF.jpg), 2003.
- [33] C. N. Thai, *Exploring Robotics with ROBOTIS Systems*. Springer, 2017.
- [34] D. Tolani and N. I. Badler, "Real-time inverse kinematics of the human arm," *Presence: Teleoperators & Virtual Environments*, vol. 5, no. 4, pp. 393–401, 1996.
- [35] K. M. Reed, "Musical drum," June 16 2009. US Patent 7,547,836.
- [36] A. Tommasini, "How long, in opera, is too long?," Jan 2000.
- [37] S. Sonnentag, H. Arbeus, C. Mahn, and C. Fritz, "Exhaustion and lack of psychological detachment from work during off-job time: Moderator effects of time pressure and leisure experiences.," *Journal of Occupational Health Psychology*, vol. 19, no. 2, p. 206, 2014.

- [38] Robotis, *AX-12A User Manual*. Dynamixel, 2006.
- [39] Robotis, *RX-24F User Manual*. Dynamixel, 2010. V1.29.00.
- [40] Robotis, *MX-64T User Manual*. Dynamixel, 2010. V1.29.00.
- [41] G. M. Maitra, *Handbook of gear design*. Tata McGraw-Hill Education, 1994.
- [42] A. McRitchie, "How to: Set a gear mesh on an rc vehicle-," May 2016.
- [43] K. J. Christiyan, U. Chandrasekhar, and K. Venkateswarlu, "A study on the influence of process parameters on the mechanical properties of 3d printed abs composite," in *IOP Conference Series: Materials Science and Engineering*, vol. 114, p. 012109, IOP Publishing, 2016.
- [44] F. Malagelada, M. Dalmau-Pastor, J. Vega, and P. Golano, *Elbow Anatomy*, pp. 1–30. 01 2014.
- [45] G. Woan, *The Cambridge handbook of physics formulas*. Cambridge University Press, 2000.
- [46] J. E. Shigley, *Shigley's mechanical engineering design*. Tata McGraw-Hill Education, 2011.
- [47] U. S. Plastic Corporation, *Average weight per square foot for the acrylic sheet*. 884, 2010.
- [48] Altuglas International Arkema Group, *Average Physical Properties of Acrylic Sheets?* Plexiglas G, 2002.
- [49] O. Electronics, *Basic / Snap Action Switches 250VAC 5A 1.47 N. D2F-5L*, 2017.
- [50] G. R. North, J. A. Pyle, and F. Zhang, *Encyclopedia of atmospheric sciences*, vol. 1. Elsevier, 2014.
- [51] W. H. Organization *et al.*, "Hearing loss due to recreational exposure to loud sounds: A review," tech. rep., World Health Organization, 2015.
- [52] H. . Littelfuse, *Magnetic/Reed Switches 10-15AT 200Vdc @ 10W. MASM-14R-10-15*, 2015.
- [53] J. McGrath, R. Eady, and F. Pope, "Anatomy and organization of human skin," *Rook's textbook of dermatology*, vol. 1, pp. 3–1, 2010.
- [54] P. G. Agache, C. Monneur, J. L. Leveque, and J. De Rigal, "Mechanical properties and young's modulus of human skin in vivo," *Archives of dermatological research*, vol. 269, no. 3, pp. 221–232, 1980.

- [55] J. A. Saunders and D. C. Knill, "Humans use continuous visual feedback from the hand to control both the direction and distance of pointing movements," *Experimental brain research*, vol. 162, no. 4, pp. 458–473, 2005.
- [56] F. Azzarto, "What you need to know about...drumsticks." <https://www.moderndrummer.com/2014/12/need-know-drumsticks/>, Feb 2010.
- [57] J. Tan, "Radial nerve entrapment at the elbow; radial tunnel syndrome and posterior interosseous nerve syndrome." <https://bit.ly/2TbpdMh>, Jul 2014.
- [58] Interlink, *Force-Sensing Resistor: 0.25 Diameter Circle, Short Tail*. FSR 400 Short, 2010.
- [59] C. Coward, *3D Printing*. Penguin, 2015.
- [60] K. B. Shimoga and A. A. Goldenberg, "Soft robotic fingertips: Part i: A comparison of construction materials," *The International Journal of Robotics Research*, vol. 15, no. 4, pp. 320–334, 1996.
- [61] N. Elango and A. Faudzi, "A review article: investigations on soft materials for soft robot manipulations," *The International Journal of Advanced Manufacturing Technology*, vol. 80, no. 5-8, pp. 1027–1037, 2015.
- [62] H. Iwata and S. Sugano, "Design of anthropomorphic dexterous hand with passive joints and sensitive soft skins," in *2009 IEEE/SICE International Symposium on System Integration (SII)*, pp. 129–134, IEEE, 2009.
- [63] H. Qi, K. Joyce, and M. Boyce, "Durometer hardness and the stress-strain behavior of elastomeric materials," *Rubber chemistry and technology*, vol. 76, no. 2, pp. 419–435, 2003.
- [64] C. Edwards and R. Marks, "Evaluation of biomechanical properties of human skin," *Clinics in dermatology*, vol. 13, no. 4, pp. 375–380, 1995.
- [65] Pit Stop USA, "Durometer indenter testing pressed into rubber." [https://www.speednik.com/wp-content/blogs.dir/1/files/2011/03/durometer1\\_640-400x285.jpg](https://www.speednik.com/wp-content/blogs.dir/1/files/2011/03/durometer1_640-400x285.jpg), 2011.
- [66] S.-O. Plastics, "Durometer chart." <https://www.smooth-on.com/pw/site/assets/files/30090/durometerchart.png>, 2012.
- [67] C. Rao, "Physical modelling for electronics enclosures using rapid prototyping."

- [68] R. M. Foster, "Geometrical circuits of electrical networks," *Transactions of the American Institute of Electrical Engineers*, vol. 51, no. 2, pp. 309–317, 1932.
- [69] E. Suhir, "Thermal stress in through-silicon-vias: theory-of-elasticity approach," *Microelectronics Reliability*, vol. 54, no. 5, pp. 972–977, 2014.
- [70] V. K. Tamarkin and R. H. Fix, "Printed circuit board routing techniques," July 3 2001. US Patent 6,256,769.
- [71] J. Rothstein, *MIDI: A comprehensive introduction*, vol. 7. AR Editions, Inc., 1995.
- [72] MOLEX, *Mini-fit Jr. Wire-to-board*. 39-02-7028, 2018.
- [73] R. Widlar, "New developments in ic voltage regulators," in *1970 IEEE International Solid-State Circuits Conference. Digest of Technical Papers*, vol. 13, pp. 158–159, IEEE, 1970.
- [74] ON Semiconductors, *1.0 A Positive Voltage Regulators*. MC7805, 2010.
- [75] S. V. Karuppana, A. A. Jetha, and J. Thomsen, "System and method for providing surge, short, and reverse polarity connection protection," Aug. 20 2002. US Patent 6,437,957.
- [76] Vishay/Siliconix, *MOSFET -30V Vds PowerPAK AEC-Q101 Qualified*. SQJ407EP-T1GE3, 2014.
- [77] J. Rothstein, *MIDI: A comprehensive introduction*, vol. 7. AR Editions, Inc., 1995.
- [78] LITEON Technology Corporation, *Single channel, High speed optocoupler*. 6N138, 2012.
- [79] T. CHEN and C. XIE, "Design of software and hardware in serial-communication between pc and multiple mcus based on rs 485 [j]," *Modern Electronics Technique*, vol. 5, 2007.
- [80] A. I. Leibovich, "Build rs-422/rs-485 transceivers with configurable mixed-signal ics," Feb 2017.
- [81] M. Soltero, J. Zhang, C. Cockril, *et al.*, "Rs-422 and rs-485 standards overview and system configurations," 2002.
- [82] MAXLinear, *3.3V Low Power Half-Duplex RS-485 Transceiver with 10Mbps Data Rate*. SP3485EN-LTR, 2016.

- [83] Maxim Integrated, "Determining clock accuracy requirements for uart communications." <https://pdfserv.maximintegrated.com/en/an/AN2141.pdf>, 2003.
- [84] P. J. Stoffregen and R. C. Coon, "Teensy usb development board," *Code Library*, 2014.
- [85] NXP-Semiconductors, *120 MHz ARM® Cortex®-M4-based Microcontroller with FPU. Kinetis K64F*, 2015. Rev. 6.
- [86] M. R. Jouppi, "Current carrying capacity in printed circuits," *Past, Present and Future*, [www.thermalman.com](http://www.thermalman.com), 2007.
- [87] Topward, *6303D Triple Output Power Supply. T 6303D*, 2005.
- [88] M. Dewadasa, A. Ghosh, and G. Ledwich, "Dynamic response of distributed generators in a hybrid microgrid," in *2011 IEEE Power and Energy Society General Meeting*, pp. 1–8, IEEE, 2011.
- [89] J. I. Choi, M. Jain, K. Srinivasan, P. Levis, and S. Katti, "Achieving single channel, full duplex wireless communication," in *Proceedings of the sixteenth annual international conference on Mobile computing and networking*, pp. 1–12, ACM, 2010.
- [90] Texas Instruments, *Dual Bus Buffer Gate With 3-State Outputs. SN74LVC2G125DCTR*, 2017.
- [91] A. Savage, *Arduino and Dynamixel Library for AX-12A*. Savage Electronics, 2011.
- [92] J. Bayle, *C programming for Arduino*. Packt Publishing Ltd, 2013.
- [93] FLIR Systems, *ThermaCAM T400 Technical Specifications. T400*, 2010.
- [94] Tenma, *Sound Level Meter w/ USB Interface. 72-947*, 2018. Rev 1.1.
- [95] L. Morissette, *Basic Contact Microphone*. Cold Gold, 2015.
- [96] G. Luck, S. Saarikallio, B. Burger, M. R. Thompson, and P. Toiviainen, "Effects of the big five and musical genre on music-induced movement," *Journal of Research in Personality*, vol. 44, no. 6, pp. 714–720, 2010.
- [97] R. W. Schafer *et al.*, "What is a savitzky-golay filter," *IEEE Signal processing magazine*, vol. 28, no. 4, pp. 111–117, 2011.
- [98] T. Little, "Mechatronic percussion system - three arms in unison, recording 2." <https://vimeo.com/user95788337/review/321146629/9a7b39a8d3>, 2019.

- [99] T. Little, "Mechatronic percussion system - three arms in unison, recording 2." <https://vimeo.com/user95788337/review/321146786/a01c70c4ad>, 2019.
- [100] T. Little, "Mechatronic percussion system - three stationary arms." <https://vimeo.com/user95788337/review/321145825/81e0c686b9>, 2019.
- [101] T. Little, "Mechatronic percussion system - one arm displaying verticality." <https://vimeo.com/user95788337/review/321145802/56ea95f8f4>, 2019.
- [102] T. Little, "Mechatronic percussion system - one arm drum roll." <https://vimeo.com/user95788337/review/321145784/9698290114>, 2019.
- [103] T. Little, "Mechatronic percussion system - one arm double stroke pan." <https://vimeo.com/user95788337/review/321145765/ee5d8fe4a8>, 2019.
- [104] T. Little, "Mechatronic percussion system - one arm single strike pan." <https://vimeo.com/user95788337/review/321145748/a3144d628e>, 2019.